4th Croatian Microscopy Congress

with International Participation

BOOK OF ABSTRACTS

Poreč, Croatia

18-20 May, 2022

4th CROATIAN MICROSCOPY CONGRESS with International Participation: Book of Abstracts

18-20 May 2022, Poreč, Croatia

Editors: Jelena Macan and Goran Kovačević

Technical editors: Vida Strasser, Ina Erceg, Darija Domazet Jurašin and Ana Hant

Publishers: Croatian Microscopy Society and Ruđer Bošković Institute

ISBN 978-953-7941-41-3

Scientific Committee

Suzana Šegota

Igor Weber

Andreja Gajović

Jelena Macan

Goran Kovačević

Maja Herak Bosnar

Maja Dutour Sikirić

Organizing Committee

Danijela Poljuha

Vida Strasser

Damir Sirovina

Darija Domazet Jurašin

Ina Erceg

Ana Hant

GOLDEN SPONSOR

SILVER SPONSORS

BRONZE SPONSORS

ANSAR-ANALITIKA
ANALYTICAL EQUIPMENT

ZEISS

mikrolux
www.mikrolux.hr

TESCAN
PERFORMANCE IN NANOSPACE

EXHIBITORS

ANIMA LAB

KEFO
SINCE 1949

ETS
MEDICAL

OXFORD
INSTRUMENTS

ANDOR

AstraFokus
FOKUSIRANI NA MIKROSKOPIJU

EDC

WELCOME TO THE CMC2022

We welcome you to the 4th Croatian Microscopy Congress (CMC2022) in Poreč, Croatia (18th – 20th May 2022). The Congress is jointly organized by the Croatian Microscopy Society and the Ruđer Bošković Institute, Zagreb, Croatia's leading scientific institute in natural sciences, biomedicine, marine and environmental research.

CMC2022 has gathered more than 100 researchers, industry representatives and exhibitors from the region and Europe, focusing on the latest methodological developments in microscopy and applications of electron, light and scanning probe microscopy in biomedicine, biology, physics and chemistry of materials and related research areas. The Congress will include invited, oral, and poster presentations, as well as industry exhibits.

This edition of the Congress also marks the 30th anniversary of the Croatian Microscopy Society as an independent society and the 40th anniversary of the Electron Microscopy Section of the Croatian Society of Natural Sciences. We are particularly pleased to have the opportunity to award the "Spiridion Brusina" medal to prof. dr. sc. Miran Čeh, which will be presented to him by the President of the Croatian Society of Natural Sciences as a token of our gratitude for his contribution to microscopy in Croatia. In addition, the Congress will present a brief history of microscopy in Croatia through a lecture and an exhibition of historical photographs and events.

We are glad that you will spend three days dedicated to microscopy with us and we thank you for your participation in this event.

Suzana Šegota, chair of the Scientific Committee and
Danijela Poljuha, chair of the Organizing Committee

TABLE OF CONTENTS

PROGRAM

PROGRAM OVERVIEW ..... **I**

Wednesday, 18th May 2022 II

Thursday, 19th May 2022 IV

Friday, 20th May 2022 VIII

SPIRIDION BRUSINA LECTURE

SEM and TEM investigations of materials at the Centre for Electron Microscopy and Microanalysis (CEMM)

Miran Čeh, Sandra Drev, Jitka Hreščak, Maja Koblar, Andreja Šestan 1

PLENARY LECTURE (Materials Science)

Dynamics at catalytically active interfaces studied by multi-scale *operando* electron microscopy

Marc Willinger 3

PLENARY LECTURE (Life Sciences)

Microscopy approaches for the analysis of biomimetic *in vitro* models used in preclinical testing

Mateja Erdani Kreft 5

INVITED LECTURES (Life Sciences)

Functions of *Dictyostelium* protein IqgC in macropinocytosis

Vedrana Filić 7

The subcellular localization and oligomerization preferences of NME1/NME2 upon radiation-induced DNA damage

Martina Radić, Marko Šoštar, Igor Weber, Helena Ćetković, Neda Slade, Maja Herak Bosnar 8

Astrocyte energy metabolism measured by genetically encoded FRET nanosensors

Marko Kreft 9

Comet assay through the history and microscopy demands to follow it

Davor Želježić 10

INVITED LECTURES (Materials Science)

Chemical dynamics of nanocatalysts revealed by *operando* transmission electron microscopy

Milivoj Plodinec, Hannah Catherine Nerl, Thomas Lunkenbein, Robert R. Schlögl 12

Nucleation pathways of nanomaterials studied by advanced transmission electron microscopy

Sašo Šturm, Bojan Ambrožič, Kristina Žužek, Anže Prašnikar, Blaž Likozar 14

Micro-textural and micro-chemical evidences of mineral origin, alteration and weathering – case studies on REE minerals to understand REE distribution and accumulation in nature

Nenad Tomašić 16

Microscopy of polymer blends and polymer composites for 3D printing

Domagoj Vrsaljko, Filip Car, Ivan Karlo Cingesar, Marijan-Pere Marković 17

SELECTED LECTURES (Life Sciences)

Peripheral chromosomes positioned behind the spindle poles are prone to chronic unalignment in tumour cell lines

Kruno Vukušić, Snježana Kodba, Patrik Risteski, Iva M. Tolić 20

Rac1 dynamics in *Dictyostelium* cells: A combined experimental and theoretical approach

Marko Šoštar, Maja Marinović, Vedrana Filić, Nenad Pavin, Igor Weber 21

Reactive oxygen species (ROS) confocal laser scanning imaging in TROL mutants

Ena Dumančić, Hrvoje Fulgosi 22

Marine microalgae under temperature and salinity stress – insight from AFM study

Tea Mišić Radić, Maja Levak Zorinc, Nives Novosel, Nadica Ivošević DeNardis 24

Fully automatic whole slide imaging using a faster than real-time image recognition neural network

Krunoslav Vinicki, Dora Machaček 25

Organotypic culture as a 3D model to study Alzheimer's disease in porcine brain

Sowmya Sunkara 27

Segmentation of 3D SEM images of neurons: pre-processing steps

Snježana Radulović, Lucie Chalet, Benjamin Gottschalk, Stefan Wernitznig, Armin Zankel, Gerd Leitinger 28

Expression of NF, GFAP, and dendrin in the brain of small-spotted catshark *Scyliorhinus canicula* L.

Ivana Restović, Marko Vučemilo, Mia Obad, Nives Kević, Nela Kelam, Anita Racetin, Ivana Bočina 30

Thick and cleared – Blood vessels and neurons can be visualized in the cleared mouse brain using inverted fluorescence microscopy

Dominik Hamer, Daniela Petrinec, Monika Berecki, Laura Skukan, Srećko Gajović 32

Structural characteristics of femoral arteries in wild-type and Tff3 knock-out mice on standard and high-salt diet

Nikola Bijelić, Nataša Kozina, Edi Rođak, Iva Bazina, Kate Šešelja, Mirela Baus Lončar, Tatjana Belovari, Ivana Jukić, Ines Drenjančević 34

SELECTED LECTURES (Materials Science)

Decoding the multi-spatial-scale structure of high-entropy alloys by electron microscopy

Andreja Jelen, Stanislav Vrtnik, Primož Koželj, Sheng Guo, Guim Hwanuk, Kim Hae Jin, Anton Meden, Janez Dolinšek 37

Structural and electrical studies of sodium vanadium niobium phosphate glasses and glass-ceramics

Sara Marijan, Marta Razum, Teodoro Klaser, Marijan Marciuš, Željko Skoko, Jana Pisk, Luka Pavić 39

Chemical synthesis of manganite catalysts for simultaneous oxidation of aromatic compounds

Jelena Macan, Andreja Žužić, Filip Car, Vesna Tomašić, Andreja Gajović 41

Tungsten doped titania porous thin films for photocatalytic purification of water

Tayebeh Sharifi, Mario Bohač, Vedran Kojić, Krešimir Salamon, Krunoslav Juraić, Andreja Gajović 43

Nanostructured CuO@TiO_2: an efficient photocatalyst for degradation of diclofenac from the aqueous solution

Tihana Čižmar, Ivana Panžić, Lidija Brkljačić, Zaoli Zhang, Andreja Gajović 45

Surface morphology of textured transparent conductive oxide thin film seen by various probes: visible light, X-rays, electron scattering and contact probe

Krunoslav Juraić, Pavo Dubček, Mario Bohač, Andreja Gajović, Sigrid Bernstorff, Miran Čeh, Davor Gracin 47

Specific and abstract feature analysis of wide area CVD grown 2D islands using deep learning

Antonio Supina, Ana Senkić, Antun Lovro Brkić, Marko Jaklin, Marko Kralj 49

Large-scale synthesis and electrochemical transfer of borophene

B. Radatović, V. Jadriško, S. Kamal, M. Kralj, D. Novko, N. Vujičić, M. Petrović 51

Simultaneous influence of titanate nanomaterials and chitosan on precipitation of calcium phosphate

Ina Erceg, Ana–Marija Milisav, Vida Strasser, Maja Dutour Sikirić 53

SEM and EDS analyses of zeolite clinoptilolite water supernatants upon centrifugation

Rumenka Markoska, Vedrana Spada, Dean Marković, Krešimir Pavelić, Sandra Kraljević Pavelić 54

POSTER PRESENTATIONS (Life Sciences)

P1: Pancreatic islet surface and share of insulin granules after streptozotocin treatment in wild-type and Tff3 knock-out mice

Nikola Bijelić, Edi Rođak, Kate Šešelja, Iva Bazina, Tatjana Belovari, Mirela Baus Lončar 57

P2: Lipid profile of epicardial adipose tissue in obese individuals – preliminary data

Nikola Bijelić, Milorad Zjalić, Edi Rođak, Domagoj Vučić, Željko Debeljak, Boris Dumenčić, Jasmina Rajc, Tatjana Belovari, Kristina Selthofer Relatić 59

P3: The golden days are back: modern application of gold impregnation technique on rat brain cryosections

Milorad Zjalić, Sara Cibok, Edi Rođak, Marija Heffer, Tatjana Belovari, Nikola Bijelić 61

P4: Particle surface functionalization affects mechanism of endocytosis of silver nanoparticles in mammalian kidney cells

Maja Beus, Marija Ćurlin, Igor M. Pongrac, Ivona Capjak, Krunoslav Ilić, Ena Vrček, Mirta Milić, Ana Marija Marjanović Čermak, Ivan Pavičić 62

P5: Dependence of cell shape on spatial confinement

Blaž Ivšić, Tomislav Vuletić, Marko Šoštar, Igor Weber 64

P6: Effect of silver nanoparticles and ions on oxidative stress formation and antioxidative machinery of *Chlorella vulgaris*

Bruno Komazec, Daniel Mark Lyons, Petra Peharec Štefanić 65

P7: *In situ* fluorescence-based confocal imaging for detecting early stress responses of tobacco plants after exposure to silver nanoparticles or silver nitrate

Karla Košpić, Renata Biba, Petra Peharec Štefanić, David Vondrášek, Ilse Letofsky Papst, Biljana Balen 67

P8: Morphometric characteristics of *Dreissena polymorpha* oocytes in the Drava River and in the Dubrava Reservoir

Jasna Lajtner 69

P9: Histomorphometric evaluation of toxic effects of Na-PCP on the gill of the freshwater snail *Holandriana holandrii*

Romana Gračan, Jasna Lajtner, Maria Špoljar, Ines Tkalčec, Goran Kovačević, Blaženka Banjad Ostojić, Martina Ivšić, Ana Miletić, Radovan Erben 71

P10: Tracking polystyrene nanoparticles and resolving their effect on the immune system in mussel *Mytilus galloprovincialis*

Matea Marelja, Petra Peharec Štefanić, Daniel Mark Lyons 73

P11: Glandular trichomes micromorphology of aerial parts of *Sideritis romana* L. and *Sideritis montana* L.

T. Marić, M. Friščić, Ž. Maleš 74

P12: IqgC at the crossroads of RasGAP and IQGAP protein families

Lucija Mijanović, Darija Putar, Vedrana Filić, Igor Weber 76

P13: *In vivo* imaging to tackle the challenge of visualisation of dynamic processes – example of brain damage evolution after ischemic stroke

Daniela Petrinec, Dominik Hamer, Sanja Sarkočić, Paula Josić, Rok Ister, Monika Berecki, Laura Skukan, Marina Dobrivojević Radmilović, Siniša Škokić, Anton Glasnović, Srećko Gajović 78

P14: *Dictyostelium* IqgD is a Rho-regulated IQGAP involved in large-scale endocytosis

Anja Privara, Darija Putar, Igor Weber, Vedrana Filić 80

P15: Small GTPases interacting with IqgC on *Dictyostelium* macropinosomes

Darija Putar, Tamara Ćutić, Igor Weber, Vedrana Filić 81

P16: Microscopic insight into the intriguing world of broccoli

Ivana Šola, Danijela Poljuha 83

P17: A new approach to teaching about invasive species using a pocket paper Foldscope microscope

Mirela Uzelac, Ida Linić, Barbara Sladonja, Danijela Poljuha 85

P18: DNA damage and morphological changes to symbiotic and free-living hydra caused by norflurazon and UVB radiation

Goran Kovačević, Davor Želježić, Ana Matijević, Petra Korać, Katarina Caput Mihalić, Martina Ivšić 87

P19: Deleterious effect of quercetin on green hydra and its endosymbiotic alga

Goran Kovačević, Ana Matulić 88

P20: Microalgae as „triggers“ to dynamics in freshwater microcosm

Goran Kovačević, Daniela Petrinec, Petra Tramontana, Damir Sirovina, Siegfried Reipert, Davor Želježić, Petra Peharec Štefanić 89

POSTER PRESENTATIONS (Materials Science)

P21: Photocatalytic properties of thin PE-ALD ZnO films: the role of crystal structure

D. Jardas, R. Peter, M. Podlogar, D. Vengust, K. Salamon, M. Petravić, A. Omerzu 91

P22: Atomic layer deposition of ZnO and Al_2O_3 on cellulose for photocatalytic antibacterial performance

Ivana Jelovica Badovinac, Silvestar Mežnarić, Dalibor Broznić, Iva Šarić, Robert Peter, Maria Kolympadi Marković, Gabriela Ambrožić, Ivana Gobin 93

P23: Photocatalytic activity of thin ZnO ALD films deposited on porous substrates

Ivna Kavre Piltaver, Ivana Jelovica Badovinac, Karlo Veličan, Aleš Omerzu 95

P24: Ceria-zirconia-based high entropy oxides as catalysts for pinacol-type reactions

I. Kojčinović, D. Tatar, I. Szenti, S. Balász Nagy, S. Ziegenheim, Y. Tang, D. Stenzel, G. Varga, I. Djerdj 97

P25: Poster was retracted

P26: Experimental validation of novel fluorite-type rare earth high-entropy oxides for photocatalytic water splitting applications

D. Tatar, J. Kojčinović, S. Nundy, H. Ullah, A. Ghosh, A. A. Tahir, R. Meinusch, B. M. Smarsly, I. Djerdj 99

P27: Split-second photothermal processing of thin film titania nanotubes using intense pulsed (white) light

M. Bohač, M. Zubak, V. Kojić, P. Kassal, K. Juraić 101

P28: Correlation between synthesis parameters and optical/morphological properties of PbI_2 nanocrystals

Tomislav Damjanović, Livio Žužić, Antonio Supina, Ana Senkić, Iva Šrut Rakić, Nataša Vujičić 102

P29: Role of polyvinylpyrrolidone glass transition temperature in the performance of formamidinium perovskite solar cells

Vedran Kojić, Mario Bohač, Tihana Čižmar, Krešimir Salamon, Pavo Dubček, Andreja Gajović 104

P30: Morphological analysis of fibres extracted from lignocellulosic biomass – resources of renewable bioenergy

Zorana Kovačević, Sofia Šoufek, Ksenija Višić, Sandra Bischof 106

P31: Voltage cycling induced surface changes for enhancing sensing characteristics of graphene paste modified screen-printed electrodes

P. Živković, M. Medvidović Kosanović, A. Sečenji 108

P32: Determination of morphology, dopant amount and oxygen nonstoichiometry in lanthanum manganites by SEM-EDXS technique

Andreja Žužić, Jelena Macan 110

P33: Optical characterization of PbI_2 nanosheets prepared by a simple precipitation process

Livio Žužić, Tomislav Damjanović, Ana Senkić, Antonio Supina, Iva Šrut Rakić, Nataša Vujičić 112

P34: Microscopy study of calcium phosphates and calcium carbonates precipitation in the presence of differently charged liposomes

Ina Erceg, Jasminka Kontrec, Vida Strasser, Atiđa Selmani, Darija Domazet Jurašin, Marija Ćurlin, Branka Njegić Džakula, Nives Matijaković Mlinarić, Suzana Šegota, Daniel M. Lyons, Damir Kralj, Maja Dutour Sikirić 114

P35: Light microscopy application in determination of visible particles in injections

A. Giacobi Martinelli, N. Košutić Hulita, B. Martinić, B. Gudeljević 116

P36: Effect of silver nanoparticles on the precipitation of calcium phosphates

Ana-Marija Milisav, Ina Erceg, Vida Strasser, Maja Dutour Sikirić 117

P37: The impact of a novel photo-activation protocol on dental composite's degree of conversion – a Raman study

E. Novta, T. Lainović, S. Savić-Šević, D. Pantelić, E. Toth, Ž. Cvejić, L. Blažić 119

P38: The importance of SEM BSED in paintings and wooden polychrome cross-sections analysis

Tea Zubin Ferri 121

Author Index 123

PROGRAM

4th Croatian Microscopy Congress

18th – 20th May 2022.

PROGRAM OVERVIEW

WED 18th May

08:00 -13:00	BUS Zagreb-Poreč	
15:30 16:30	Poreč guided tour	
16:00 17:30	Registration and poster setup	
17:30 18:00	Opening ceremony	
18:00	Miran Čeh S. Brusina lecture	
19:00	Welcome reception	

THU 19th May

09:00 09:50	**IL: Vedrana Filić** **IL: Martina Radić**	**IL: Milivoj Plodinec** **IL: Sašo Šturm**
09:50 10:20	**SL**: Kruno Vukušić **SL**: Marko Šoštar	**SL**: Andreja Jelen **SL**: Sara Marijan
10:20 11:00	**Coffee break**	
11:00 11:45	**SL**: Ena Dumančić **SL**: Tea Mišić Radić **SL**: Krunoslav Vinicki	**SL**: Jelena Macan **SL**: Andreja Gajović **SL**: Tihana Čižmar
12:00 13:00	**Lunch break**	
13:00 13:40	**Plenary lecture: Marc Willinger**	
13:40 14:40	**Presentation of equipment**	
14:40 16:00	**Poster session with refreshments**	
16:00	**Visit to the Institute of Agriculture and Tourism, olive oil degustation**	
18:30	**Gala dinner - agrotourism Paladnjaki (at 19:00 h)**	

FRI 20th May

09:00 09:45	**SL**: Sowmya Sunkara **SL**: Snježana Radulović **SL**: Ivana Bočina	**SL**: Krunoslav Jurić **SL**: Antonio Supina **SL**: Marin Petrović
09:45 10:20	**Coffee break**	
10:20 11:10	**IL: Marko Kreft** **IL: Davor Želježić**	**IL: Nenad Tomašić** **IL: Domagoj Vrsaljko**
11:10 11:40	**SL**: Dominik Hamer **SL**: Nikola Bijelić	**SL**: Ina Erceg **SL**: Rumenka Markoska
12:00 13:00	**Lunch break**	
13:00 14:00	**Presentation of equipment**	
14:00 14:40	**Plenary lecture: Mateja Erdani Kreft**	
14:40 15:00	**Closing ceremony**	
15:15	**Cossetto winery tour with vine tasting**	

Plenary Lecture: 35 + 5 min - Invited Lecture : 20+5 min - Selected Lecture : 10+5 min

Life Sciences: Lavanda | Materials Science: Lovor

Wednesday, 18th May 2022

08:00–13:00

BUS ZAGREB-POREČ

Departure from Ruđer Bošković Institute at 8:00
30' stop at Vrata Jadrana

15:30–16:30

POREČ CITY WALKING TOUR

16:00–17:30

REGISTRATION AND POSTER SETUP

Lobby

17:30–18:00

OPENING CEREMONY

Lecture hall Lavanda

18:00–18:45

SPIRIDION BRUSINA LECTURE

MIRAN ČEH

SEM and TEM investigations of materials at the centre for electron microscopy and microanalysis (CEMM)

Lecture hall Lavanda

19:00

WELCOME RECEPTION

Restaurant / Outdoor


NanoWizard 4 XP
STEDYcon
JPK BIOAFM
BRUKER
abberior INSTRUMENTS
EVIDENT
OLYMPUS
Labena

Thursday, 19th May 2022

PARALLEL SECTIONS

09:00–10:20

LIFE SCIENCES

Lecture hall Lavanda

Chairpersons: M. Radić, V. Filić

INVITED LECTURES

09:00–09:25

VEDRANA FILIĆ

Functions of Dictyostelium protein IqgC in macropinocytosis

09:25–09:50

MARTINA RADIĆ

The subcellular localization and oligomerization preferences of NME1/NME2 upon radiation-induced DNA damage

SELECTED LECTURES

09:50–10:05

KRUNO VUKUŠIĆ

Peripheral chromosomes positioned behind the spindle poles are prone to chronic unalignment in tumour cell lines

10:05–10:20

MARKO ŠOŠTAR

Rac1 dynamics in Dictyostelium cells: A combined experimental and theoretical approach

MATERIALS SCIENCE

Lecture hall Lovor

Chairpersons: J. Macan, T. Čižmar

INVITED LECTURES

09:00–09:25

MILIVOJ PLODINEC

Chemical dynamics of nanocatalysts revealed by operando transmission electron microscopy

09:25–09:50

SAŠO ŠTURM

Nucleation pathways of nanomaterials studied by advanced transmission electron microscopy

SELECTED LECTURES

09:50–10:05

ANDREJA JELEN

Decoding the multi-spatial-scale structure of high-entropy alloys by electron microscopy

10:05–10:20

SARA MARIJAN

Structural and electrical studies of sodium vanadium niobium phosphate glasses and glass-ceramics

10:20-11:00

COFFEE BREAK

outdoor / Lecture hall Magnolia

PARALLEL SECTIONS

11:00–11:45

LIFE SCIENCES

Lecture hall Lavanda

Chairpersons: M. Herak Bosnar, I. Weber

SELECTED LECTURES

11:00–11:15

ENA DUMANČIĆ

Reactive oxygen species (ROS) confocal laser scanning imaging in TROL mutants

11:15–11:30

TEA MIŠIĆ RADIĆ

Marine microalgae under temperature and salinity stress–insight from AFM study

11:30–11:45

KRUNOSLAV VINICKI

Fully automatic whole slide imaging using faster than real-time image recognition neural network

MATERIALS SCIENCE

Lecture hall Lovor

Chairpersons: I. Jelovina Badovinac, K. Juraić

SELECTED LECTURES

11:00–11:15

JELENA MACAN

Chemical synthesis of manganite catalysts for simultaneous oxidation of aromatic compounds

11:15–11:30

ANDREJA GAJOVIĆ

Tungsten doped titania porous thin films for photocatalytic purification of water

11:30–11:45

TIHANA ČIŽMAR

Nanostructured CuO@TiO_2: an efficient photocatalyst for degradation of diclofenac from the aqueous solution

12:00–13:00

LUNCH BREAK*

hotel restaurant
*Lunch is included for all CMC participants

13:00–13:40

PLENARY LECTURE

Lecture hall Lavanda

MARC WILLINGER

Dynamics at catalytically active interfaces studied by multi-scale operando electron microscopy

Chairperson: A. Gajović

13:40–14:40

EQUIPMENT PRESENTATION

Lecture hall Lavanda

13:40–14:00

CARL ZEISS

ZEISS fs-laser assisted FIB/SEM & Correlative Cryo Workflow
Wolfgang Schwinger, Carl Zeiss

14:00–14:20

SCAN / JEOL

Latest JEOL developments for biology and material sciences
Guillaume Brunetti, JEOL

14:20–14:40

ITR LAB / THERMOFISHER SCIENTIFIC

DualBeams for diverse applications
Daniel Phifer, Thermofisher scientific

14:40–16:00

POSTER SESSION WITH REFRESHMENTS

Lobby

16:00–17:50

VISIT TO THE INSTITUTE OF AGRICULTURE AND TOURISM, OLIVE OIL DEGUSTATION

GROUP 1 16:00 – 16:50
GROUP 2 17:00 – 17:50

18:30

GALA DINNER IN THE AGROTOURISM PALADNJAKI

Dinner starts at 19:00, return will be organized at 22:00, 23:00 and 24:00

Friday, 20th May 2022

PARALLEL SECTIONS

09:00–09:45

LIFE SCIENCES

Lecture hall Lavanda

Chairpersons: I. Bočina, N. Bijelić

SELECTED LECTURES

09:00–09:15

SOWMYA SUNKARA

Organotypic culture as a 3D model to study Alzheimer's disease in porcine brain

09:15–09:30

SNJEŽANA RADULOVIĆ

Segmentation of 3D SEM images of neurons: pre-processing steps

09:30–09:45

IVANA BOČINA

Expression of NF, GFAP, and dendrin in the brain of small-spotted catshark Scyliorhinus canicula L.

MATERIALS SCIENCE

Lecture hall Lovor

Chairpersons: N. Tomašić, D. Vrsaljko

SELECTED LECTURES

09:00–09:15

KRUNOSLAV JURAIĆ

Surface morphology of textured transparent conductive oxide thin film seen by various probes: visible light, X-rays, electron scattering and contact probe

09:15–09:30

ANTONIO SUPINA

Specific and abstract feature analysis of wide area CVD grown 2D islands using deep learning

09:30–09:45

MARIN PETROVIĆ

Large-scale synthesis and electrochemical transfer of borophene

09:45–10:20

COFFEE BREAK

outdoor / Lecture hall Magnolia

PARALLEL SECTIONS
10:20–11:40

LIFE SCIENCES

Lecture hall Lavanda

Chairpersons: G. Kovačević, M. Kreft

INVITED LECTURES

10:20–10:45

MARKO KREFT

Astrocyte energy metabolism measured by genetically encoded FRET nanosensors

10:45–11:10

DAVOR ŽELJEŽIĆ

Comet assay through the history and microscopy demands to follow it

SELECTED LECTURES

11:10–11:25

DOMINIK HAMER

Thick and cleared - Blood vessels and neurons can be visualized in the cleared mouse brain using inverted fluorescence microscopy

11:25–11:40

NIKOLA BIJELIĆ

Structural characteristics of femoral arteries in wild-type and Tff3 knock-out mice on standard and high-salt diet

MATERIALS SCIENCE

Lecture hall Lovor

Chairpersons: T. Zubin Ferri, M. Petrović

INVITED LECTURES

10:20–10:45

NENAD TOMAŠIĆ

Micro-textural and micro-chemical evidences of mineral origin, alteration and weathering – case studies on REE minerals to understand REE distribution and accumulation in nature

10:45–11:10

DOMAGOJ VRSALJKO

Microscopy of polymer blends and polymer composites for 3D printing

SELECTED LECTURES

11:10–11:25

INA ERCEG

Simultaneous influence of titanate nanomaterials and chitosan on precipitation of calcium phosphate

11:25–11:40

RUMENKA MARKOSKA

SEM and EDS analyses of zeolite clinoptilolite water supernatants upon centrifugation

12:00–13:00

LUNCH BREAK*

hotel restaurant
*Lunch is included for all CMC participants

13:00–14:00

EQUIPMENT PRESENTATION

Lecture hall Lavanda

13:00–13:20

MIKROLUX / TESCAN
Gain the maximum throughput with artifact-free surfaces for sample characterization by using high current plasma FIB-SEM
Martin Suchanek, Tescan

13:20–13:40

ANSAR ANALITIKA
News related to Oxford Instruments/Asylum Research Atomic Force Microscopy (AFM) instruments
Krešo Mesarek, Ansar analitika

13:40–14:00

LABENA / ABERRIOR
STED nanoscopy in tissues using adaptive optics and MATRIX array detection
Jan Vavra, Abberior Instruments GmbH

14:00–14:40

PLENARY LECTURE

Lecture hall Lavanda

MATEJA ERDANI KREFT

Microscopy approaches for the analysis of biomimetic in vitro models used in preclinical testing

Chairperson: I. Weber

14:40–15:00

CLOSING CEREMONY

Lecture hall Lavanda

15:15

COSSETTO WINERY TOUR/WINE TASTING & DEPARTURE TO ZAGREB

Departure to Zagreb is expected around 17:00

30 minute break at Vrata Jadrana around 18:30

return to Zagreb around 21:00

SPIRIDION BRUSINA LECTURE

SEM and TEM investigations of materials at the Centre for Electron Microscopy and Microanalysis (CEMM)

Miran Čeh (1), Sandra Drev (2), Jitka Hreščak (1), Maja Koblar (1), Andreja Šestan (1)

1) Centre for Electron Microscopy and Microanalysis (CEMM), Jožef Stefan Institute, Ljubljana, Slovenia

2) Nanostructured Materials, Jožef Stefan Institute, Ljubljana, Slovenia

Modern *state-of-the-art* electron microscopy (EM) techniques are among the most versatile and useful analytical methods for non-destructive morphological, structural and chemical characterization of materials. Both scanning electron microscopy techniques (SEM) and transmission electron microscopy techniques (TEM), in essence complementary analytical methods, are capable of providing insight into the structure and chemical composition of materials from micrometer range to sub-atomic range. By recent developments of liquid-cell TEM *in situ* techniques, the dynamic component of processes in liquids/gases and during electrochemical reactions can be observed as well. The present work will focus on more recent SEM and TEM investigations that were carried out at the Centre for Electron Microscopy and Microanalysis (CEMM) at the Jožef Stefan Institute (JSI). The EM techniques available within the CEMM will be demonstrated with the results of EM investigations performed on various inorganic and organic materials. The CEMM function and strategy will also be commented on.

Keywords: SEM and TEM techniques, Centre for Electron Microscopy and Microanalysis (CEMM)


AstraFokus
FOKUSIRANI NA MIKROSKOPIJU
3i Intelligent Imaging Innovations
ZEISS
delmic
NANOMAGNETICS INSTRUMENTS
DeltaPix
- Discover the Details
abbelight
Now, we see.
iolight
AstraFokus d.o.o., 385 91 48 99 025, luka@astrafokus.hr, www.astrafokus.hr

PLENARY LECTURE
(Materials Science)

Dynamics at catalytically active interfaces studied by multi-scale *operando* electron microscopy

Marc Willinger (1)

1) ETH Zürich, Zürich, Switzerland

Our aim is to understand processes that lead to the emergence of catalytic function through direct observation using a combination of *operando* scanning and transmission electron microscopy. Starting with simple model catalysts, such as polycrystalline metal foils, we observe the propagation of chemical waves and reveal how catalytic activity depends on grain orientation, coupling mechanisms and reaction conditions [1]. In the case of redox-reactions on non-noble metals, we find that the active catalyst is operating near a phase-boundary where metallic and oxidized phases co-exist [2]. Real-time imaging reveals fascinating oscillatory redox dynamics that increase in complexity with the increasing chemical potential of the gas-phase. When moving from simple model catalysts to industrially relevant metal nanoparticles supported on reducible oxide carriers, we apply *in situ* transmission electron microscopy to study effects related to a strong metal-support interaction (SMSI) under reactive conditions [3]. Using the archetypical titania supported platinum nanoparticles as a reference system, and hydrogen oxidation as model redox reaction, it will be shown that the well-described encapsulated state of platinum particles is lost as soon as the system is exposed to a redox-active environment. Structural incoherence at the platinum-titania interface lowers the barrier for redox processes, which gives rise to dynamic reconstructions and particle migration. The particle orientation on the support determines the structure of the interface and the resulting particle dynamics, migration, and sintering behaviour. The aim of the presentation is to demonstrate that active catalysts are dynamically adapting to the reaction environment and that catalytic function is related to the catalysts' ability to participate in the reaction through reversible changes in its structure and/or (local) composition.

Keywords: *operando* electron microscopy, chemical dynamics, redox processes, catalysis

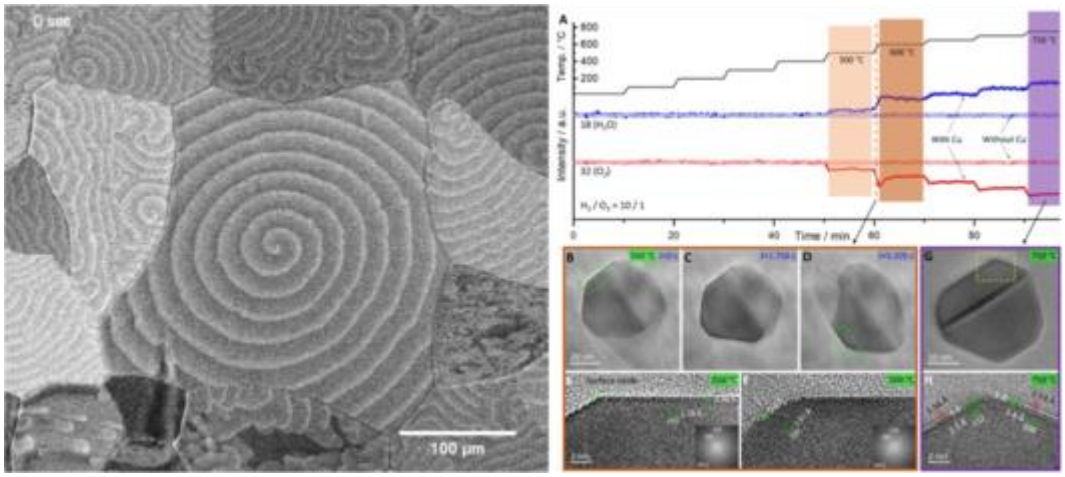

Figure 1. Left: Propagating reaction fronts observed during NO_2 hydrogenation on a polycrystalline Pt foil [1]. Right: MS data recorded during H_2 oxidation on Cu particles. Simultaneously recorded TEM images reveal oscillatory redox dynamics and the co-existence of Cu and Cu_2O [2].

References:
1. C. Barroo et al., Nat. Catal. 3 (2020) 30–39.
2. X. Huang et al., Adv. Mater. 33 (2021) 2101772.
3. A. Beck et al., Nat. Catal. 4 (2021) 488-497.

PLENARY LECTURE

(Life Sciences)

Microscopy approaches for the analysis of biomimetic *in vitro* models used in preclinical testing

Mateja Erdani Kreft (1)

1) University of Ljubljana, Faculty of Medicine, Institute of Cell Biology, Ljubljana, Slovenia

Biomimetic *in vitro* models resemble the closest alternative to *in vivo* tissue or organ for basic and preclinical studies. They must have molecular, ultrastructural, and physiological characteristics similar to *in vivo* tissue that are proven by different cytochemistry and cell- physiology methods and finally unequivocally confirmed by the "seeing is believing" approach in live-cell imaging and electron microscopy. Biomimetic *in vitro* models can significantly contribute to the principle of the three Rs, which are refining, reducing, and replacing the use of laboratory animals and have good transferability to animal and human studies. Our work over the past few years has shown the key contribution of microscopy in determining the functionality and potency of the urinary and respiratory tract *in vitro* models. Using different microscopy techniques and applied qualitative and quantitative evaluation, new insights into the urinary and respiratory tissue ultrastructure and function have emerged. Both systems are exposed to a variety of possible infections and injures that may lead to organ damage or loss. New approaches for the preparation of biomimetic normal and cancerous *in vitro* models, and high-resolution light and electron microscopes allow us to study the cell's subcellular organization and dynamics, drug candidates, and to assess drug permeability and their intracellular function. The high-speed phase-contrast microscopy shows great potential as an *in vitro* method for screening and testing of long-term ciliotoxicity and cytotoxicity after repeated doses in the growing field of potential nasal therapies. In this lecture, the microscopy approaches that enable us to test bacterial uropathogenicity and corresponding cellular responses and study the cytotoxicity and clinical relevance of developing urothelial and nasal drugs on biomimetic normal and cancerous *in vitro* models, will be presented.

Keywords: high-resolution microscopy, biomimetic *in vitro* model, preclinical study, nasal drugs, urinary bladder

INVITED LECTURES

(Life Sciences)

Functions of *Dictyostelium* protein IqgC in macropinocytosis

Vedrana Filić (1)

1) Ruđer Bošković Institute, Division of Molecular Biology, Zagreb, Croatia

Dictyostelium IqgC is an IQGAP-related protein. IQGAPs from higher eukaryotes are large, multidomain proteins whose name derives from the IQ motifs and a GAP-related domain (GRD) or RasGAP domain (GAP, GTPase-activating protein). Although they belong to a large group of RasGAP domain-containing proteins, they have lost catalytic activity, i.e. they are unable to promote GTP-hydrolytic activity of small GTPases from the Ras family. Instead, they interact with Rho family GTPases, Rac1 and Cdc42, and act as their effectors in the regulation of the actin cytoskeleton [1]. *Dictyostelium discoideum* harbours four IQGAP-related proteins that are substantially smaller than their mammalian relatives, but still contain conserved RasGAP-RasGAP_C-terminal domain architecture found only in IQGAPs. *Dictyostelium* DGAP1 (DdIQGAP1) and GAPA (DdIQGAP2) are Rac1 effectors that mediate the bundling of actin filaments. They are essential for normal cytokinesis and localize to the cleavage furrow of dividing cells and to the retracting tail of polarized interphase cells [2]. We have investigated the role of IqgC (DdIQGAP3) [3]. IqgC is an atypical IQGAP because it does not bind Rho GTPases and has preserved RasGAP activity exerted specifically toward RasG protein. Besides, unlike DGAP1 and GAPA, IqgC strongly localizes to protrusive structures, such as forming macropinocytic and phagocytic cups, and nascent macropinosomes and phagosomes, where it colocalizes with active Ras. Moreover, we have demonstrated interaction with RasG to be indispensable for the recruitment of IqgC to membrane patches primed for macropinocytosis. Since RasG is one of the major regulators of macropinocytosis in *D. discoideum*, by suppressing its activity, IqgC negatively regulates fluid uptake. More specifically, we have demonstrated that IqgC limits the size of macropinocytic cups. Similarly, phagocytosis of large particles is more effective in cells deficient for IqgC. Next, we used lattice light-sheet microscopy to compare IqgC dynamics with the active Ras probe and revealed that IqgC lingers on the internalized macropinosome after Ras has dissociated from the vesicle. This finding suggests additional, RasG-independent functions of IqgC, probably during early macropinosome maturation. Indeed, using biochemical methods, we identified an early endosome marker, the GTPase Rab5A, as a direct binding partner of IqgC. Furthermore, we found Rab5A to colocalize with IqgC on the nascent macropinosome. However, a biological consequence of this interaction is not clear at the moment.

Keywords: IqgC, IQGAP, Ras, Rab5A, macropinocytosis

References:

1. T. Watanabe et al., Cell Struct. Funct. 40 (2015) 69–77.
2. J. Faix et al., EMBO J. 20 (2001) 3705–3715.
3. M. Marinović et al., Proc. Natl. Acad. Sci. U.S.A. 116 (2019) 1289–1298.

This work has been supported in part by FP7-REGPOT project InnoMol, the ESF project INTERBIO and Croatian Science Foundation under the project IP-2020-02-1572.

The subcellular localization and oligomerization preferences of NME1/NME2 upon radiation-induced DNA damage

Martina Radić (1), Marko Šoštar (2), Igor Weber (2), Helena Ćetković (2), Neda Slade (2), Maja Herak Bosnar (2)

1) University of Bern, Bern, Switzerland

2) Ruđer Bošković Institute, Zagreb, Croatia

Nucleoside diphosphate kinases (NDPK/NME/Nm23) are housekeeping enzymes responsible for the maintenance of the cellular NTP pool by catalyzing the exchange of terminal phosphate from trinucleotides to dinucleotides through a high-energy phosphohistidine intermediate. At least 80 % of the cytoplasmic NDPK activity is being exerted by NME1/NDPK A and NME2/NDPK B which combine to form isoenzymes (A6, A5B1, …, B6). The NME1/NDPK A and NME2/NDPK B subunits have a variety of additional biological functions, from metastasis suppression and DNA damage repair to proliferation and development. Although eukaryotic NDPKs are active only as hexamers, it is unclear whether other NME functions require the hexameric form and how the isoenzyme composition varies in different cellular compartments. To investigate the effect of DNA damage on the intracellular localization of NME1 and NME2 and the composition of NME oligomers in the nucleus and cytoplasm, we used live-cell imaging and the FRET/FLIM technique. We demonstrated that exogenous NME1 and NME2 proteins colocalize in the cytoplasm of non-irradiated cells and move simultaneously to the nucleus after gamma irradiation. The FRET/FLIM experiments suggest that there is a slight shift in the homomer/heteromer balance between the nucleus and cytoplasm after DNA damage. Overall, our results suggest that NME1 and NME2 engage in mutual functions in the nucleus after irradiation, possibly performing specific functions in their homomeric state.

Keywords: NME protein family, NDPK, DNA damage, FRET/FLIM, live-cell imaging

Astrocyte energy metabolism measured by genetically encoded FRET nanosensors

Marko Kreft (1)

1) Laboratory of Neuroendocrinology-Molecular Cell Physiology, Institute of Pathophysiology, Faculty of Medicine, University of Ljubljana, Ljubljana, Slovenia & Celica Biomedical Center, Ljubljana, Slovenia & Department of Biology, Biotechnical Faculty, University of Ljubljana, Ljubljana, Slovenia

Astrocytes play a significant role in a number of processes, including the brain energy metabolism. Their anatomical position between blood vessels and neurons makes them an interface for effective glucose uptake from blood. Astrocytes contain glycogen, an energy buffer, which can bridge local short-term energy requirements in the brain. Glycogen levels reflect a dynamic equilibrium between glycogen synthesis and glycogenolysis. Many factors that include hormones and neuropeptides such as insulin and adrenaline likely modulate glycogen stores in astrocytes, but detailed mechanisms at the cellular level are sparse. During cognitive efforts mediated by local neuronal networks, approximately 20 % of additional energy is required; this is mediated by chemical messengers such as noradrenaline (NA). We used a glucose nanosensor based on Förster resonance energy transfer to monitor cytosolic glucose and lactate concentration with high temporal resolution and a cytochemical approach to determine glycogen stores in single cells. We show that, following the adrenaline or noradrenaline stimulation, the availability of cytosolic glucose and lactate is increased promptly after stimulation. Insulin boosts the process of glycogen formation. We showed that D-glucose uptake is essential for the NA-induced increase in lactate concentration, and that this exclusively arises from glycogen degradation, indicating that most, if not all, D-glucose molecules in NA-stimulated cells transit the glycogen shunt during glycolysis. Moreover, under the defined transmembrane D-glucose gradient, the glycolytic intermediates were not only used to produce L-lactate, but also to significantly support oxidative phosphorylation, as demonstrated by an elevation in lactate concentration when the Krebs cycle was inhibited.

Keywords: FRET nanosensors, glycogen, astrocytes, metabolism, glucose

Comet assay through the history and microscopy demands to follow it

Davor Želježić (1)

1) Institute for Medical Research and Occupational Health, Mutagenesis Unit, Zagreb, Croatia

Nowadays, the comet assay is one of the most widely used methods in genotoxicity assessment. It owes its wide application to ease of the performance, short time to get results, and ability to be performed either *in vitro* or *in vivo*. Unlike other techniques, when performed *in vivo* it may detect genotoxicity in cells of a variety of organs and tissues. It does not require cells to be actively dividing as the other genotoxic methods do. Beginnings of the comet assay reach back to 1984 when Östling and Johanson [1] for the very first time applied the microelectrophoresis method to detect DNA damage in gamma-source irradiated cells. The DNA had to be labeled with radionuclides and the evaluation was autoradiogramic. In 1988 two independent teams of scientists (Singh et al. [2], Olive et al. [3]) shaped the comet assay more or less in the form we know today. Of the highest significance was that they made the assay more scientist-friendly. Instead of radiolabeling, fluorescent dyes were introduced and epifluorescent microscopy was applied to analyse genotoxic events. Nowadays, even less mutagenic dyes such as YOYO-1 are being introduced in the staining of the comet assay preparations. The induction of specific repair enzymes in the methodology enables us to specifically detect one targeted type of lesions in DNA. Still, a major issue of the assay's implementation in the regulatory toxicology is that the method is not sufficiently validated *in vitro* and that no consensus regarding the protocol has been reached. Besides, the lesions detectable by the comet assay are of the primary nature, being rapidly repaired. Thus, its relevance in assessing the risk from carcinogenesis has been deduced. The ever-growing number of papers applying the method will contribute to its validation and unification and estimating the relevance in the carcinogenesis risk assessment.

Keywords: comet assay, DNA damage, staining techniques, microscopy

References:

1. O. Ostling and K.J. Johanson, Biochem. Biophys. Res. Commun. 123 (1984) 291–298.
2. N.P. Singh et al., Exp. Cell. Res. 175 (1988) 184–191.
3. P.L. Olive et al., Cancer Res. 48 (22) (1988) 6444-6449.

INVITED LECTURES

(Materials Science)

Chemical dynamics of nanocatalysts revealed by *operando* transmission electron microscopy

Milivoj Plodinec (1), Hannah Catherine Nerl (2), Thomas Lunkenbein (3), Robert R. Schlögl (3)

1) ScopeM, ETH-Zürich, Zürich, Switzerland

2) Humboldt University of Berlin, Berlin, Germany

3) Department of Inorganic Chemistry, Fritz Haber Institute, Berlin, Germany

Humanity is facing great environmental challenges due to the excessive and unsustainable use of natural resources. The severity of the situation is apparent in the changing climate. Chemistry, catalysis, and material science will play an important role in the necessary transition towards an energy supply that is fully based on renewable and sustainable energy sources. Therefore, it is of crucial importance to improve our present knowledge in catalysis to ultimately lead to the rational design of better, more efficient catalysts for industrially relevant reactions such as CO_2 reduction, propane dehydrogenation (DHP) and dry reforming of methane (DRM). Many studies have shown that catalysts are metastable and dynamic systems, where the nature of the active state depends on the applied chemical potential, associated chemical dynamics and formation of transient active sites [1,2]. Moreover, since the working catalysts are thought to be metastable, the active surfaces could be unstable under non-active conditions, which could lead to the misinterpretation in *ex situ* studies of inactive structures as active states [3,4]. However, recent progress in developing *in situ* and *operando* transmission electron microscopy (TEM) techniques allows to study dynamical processes live as they happen, probe the active-state/-sites of catalysts under reaction conditions (temperature, pressure, flow) at high spatial and temporal resolution [5-8]. In this presentation, it will be shown that the *operando* TEM techniques allow to directly visualize local structural and morphological transformations of catalysts induced by the different reaction conditions in several relevant catalytic processes. Using this approach, we were able to gain direct insights into different active states of Pt and Ni catalysts and the influence of reaction conditions during carbon nanotubes growth, DHP and DRM. Furthermore, it will be shown that the combination of real-time high-resolution imaging and electron diffraction with on-line mass spectroscopy and calorimetry enables correlative observation of local changes in structure, morphology and chemical composition, which is directly related to changes in catalytic function. In summary, using *operando* TEM techniques we were able to gain meaningful insights into structural and morphological transformations of catalysts and to establish structure-function relationship in a range of industrially relevant catalytic reactions. In the future, *operando* TEM in combination with other macroscopic characterization techniques will provide crucial insights into the fundamentals underlying heterogeneous catalysis and at relevant reaction conditions, ultimately paving the way for the design of better catalysts.

Keywords: *operando* transmission electron microscopy, chemical dynamics, catalyst, structure-function relationship, active state

References:
1. R. Schlögl, Angew. Chem. Int. Ed. 54 (2015) 3465-3520.
2. R. Schlögl, ChemCatChem 9 (2017) 533-541.
3. K.F. Kalz et al., ChemCatChem 9 (2017) 17-29.
4. A. Bergmann and B. Roldan Cuenya, ACS Catalysis 9 (2019) 10020-10043.
5. S.B. Vendelbo et al., Nat. Mater. 13 (2014) 884-900.
6. M. Plodinec et al., Microsc. Microanal. 26 (2020) 220-228.
7. M. Plodinec et al., ACS Catalysis 10 (2020) 3183-3193.
8. S.W. Chee et al., J. Phys. Condens. Matter 33 (2021) 15301.

Nucleation pathways of nanomaterials studied by advanced transmission electron microscopy

Sašo Šturm (1), Bojan Ambrožič (1), Kristina Žužek (1), Anže Prašnikar (2), Blaž Likozar (2)

1) Jožef Stefan Institute, Ljubljana, Slovenia

2) National Institute of Chemistry, Ljubljana, Slovenia

Transmission electron microscopy (TEM) has been revolutionizing our way of understanding materials' properties and, in many ways, facilitated the rise of nanomaterials and nanotechnology by providing atomic-scale structural and chemical information. Despite all these advancements, a key challenge of understanding the final performance of a material is still hindered by the fact that it is being investigated in its stationary state, post-mortem. This means that the insights into the dynamic history that brought the material to its current state are excluded. Therefore, the utilization of suitable microscopy methods that allow investigations of materials in their dynamic environments at high spatial and temporal resolution offers significant advances in developing novel functional materials. This promising approach has triggered a whole scientific sub-field that studies the materials' dynamic effects in various environments inside the TEM. The latter could be represented by changes in temperature, mechanical deformation, electrical biasing, gas-imposed catalytic activity, and electrochemical reactions in aqueous environments. In this lecture, I will cover the basic concepts of TEM in dynamic environments and present examples of differently designed experiments. Firstly, I will introduce several case studies where a TEM specimen served as an inherent part of the experiments related to nanoparticle nucleation from the gaseous phase. These studies represent a semi-dynamical environment. Fully dynamic studies of nanoparticles formation in aqueous environments using specialized liquid-cells inside the TEM will then be introduced. The method is often referred to as Liquid-Cell TEM (LCTEM) microscopy. This ground-breaking approach can open a wide range of possibilities where case by-case custom-made experiments can be performed. For example, tailoring of liquid cell design can allow a direct study of nanoparticles' nucleation and growth from aqueous solutions at elevated temperatures or during the electrodeposition at both high spatial and temporal resolution. As the TEM instrument itself applies an additional dynamic condition of a high-energy electron beam to the specimen, special emphasis will be given to modelling chemical environments inside LCTEM cells. Here, a thorough understanding of the water radiolysis under the high-energy beam conditions needs to be acquired. A calculated radiolysis model can then be validated by dedicated LCTEM experiments. These have demonstrated in our case study that the nanoparticle precipitation/dissolution reactions can be dynamically and reversibly controlled by altering the chemical environment of the liquid cell, which poses both challenges and opportunities that will shape the near future of this powerful multidisciplinary TEM technique.

Keywords: TEM, *in situ*, liquid TEM, nucleation, nanoparticles

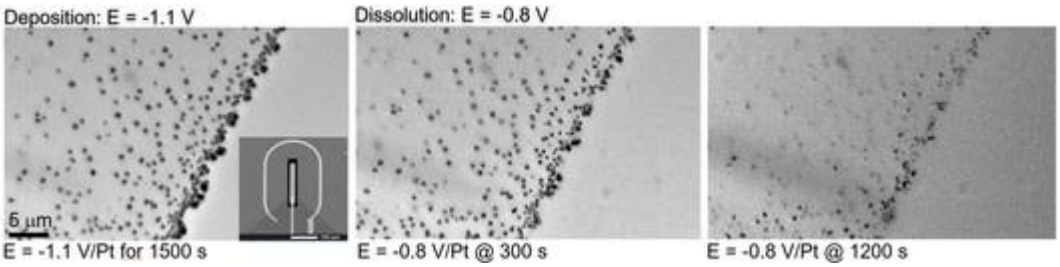

Figure 1. Dynamic electrochemical deposition-dissolution process of iron nanoparticle inside LCTEM cell.

References:

1. B. Ambrožič et al., Chem. Sci. 10 (2019) 8735-8743.

We acknowledge the Slovenian research agency through programme: P2-0084 and EU's Horizon 2020 research and innovation programme under grant agreement No. 823717 (ESTEEM3).

Micro-textural and micro-chemical evidences of mineral origin, alteration and weathering – case studies on REE minerals to understand REE distribution and accumulation in nature

Nenad Tomašić (1)

1) University of Zagreb, Faculty of Science, Department of Geology, Zagreb, Croatia

Rare-earth elements (REE) are a valuable commodity in modern industry and technology, used to optimize the properties of many materials. Also, the distribution patterns and various modes of the occurrence of these metals in nature are of a great significance in interpreting geological processes. All these make REE and REE minerals a frequent topic in geological studies. REE are widespread in various geological environments, though they rarely occur in large amounts at the same place, which makes a search for REE deposits not an easy task. Employment of diverse micro-techniques is essential for the characterization of REE minerals, particularly in the study of their structural, textural, and chemical properties. Here, two case studies on REE minerals originating from two different environments will be presented, showing features imprinted by their formation and alteration history. Certain types of granitic pegmatites usually accommodate various REE minerals, such as monazite-(Ce), xenotime-(Y), aeschynite-(Y), euxenite-(Y), gadolinite-(Y), and many others. Monazite-(Ce) is a REE mineral frequently used as a REE ore mineral, but also employed in many studies for interpretation of geological settings and a common mineral of choice in geochronology due to U and Th content. Various late- and post-magmatic processes influence the chemistry of the mineral, producing alteration patterns ruled by the dissolution-reprecipitation process and causing redistribution of REE. Similar processes have been observed in gadolinite-(Y), thus helping us understand the nature of REE mobility and constraints in the dating application of these minerals. Micro-chemical studies indicate the alteration paths and evolution of these minerals in granitic pegmatites. Bauxite is a sedimentary rock and aluminium ore, which can also contain elevated abundances of REE relative to its hosting rocks. Thus, it is a potential future source of REE, particularly after its processing in Bayer process for alumina production. Bayer process frequently doubles REE concentrations in the remaining red mud, an industrial by-product, so far considered a harmful waste. REE occurrence in bauxite can be related to various mineral phases and mechanisms, like adsorption to aluminium and iron oxides/oxyhydroxides. Thorough microscopy studies indicate a presence of REE minerals, which can be detrital (inherited from weathered parent rocks) or authigenic (formed in bauxite during episodes of weathering and bauxitization). Micro-textural studies reveal their sedimentation history but also give insight into mobility and accumulation of REE in a bauxite profile.

Keywords: rare earth element minerals, granitic pegmatites, bauxite

Microscopy of polymer blends and polymer composites for 3D printing

Domagoj Vrsaljko (1), Filip Car (1), Ivan Karlo Cingesar (1), Marijan-Pere Marković (1)

1) University of Zagreb, Faculty of Chemical Engineering and Technology, Zagreb, Croatia

The increasing demand for polymeric materials with special bulk and surface properties has led to a variety of strategies for the development of new materials aimed at synergistic effects through combinations of polymeric materials. Polymer blending is an attractive field for scientific and industrial investigation because it is a simple method to obtain new materials with improved performance without having to produce new polymers. Immiscible polymer blends form two discrete phases, and compatibilization is necessary to achieve maximum synergy. 3D printing or additive manufacturing is a fabrication of a three-dimensional object using a 3D digital model. The term 3D printing can refer to a range of processes in which material is applied, bonded, or solidified by computer control to create a three-dimensional object, typically adding the material (e.g. plastics, liquids, or powder grains that are fused together) layer by layer. Over the past ten to twenty years, 3D printing has evolved into a technology that enables the production of complex, yet cost-effective 3D components. As 3D printing technologies become more affordable, it seems inevitable that this technology will become the tool of choice for manufacturing flow reactors and other reactionware. The talk will present examples of the development of polymer blends and polymer composites for 3D printing, as well as an overview of their properties. The influence of the filler addition on the morphology of the polymer blends and the influence of the surface properties of the fillers on the selectivity of placement within the polymer blends will be presented. A brief overview of the appearance of the surfaces of 3D printed objects depending on the printing settings and the possibilities of modifying these surfaces by plasma treatment with the aim of adjusting the hydrophobic properties will be given.

Keywords: 3D printing, polymer blends, polymer composites

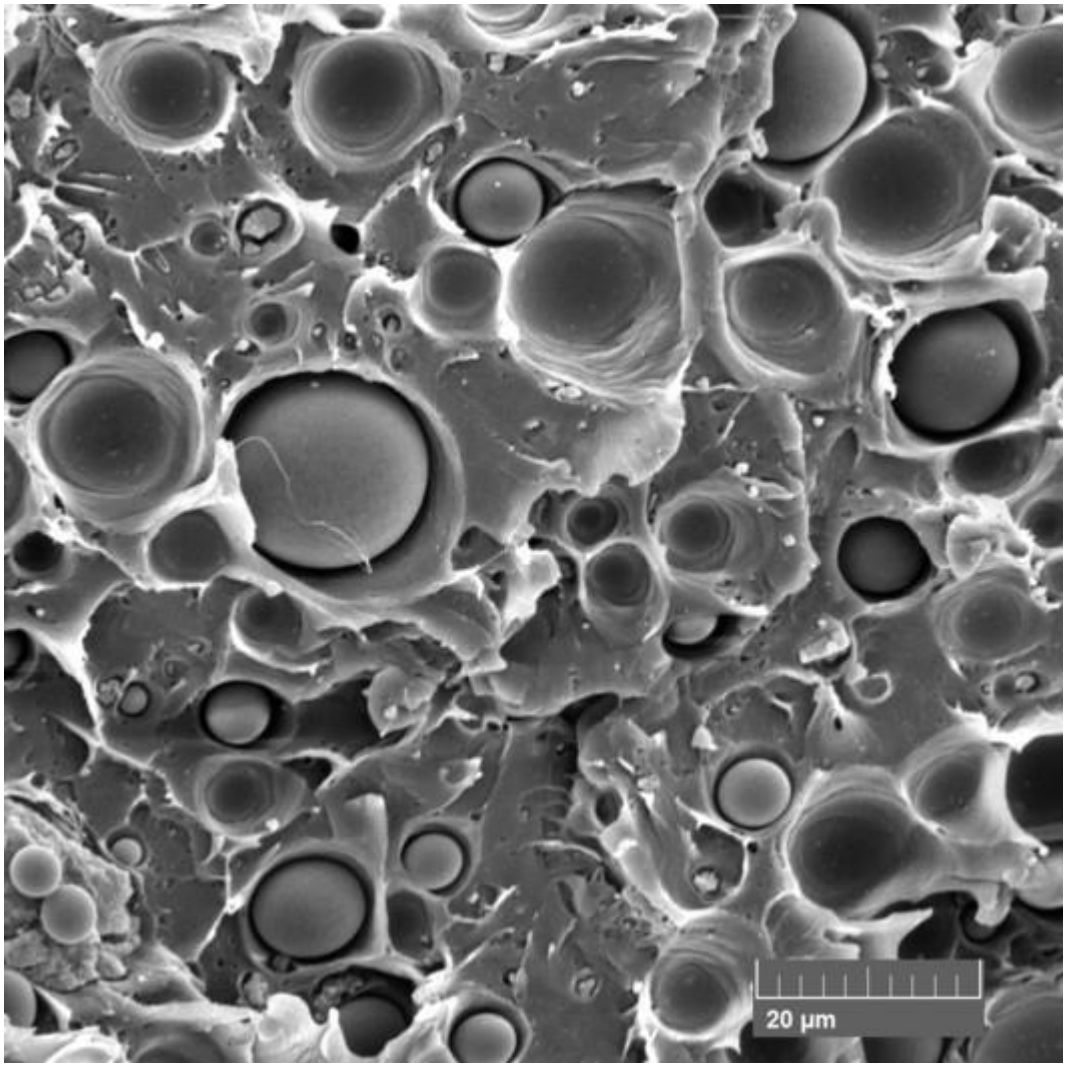

Figure 1. Scanning electron micrograph of the fracture surface of elongated specimen PLA/PE-HD 90/10 + 5 % TiO_2 after the failure.

This work has been supported by European Regional Development Fund under the project: OS-Mi (KK.01.1.1.04.0006) and by Croatian Science Foundation under the projects DOK-2020-01-8955 and DOK-2021-02-5999.

SELECTED LECTURES

(Life Sciences)

Peripheral chromosomes positioned behind the spindle poles are prone to chronic unalignment in tumour cell lines

Kruno Vukušić (1), Snježana Kodba (1), Patrik Risteski (1), Iva M. Tolić (1)

1) Ruđer Bošković Institute, Division of Molecular Biology, Zagreb, Croatia

Mitosis encompasses series of ordered and controlled events that result in a precise separation of sister chromatids into two daughter cells. At a core of mitotic fidelity is the process of congression, movement of chromosomes towards the equatorial plane of the mitotic spindle. At metaphase in a healthy cell, most chromosomes have successfully aligned at the spindle equator. However, by large-scale and long-term live-cell imaging of several human cell lines from prophase to telophase, we observed that congression occasionally fails, resulting in chronically unaligned chromosomes, which remain close to the pole and induce substantial mitotic delays. We observed that the frequencies of unaligned chromosomes range from 42-22 % in tumour U2OS and HeLa cells, to 1.9 % in non-transformed RPE-1 cells. Furthermore, in 4 % of tumour cells, the unaligned chromosome remained at the pole through mitosis, resulting in aneuploidy. However, it is unknown whether there is any intrinsic spindle-based bias that would predispose certain chromosomes to unalignment and consequentially missegregation. Here we show, by tracking the movements of chronically unaligned chromosomes in U2OS cells, that they originated mainly from the nuclear periphery during prophase, contrary to pairs that rapidly aligned. Furthermore, unaligned chromosomes were preferentially positioned behind their respective spindle poles at the beginning of mitosis, indicating that passage across the polar region can drastically impede the speed of chromosome congression in tumour cells. Interestingly, during metaphase, unaligned chromosomes were characterized by persistent positions behind and near their respective poles, indicating that incapacity to congress is often combined with a high extent of minus-end directed movements during metaphase. Furthermore, unaligned chromosomes have severely reduced stability within the metaphase plate after the attempt of congression, compared to pairs that aligned during prometaphase. Even after successful alignment, unaligned chromosomes are repeatedly followed by persistent laggards, whereas chromatin bridges are not related to this phenomenon, indicating a possible connection between late alignment and a higher incidence of merotelic attachments. Lastly, by using stimulated emission depletion (STED) super-resolution microscopy, we showed that most laggards during anaphase in U2OS cells are indeed characterized by unresolved complex merotelic attachments. In conclusion, peripheral chromosomes located behind the spindle poles at the beginning of mitosis are particularly prone to chronic unalignment, which is harmful for mitotic fidelity.

Keywords: aneuploidy, chromosome missegregation bias, mitosis, live-cell imaging, super-resolution microscopy

This research was supported by the European Research Council (Synergy Grant, GA Number 855158). We thank Geert Kops and Sjoerd Klaasen for their work in developing the chromosome missegregation bias concept.

Rac1 dynamics in *Dictyostelium* cells: A combined experimental and theoretical approach

Marko Šoštar (1), Maja Marinović (1), Vedrana Filić (1), Nenad Pavin (2), Igor Weber (1)

1) Ruđer Bošković Institute, Division of Molecular Biology, Zagreb, Croatia

2) University of Zagreb, Faculty of Science, Zagreb, Croatia

Small Rho GTPases regulate and coordinate a variety of processes driven by the actin cytoskeleton. We are particularly interested in examining and understanding their role in cell motility. As a model organism, we use *Dictyostelium discoideum* amoebas, which are capable of the fastest reorganization of the actin network among eukaryotic cells, and can reverse polarity within one minute. This makes them suitable for testing conceptual models that connect Rho signalling with cell morphodynamics during motility. Here, we present combined experimental and theoretical approaches to investigating the intracellular dynamics of the small GTPase Rac1 and its effector DGAP1. Because *Dictyostelium* cytoskeleton remodels rapidly, in order to monitor its constitutive and regulatory proteins in living cells it is crucial to use fluorescent biosensors able to follow these fast dynamics and capable to endure prolonged imaging at high recording rates. We developed a fluorescent probe highly specific for the active form of Rac1 with a low cytoplasmic background signal, which enables to resolve small variations of Rac1 activity in the cell cortex. Spatio-temporal distributions of fluorescently labelled active Rac1 and DGAP1 were recorded in living cells by point-scanning confocal microscopy, processed by QuimP software, and analyzed by principle component analysis. We observed the occurrence of three main types of patterns: standing waves, travelling waves and stably polarized states. Besides these common patterns, we noticed that the dynamics of Rac1 activity and DGAP1 were mostly anti-correlated, with the exception of rare stationary patterns with overlapping distributions. We also discuss approaches to mathematical modelling of the observed dynamics and compare the results of a reaction-diffusion model to experimentally obtained distributions of Rac1 activity and DGAP1 localization. Our reaction-diffusion model with simple mass action kinetics was able to reproduce almost all experimentally observed dynamical patterns.

Keywords: small GTPases, actin cytoskeleton, cell motility, reaction-diffusion model

Reactive oxygen species (ROS) confocal laser scanning imaging in TROL mutants

Ena Dumančić (1), Hrvoje Fulgosi (1)

1) Ruđer Bošković Institute, Zagreb, Croatia

Photosynthesis is the process in photoautotrophic organisms that converts light energy into chemical energy. The very important part of this process is the transfer of electrons from reduced ferredoxin to NADP+, which is catalyzed by the flavoenzyme Ferredoxin-NADP+ oxydoreductase (FNR) [1]. Binding of the FNR to photosynthetic membranes of many vascular plants is assisted by the thylakoid rhodanase-like protein (TROL) [2]. Within my PhD project, I am examining the influences of the TROL-FNR protein complex on electron transport and ROS scavenging, which indicates a protective role of this complex. I will carry out the detection and visualization of ROS using fluorescent probes (DHE for superoxides, SOSG for singlet oxygen molecules, spy-LHP for peroxides) for staining ROS molecules and confocal laser scanning microscopy technique for detecting them. This experiment will show the presence and propagation of ROS molecules in chloroplasts and whole plant cells. Imaging is performed using a CCD camera. *Arabidopsis thaliana* (L.) Heynh was used as a model plant; wild type (WT), TROL KO, ΔRHO mutants were grown under normal humidity and in arid conditions. The main goal of these experiments is to demonstrate how TROL-FNR complex affects electron transport, ROS scavenging, management and distribution of high energy electrons in energetic processes of photosynthesis [3] under normal soil humidity conditions and under abiotic stress conditions, in this case drought, and how deficiency of some components of this complex affects the efficiency of the TROL-FNR pair. The research will contribute to the understanding of the behavior of plants under severe stress conditions.

Keywords: microscopy, imaging, ROS, TROL

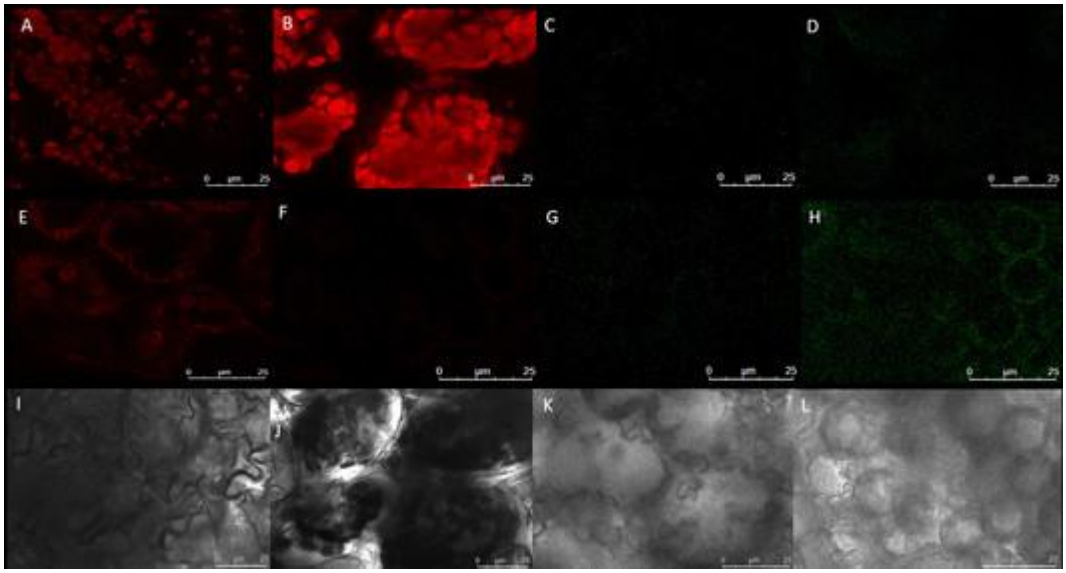

Figure 1. ROS imaging WT. A,E ctrl, SOSG normal humidity autoflr B,F ctrl, SOSG arid conditions autoflr C,G ctrl, SOSG normal humidity, D,H ctrl, SOSG arid conditions, I,J ctrl chl normal humidity, arid conditions K,L SOSG chl normal humidity, arid conditions. Scale bar, 25 μm.

References:

1. M. Lintala et al., Plant J. 70 (2012) 809-817.
2. S. Jurić et al., Plant J. 60 (2009) 783-794.
3. L. Vojta et al., Sci. Rep. 5 (2015) 1-9.

Marine microalgae under temperature and salinity stress – insight from AFM study

Tea Mišić Radić (1), Maja Levak Zorinc (1), Nives Novosel (1), Nadica Ivošević DeNardis (1)

1) Division for Marine and Environmental Research, Ruđer Bošković Institute, Zagreb, Croatia

Global climate change is causing an increase in ocean temperature and models predict a possible decrease in salinity of the sea surface layer, which will inevitably affect microalgae. The objective of this study was to investigate the response of three microalgal species (*Cylindrotheca closterium*, *Dunaliella tertiolecta* and *Tetraselmis suecica*) to temperature and salinity stress in terms of growth, surface morphology and physiological activity (extracellular polymeric substance (EPS) release). Structural details of the cell surface and the organization of released biopolymers were studied using high-resolution atomic force microscopy (AFM). Microalgae were exposed to single stressors, temperature fluctuations (12, 18, and 30 °C) and salinity fluctuations (9, 19, 27, and 38 ppt) under controlled laboratory conditions [1]. Regarding cell growth, for *D. tertiolecta* and *T. suecica*, the fastest growth and shortest doubling time were obtained at 18 °C, which was considered a favourable temperature. For *C. closterium*, the fastest growth and shortest doubling time were obtained at 30 °C. All selected microalgae survived salinity from 9 ppt to 38 ppt and had the shortest doubling time and fastest growth at the salinity of 9 ppt. Cell surface morphology did not show specific changes with temperature and salinity variations, but the change was observed in the size of microalgal species. Cells were smaller at higher temperatures and lower salinities. These results are consistent with the commonly known fact that phytoplankton cell size decreases with temperature and also with decreasing salinity. Aside from the change in cell size, loss of flagella was also observed in *T. suecica* cells under hyposaline conditions, which may indicate that the cells are transitioning to the cyst stage. Both temperature and salinity had effects on EPS release. A decrease in salinity, as well as a decrease in temperature, resulted in a significantly higher secretion of biopolymers, which allowed the stressed cells to survive under unfavourable conditions. The results of this study contribute to a better understanding of the effects of various environmental stressors on microalgae at the single-cell level.

Keywords: atomic force microscopy (AFM), climate change, microalgae, salinity stress, temperature stress

References:

1. N. Novosel et al., J. Appl. Phycol. 33 (2021) 1-17.

This work is supported by the Croatian Science Foundation Project "From algal cell surface properties to stress markers for aquatic ecosystems" (IP-2018–01-5840).

Fully automatic whole slide imaging using a faster than real-time image recognition neural network

Krunoslav Vinicki (1), Dora Machaček (1)

1) Faculty of Veterinary Medicine, University of Zagreb, Zagreb, Croatia

In pathology, digitization of glass slides with specimens utilizing whole slide imaging (WSI) opens the door for the use of computer algorithms in image analysis, greatly increasing diagnostic objectivity and productivity [1]. But, despite its numerous advantages, the WSI still faces many technical challenges, especially at high numerical apertures where field of view (FOV) and depth of field (DOF) can be significantly reduced. Under these conditions, artifacts such as tissue folds, ink, dust, and air bubbles can limit the performance of tissue slide scanners, leading to digital slides with out-of-focus areas or even completely failed scans. In modern slide scanners, this problem is solved with different scanning modes, allowing users to choose between automated and semi-automated modes in which area of interest and even focus points can be manually set. In order to make microscope slide scanners more robust to various artifacts (Fig. 1) and enable "one-button" or fully automated scanning, we developed a faster than real-time, 500 fps neural network that can be deployed during the scanning process to decide, depending on what is in the current FOV, should the autofocus and stitching algorithms be engaged for those tiles and in what way. After training our neural network on 64 000 images separated into seven different classification categories, we obtained the accuracy of 97 %, effectively attaining the performance of a human operator.

Keywords: pathology, whole slide imaging, deep learning

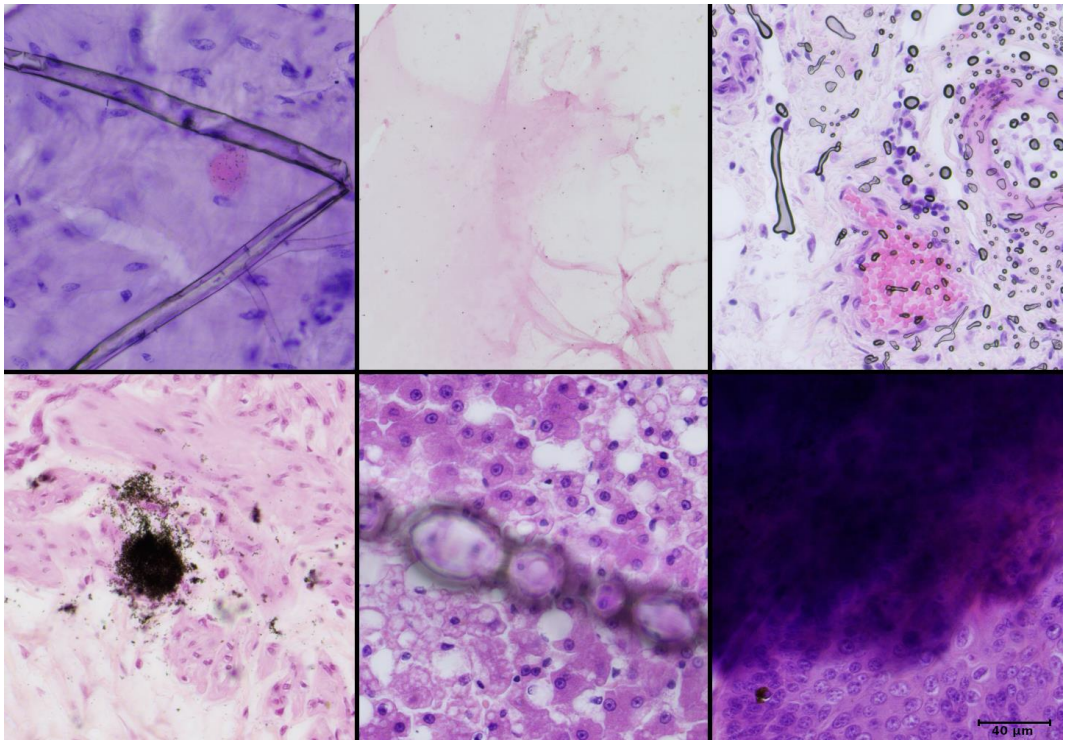

Figure 1. Regions of interest (ROIs) extracted from WSI showing various artifacts.

References:

1. F. Ghaznavi et al., Annu. Rev. Pathol. 8 (2013) 331–359.

Organotypic culture as a 3D model to study Alzheimer's disease in porcine brain

Sowmya Sunkara (1)

1) Division of Cell Biology, Histology and Embryology, Gottfried Schatz Research Center, Medical University of Graz, Graz, Austria

Organotypic culture (OTC) represents a promising method to study neurodegenerative diseases with the advantage of preservation of original architecture and connections. Counter to the classical slice cultures from model animals, we established Alzheimer's disease (AD) condition *ex vivo* in the hippocampus region of the porcine brain for our initial trials. The three-dimensional tissue culture of 160 µm thickness was treated with amyloid beta oligomers ($A\beta O_{1-42}$) and incubated for 3-5 days against a control to simulate AD. We designed a simple protocol to generate oligomers from the amyloid beta peptide prior to our treatments. Using both light microscopy and electron microscopy, we observed that the 3D architecture and the neuronal connectivity of the porcine brain sample is well-maintained, mimicking the *in vivo* system. We compared the morphology of the samples obtained from post-mortem porcine samples with OTC samples and found that the cell integrity and the neuronal connections are viable, and the cells are in an active state. There was no sign of autolysis and no dark spots were observed in the slices, indicating that the slices were respectively healthy and without any contamination. The slices exposed to $A\beta O_{1-42}$ polymerised and formed aggregates and displayed a mesh-like appearance in the extracellular matrix and in axon terminals when observed in electron microscope. We observed a few fibrils inside the axon terminal, which conforms to the studies that Aβ enters inside the axon terminals as the disease progresses. From this, we conclude that OTC is a suitable and time-saving model to study Alzheimer's disease, especially due to the preserved composition of diverse cell types, including the blood-brain barrier. Previous studies have shown that Aβ affect the neuronal connections via disturbing the synapses [1]. Our immediate follow-up studies include quantifying the synapses in $A\beta O_{1-42}$ treated slices to understand the effect of $A\beta O_{1-42}$ on neuronal communication in AD. We plan to switch to human brain samples and replicate the same, after establishing in a porcine model.

Keywords: organotypic culture, Alzheimer's disease, porcine model

References :

1. B.C. Karisetty et al., Front. Mol. Neurosci. 13 (2020) 577622.

This project is funded by the Austrian Science Fund (FWF – Der Wissenschaftsfonds).

Segmentation of 3D SEM images of neurons: pre-processing steps

Snježana Radulović (1), Lucie Chalet (2), Benjamin Gottschalk (3), Stefan Wernitznig (1), Armin Zankel (4), Gerd Leitinger (1)

1) Gottfried Schatz Research Center, Division of Cell Biology Histology and Embryology, Medical University Graz, Graz, Austria

2) University of Franche Comté, Besançon, France

3) Gottfried Schatz Research Center, Division of Molecular Biology and Biochemistry, Medical University Graz, Graz, Austria

4) Institute of Electron Microscopy and Nanoanalysis, NAWI Graz, Graz University of Technology and Graz Centre for Electron Microscopy, Graz, Austria

Traditionally, neuron reconstructions from serial EM micrographs and synapses localizations are done manually, which is extremely time-consuming [1,2]. Currently used, semi-automatic selection tools for segmenting are faster compared to manual selection. In order for those tools to work properly, noise reduction is necessary, while keeping membrane integrity and structural features of synapses preserved at the same time. We developed pre-processing steps to make the micrographs suitable for semi-automatic selection. Serial block-face scanning electron microscopy was used to produce serial electron micrographs of identified neurons of the locust, *Locusta migratoria* (Fig. 1A). Obtained stacks were sequentially processed using Image J software. First, a histogram matching algorithm was used to homogenize brightness levels, followed by a low pass Fourier transform band-filter to isolate small structures like cell membranes, a rolling ball algorithm to give the cell membranes a higher contrast, and an automated Otsu threshold. The thresholded stacks were analyzed with the particle analyzer to filter out small irregular components. In parallel, the particle analyzer was used once more with settings that enabled keeping the large particles such as mitochondria. The result was subtracted from the result of the first round with the particle analyzer. Second, mitochondria were removed; for this, the histogram-matched stacks were filtered with a median filter after a contrasting step, followed by Huang´s auto threshold to get a binary image (that contained the mitochondria) which was subtracted from the first preprocessing step. The first step successfully removed noise and small structures, but mitochondria attached to the membranes were still visible, compromising the results of segmenting (Fig. 1B). During the second preprocessing step, most of the structures inside the cells were deleted. However, at certain locations the membranes appeared discontinuous. Nevertheless, combining both steps with fast selection tools significantly enhanced segmentation efficiency compared to a traditional manual approach (Fig. 1C). In summary, pre-processing can improve the accuracy and efficiency of segmenting algorithms.

Keywords: segmentation, neuron, Image J, 3D SEM

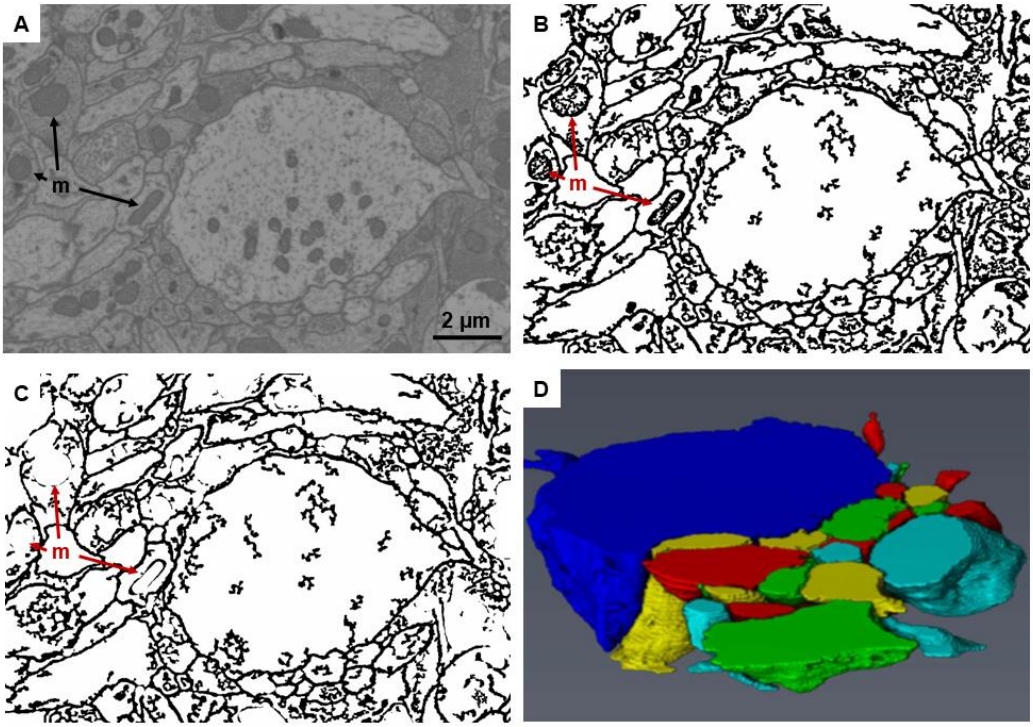

Figure 1. A) Original micrograph. B) First pre-processing step: contrasting membranes and filtering out small irregular components. C) Second pre-processing step: removing mitochondria. D) 3D reconstruction. m – mitochondria.

References:
1. F.C. Rind and P.J. Simmons, Trends Neurosci. 22 (1999) 215-220.
2. R.D. Santer et al., J. Neurophysiol. 95 (2006) 3391-3400.
3. S. Wernitznig et al., J. Neurosci. Methods. 264 (2016) 16-24.

Supported by the Austrian Science Fund FWF (P 32058 and P 32376 to GL and SW).

Expression of NF, GFAP, and dendrin in the brain of small-spotted catshark *Scyliorhinus canicula* L.

Ivana Restović (1), Marko Vučemilo (2), Mia Obad (2), Nives Kević (2), Nela Kelam (3), Anita Racetin (3), Ivana Bočina (2)

1) Faculty of Humanities and Social Sciences, University of Split, Split, Croatia

2) Faculty of Science, University of Split, Split, Croatia

3) School of Medicine, University of Split, Split, Croatia

In the present study we reported the expression of neurofilaments (NFs) and glial fibrillary acidic protein (GFAP) and for the first time the expression of dendrin in the brain of small-spotted catshark *Scyliorhinus canicula* L. Small-spotted catshark is a well-known model species of cartilaginous fishes. Its developing telencephalon shows more similarities to those of mammals than to those of bony fishes, amphibians, and birds. Neurofilaments (NFs) are members of the intermediate filament protein family which are essential for the formation of the neuronal cytoskeleton. GFAP is expressed by numerous central nervous system (CNS) cell types, including astrocytes and ependymal cells during development. Dendrin, a proline-rich protein known as a neuron and renal protein, has an important role in synaptic plasticity and as a postsynaptic component has a significant impact in modulating synaptic cytoskeleton. The tissues of sectioned forebrain, midbrain, and hindbrain of ten specimens of *Scyliorhinus canicula* L. fresh-caught in the Adriatic Sea were studied using histochemical and immunofluorescence techniques. Hematoxylin-eosin and Mallory staining were used to identify the histological structure of these brain parts. These sections were observed using a Leica DM 3000 LED microscope (Leica Microsystems, Germany). For immunofluorescence, the sections were incubated overnight with primary antibodies according to their own protocols followed by incubation with suitable secondary antibodies for one hour. The nuclei were stained with DAPI. The images were captured with epifluorescence microscope Olympus BX51 (Olympus Corporation, Tokyo, Japan). The present study has shown that morphological and histochemical composition of the forebrain and midbrain have many similarities. Most of the neuronal tissue are neuronal and glial cells bodies surrounded by neuropil. In the cerebellum, three layers could be distinguished: the most superficial layer, the middle one called the Purkinje cells layer and the deepest granular one. The other part of the hindbrain, the medulla oblongata, histologically resembles the granular cerebellum layer. NF, GFAP, and dendrin in the catshark's brain are highly expressed in all parts of the brain except in the medulla oblongata where the expression pattern was weaker for all investigated proteins. Morphological and histochemical analysis of the small-spotted catshark's brain confirmed the great potential of this cartilaginous fish not only as a model for evo-devo studies but as a model in the adult stage that shows more similarities to mammals than it was thought, with the special emphasis on the distribution of dendrin in the non-mammalian brain for the first time.

Keywords: neurofilaments, GFAP, dendrin, immunofluorescence, small-spotted catshark

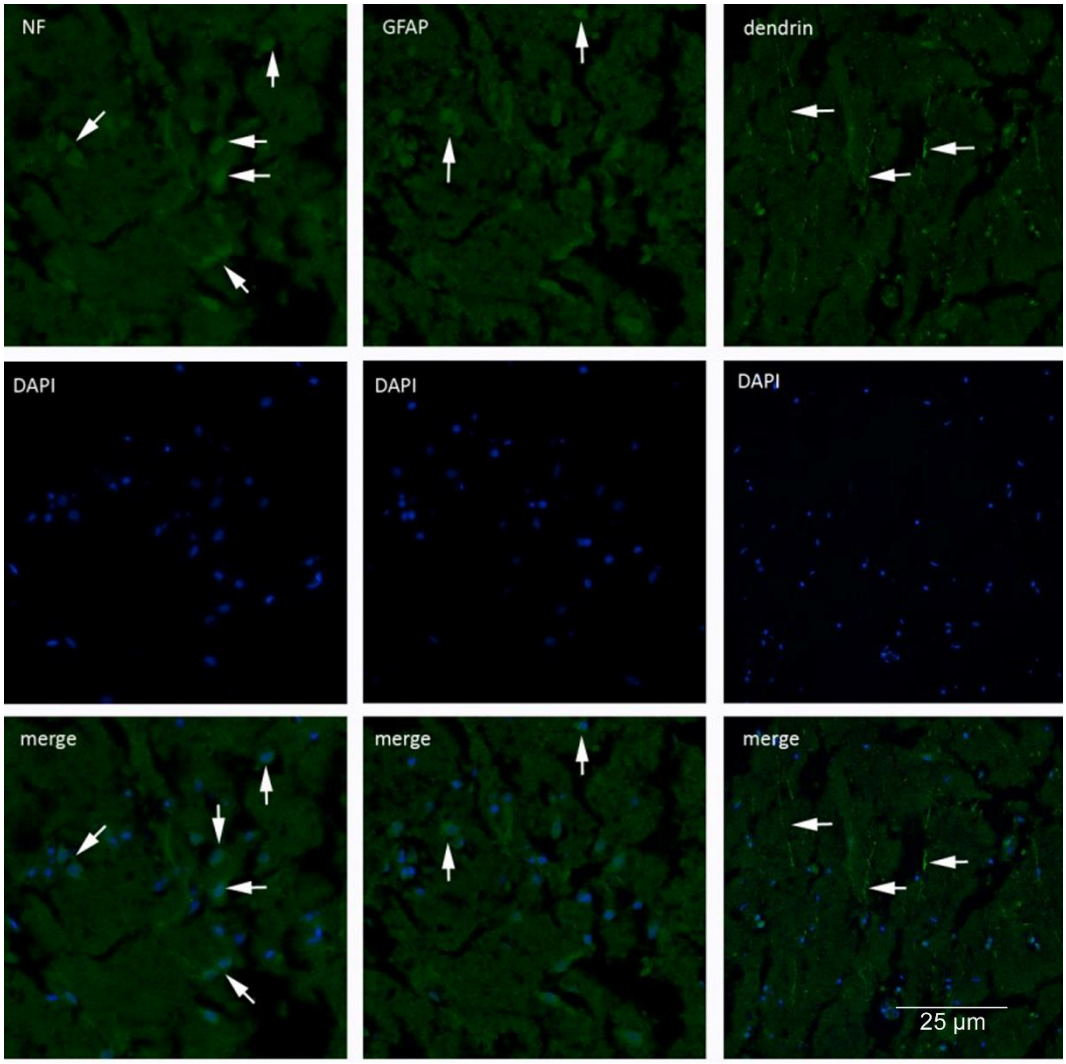

Figure 1. Expression of the NF, GFAP and dendrin in the small-spotted catshark forebrain.

References:
1. M. Kalman et al., Anat. Embryol. 204 (2001) 59-80.
2. A. Docampo-Seara et al., Brain Struct. Funct. 224 (2018) 33-56.
3. J. Kremerskothen et al., J. Neurochem. 96 (2006) 1659-1666.

Thick and cleared – Blood vessels and neurons can be visualized in the cleared mouse brain using inverted fluorescence microscopy

Dominik Hamer (1), Daniela Petrinec (1), Monika Berecki (1), Laura Skukan (1), Srećko Gajović (1)

1) Croatian Institute for Brain Research, University of Zagreb School of Medicine, Zagreb, Croatia

To visualize whole organs or whole body of humans or animals, different imaging techniques can be applied. Novel light sheet fluorescence microscopy (LSFM) allows to visualize large samples, in particular whole organs of the laboratory animals. The variety of tissue clearing procedures are used for achieving sample transparency and the visualisation is based on the labelling of structures of interest by fluorescence. The main goal of this research was to image the structures in the cleared mouse brain with a special task to verify if the clearing procedure can be beneficial even if "classical" easily available fluorescent microscopes were used for sample visualisation. The inverted fluorescence microscope (The EVOS® FL Auto Imaging System, ThermoFisher Scientific) was used as a test instrument for this purpose. Previously naturally transparent parts of mouse embryos were imaged using fluorescence microscopy by our group [1,2]. A fluorescent marker was applied to the brain of live mouse by stereotaxic injection. The fluorescent staining 10 % fluorescein solution (Fluorescite, Alcon) and Isolectin GS-IB4 from *Griffonia simplicifolia*, Alexa Fluor 568 Conjugate (Invitrogen) was injected by help of stereotaxic apparatus (David KOPF Stereotaxic Instrument Small Animal Frame 5001 H7000). Moreover, mouse brains were isolated from two months old animals (Thy1-YFP-16 strain), which naturally expressed yellow fluorescent protein in neurons. As a third approach, blood vessel visualization *Lycopersicon esculentum* Lectin Texas Red (Invitrogen) was injected in the left heart ventricle of living mouse (Fig. 1). In all three cases the mice were perfused by 1× PBS and 4 % formalin solution and subsequently cleared. For whole brain tissue clearing, three methods were used: ECi (optical clearing using ethyl-cinnamate), iDISCO (immunolabeling-enabled threedimensional imaging of solvent-cleared organs) and PEGASOS (polyethylene glycol-associated solvent system). Cleared mouse brain samples were cut on approximately 1 mm thick slices using mold (Alto Acrylic 1 mm Mouse Brain Coronal 40-75gm, CellPoint Scientific), mounted subsequently on the glass slides in the drop of the final clearing solution, covered by coverslips, and imaged using inverted fluorescence microscope. The ECi method was preferred as the protocol for clearing lasted only one day and used chemicals were nontoxic. iDISCO clearing technique made brain slices brittle and difficult to handle. Even without using LSFM, it was possible to visualize fluorescently labelled structures in thick samples. It still remains to be clarified if this type of imaging is suitable not only for qualitative description of the samples, but also for quantitative measurements. In conclusion, the clearing of mouse brain produces thick slices suitable as well for imaging and analysis by fluorescence microscopy.

Keywords: blood vessels, neurons, clearing techniques, mouse brain, fluorescence microscopy

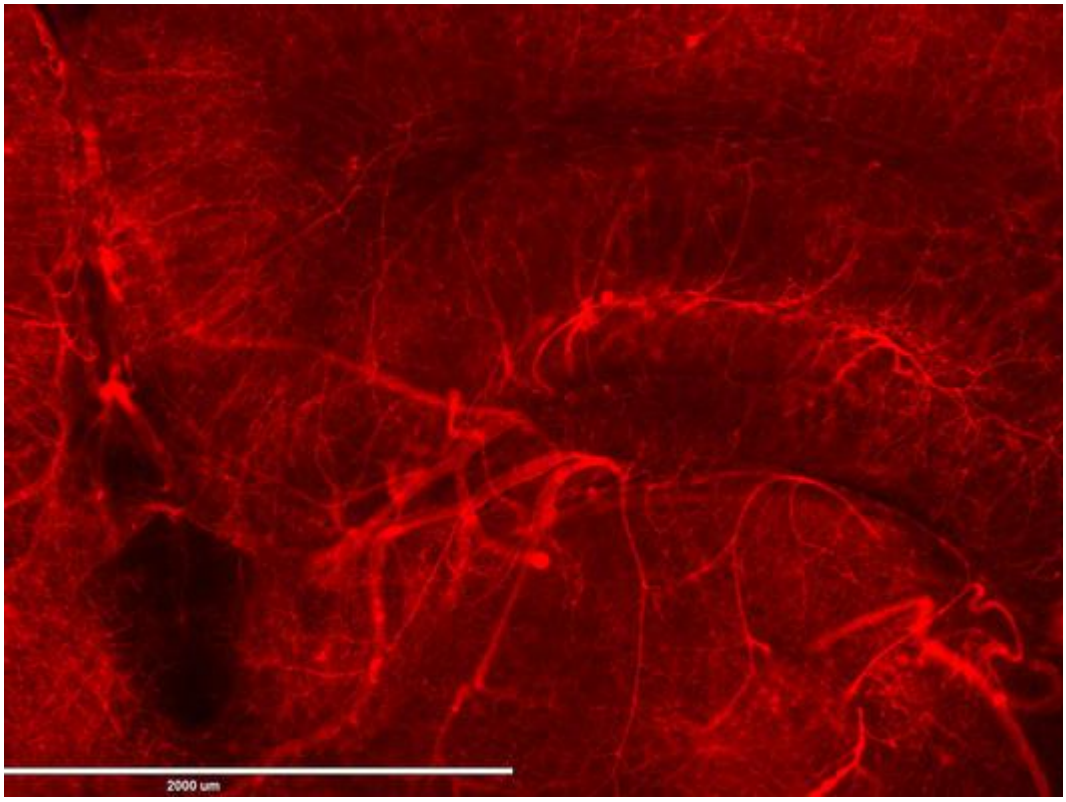

Figure 1. Blood vessels in cleared mouse brain slices (approximately 1 mm sample slice, brain clearing method ECi) labeled with *Lycopersicon esculentum* Lectin Texas Red (Invitrogen) using inverted fluorescence microscope.

References:
1. I. Alić et al., Neurosci. Lett. 634 (2016) 32–41.
2. M. Žižić Mitrečić et al., Cells Tissues Organs 192 (2010) 85–92.

Structural characteristics of femoral arteries in wild-type and Tff3 knock-out mice on standard and high-salt diet

Nikola Bijelić (1), Nataša Kozina (2), Edi Rođak (1), Iva Bazina (3), Kate Šešelja (3), Mirela Baus Lončar (3), Tatjana Belovari (1), Ivana Jukić (2), Ines Drenjančević (2)

1) Department of Histology and Embryology, Faculty of Medicine Osijek, Josip Juraj Strossmayer University of Osijek, Osijek, Croatia

2) Department of Physiology and Immunology, Faculty of Medicine Osijek, Josip Juraj Strossmayer University of Osijek, Osijek, Croatia

3) Ruđer Bošković Institute, Department of Molecular Medicine, Zagreb, Croatia

Trefoil factor family 3 (Tff3) protein is a small secretory peptide that promotes angiogenesis. Microvessel density in some malignant tumors is dependent upon Tff3 expression [1,2]. The effect of Tff3 peptide deficiency on the vascular response to a high-salt diet has not been thoroughly investigated yet. Recent research on mice showed that the lack of the *Tff3* gene was partly protective regarding structural changes of the aorta in mice on a high-salt diet. Aortae of Tff3 knock-out mice had thicker tunica media and thinner tunica adventitia than wild-type mice; mechanisms behind this phenomenon are still unknown [3]. The aim of this research was to examine the structural characteristics of femoral arteries in wild-type and Tff3 knock-out mice on standard or high-salt diet. Femoral arteries from 22 mice were isolated, fixed in 4 % paraformaldehyde and paraffin-embedded. Histological slides 6 μm-thick were prepared and stained using picrosirius red and orcein staining techniques. Animals were divided into four groups (wild-type and Tff3 knock-out mice on standard or high-salt diet). Area and diameter of the femoral artery, its lumen, wall, media, and adventitia were measured, as well as the area occupied by collagen and elastin. Free and open-source image manipulation and/or analysis programs GIMP and FIJI were used for image preparation and analysis. Femoral arteries exhibited normal morphology in all groups when examined using bright-field microscopy. No significant differences were found in the measured morphological properties of the femoral arteries, such as wall thickness, artery and lumen radius, wall to lumen radius and area ratio, share of collagen and elastin. Using Tff3 knock-out animals to study the effects of a high-salt diet on blood vessel function and morphology is a new area of research. More studies are needed to elucidate the effect of Tff3-deficiency in this experimental context. For example, research on large elastic and mid-size muscular arteries was performed until now, however, small resistance blood vessels should be also investigated, since they are important in the regulation of systemic blood pressure.

Keywords: femoral artery, morphological and microscopic findings, Tff3, high-salt diet

References:
1. A.R.H. Ahmed et al., Am. J. Pathol. 180 (2012) 904–916.
2. N. Bijelić et al., Southeast Eur. Med. J. 4 (2020) 20–27.
3. N. Kozina et al., Int. J. Mol. Sci. 20 (2019) 5188.

This work was supported by Croatian Science Foundation grant IP-06-2016-2717 and "Young researchers career development project – training of doctoral students" of the Croatian Science Foundation funded by the European Union from the European Social Fund (I. Bazina).

SELECTED LECTURES

(Materials Science)

Decoding the multi-spatial-scale structure of high-entropy alloys by electron microscopy

Andreja Jelen (1), Stanislav Vrtnik (1), Primož Koželj (1), Sheng Guo (2), Guim Hwanuk (3), Kim Hae Jin (3), Anton Meden (4), Janez Dolinšek (1)

1) Jožef Stefan Institute, Ljubljana, Slovenia

2) Chalmers University of Technology, Göteborg, Sweden

3) Korea Basic Science Institute, Daejeon, Republic of Korea

4) University of Ljubljana, Faculty of Chemistry and Chemical Technology, Ljubljana, Slovenia

High-entropy alloys (HEAs) represent novel metals-based materials with complicated microstructure, where at least five different chemical elements, all in majority concentrations, are mixed on a simple crystal lattice at the atomic level (Fig. 1 d). Likewise, the materials are usually comprised of more than one phase on different microscopic levels, ranging from 10 nm to 1 mm. The complex atomic and phase structure, together with the choice of the elements and their concentrations, determine the physical properties (magnetic, electric and thermal) of the HEAs, which are usually not the compositional average of physical properties of the constituent phases [1-3]. For complete microstructural investigation of HEAs, the following electron microscopes with corresponding techniques were used: scanning electron microscope (SE and BSE imaging, EDS, EBSD), transmission electron microscope (HAADF, EDS) and focused ion beam (channeling cont.). In order to interpret the physical properties as accurately as possible, the microstructure has to be known at different orders of magnitude (multi-spatial-scale), using different types of electron microscopes (correlative microscopy) that enable such magnifications. We have investigated the magnetism of $CoCrFeNiZr_x$ (x = 0.4–0.5) eutectic high-entropy alloys (HEAs) in relation to their microstructure by XRD, SEM, magnetization, specific heat and electrical resistivity measurements. Multilayered correlative electron microscopy of $CoCrFeNiZr_{0.45}$ eutectic HEA is presented in Figure 1. with four panels, where each panel gives us a closer look of the same sample from 1 mm range to < nm range [1]. Two structural phases develop in the $CoCrFeNiZr_x$ HEAs, a Zr-free fcc solid solution and a Zr-containing C15 Laves-phase intermetallic compound, where in both phases magnetic transition elements Co, Cr, Fe and Ni substitute each other in a random-like manner. Relative fractions of the two phases change substantially with the Zr concentration. Microstructurally, the two phases form alternatively grown fine lamellar structure typical of eutectic alloys. In addition, bulky dendrites of the fcc solid solution form in large number for the x = 0.40 concentration and in small number for x = 0.45. Two magnetic structures coexist in the $CoCrFeNiZr_x$ HEAs. The first is a disordered ferromagnetic (FM) phase that develops in the interior of large dendrites of the fcc solid solution and in some larger lamellas of this phase. The second phase is superparamagnetic-like and originates from the remaining spins of the fcc solid solution fraction, located at the surfaces and in the interfaces, and from all spins of the C15 Laves-phase fraction. The relative magnitude of the disordered FM-state magnetization with respect to the superparamagnetic magnetization in the samples with different Zr concentration is predominantly determined by the volume fraction of the fcc bulky dendrites.

Keywords: high-entropy alloys, electron microscopy, multi-spatial scale structure

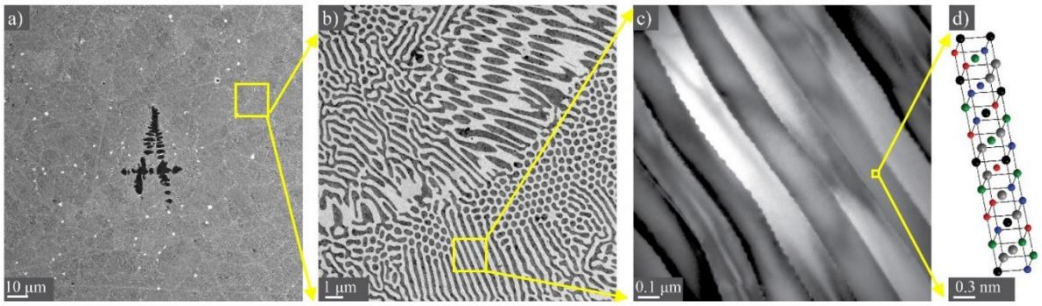

Figure 1. (a) SEM BSE image of $CoCrFeNiZr_{0.45}$ eutectic HEA at low magnification; (b) higher magnification SEM BSE image of the same sample shows finer details of the "grey" area in the panel (a); (c) TEM image shows lamellar structure; (d) schematic representation of HEA on an atomic scale.

References:
1. S. Vrtnik et al., Intermetallics 93 (2018) 122-133.
2. A. Jelen et al., JALCOM 84 (2021) 158115.
3. A. Jelen et al., Mater. Char. 172 (2021) 110837.

The Author thanks Korea Basic Science Institute, Daejeon, Korea, for a Postdoc exchange, and European C-MAC for Young Scientist Exchange at SIMaP, Physics of Metals, Grenoble, France.

Structural and electrical studies of sodium vanadium niobium phosphate glasses and glass-ceramics

Sara Marijan (1), Marta Razum (1), Teodoro Klaser (1), Marijan Marciuš (1), Željko Skoko (2), Jana Pisk (3), Luka Pavić (1)

1) Ruđer Bošković Institute, Division of Materials Chemistry, Zagreb, Croatia

2) University of Zagreb, Faculty of Science, Department of Physics, Zagreb, Croatia

3) University of Zagreb, Faculty of Science, Department of Chemistry, Zagreb, Croatia

Sodium phosphate-based glasses have been proposed as safer, cheaper, and environmentally friendly materials for electrolytes and/or electrode materials in solid-state battery development. Despite their advantages, these glasses usually suffer from relatively low ionic conductivity. Hence, to improve the electrical conductivity of these materials, new research seeks to clarify the relationship between composition, structure, and electrical properties. Numerous studies showed that significant improvement in electrical conductivity can be achieved when one glass-forming oxide is replaced by another that causes non-linear variation of conductivity, a phenomenon known as the *mixed glass former effect* (MGFE). In addition, crystallization of the glasses, brought about either by controlled heat-treatment or by spontaneous crystallization at the border of the glass-forming composition region, has been recognized as another approach to improve overall electrical conductivity, since it leads to glass-ceramic materials with substantially improved electrical features. In the present work, two series of glasses are prepared by conventional melt-quenching technique from the quaternary system Na_2O–V_2O_5–P_2O_5–Nb_2O_5. The content of V_2O_5 is kept constant, while P_2O_5 is gradually replaced by Nb_2O_5, in order to investigate the compositional dependence of the glass-forming tendency and to verify the MGFE in the presence of two conditional glass-formers, V_2O_5 and Nb_2O_5. The PXRD technique is used to confirm the amorphous character of the prepared glasses, as well as to qualitatively and quantitatively study partially crystallized samples formed by spontaneous crystallization during cooling of high content Nb_2O_5 glass melts. The thermal behaviour of the obtained glass(-ceramics) is analyzed by DTA, while their (micro)structural properties are evaluated by SEM-EDS analysis and IR-ATR spectroscopy. On the other hand, their electrical properties are investigated by solid-state impedance spectroscopy (SS-IS) in a wide range of frequencies (0.01 Hz – 1 MHz) and at different temperatures (–90 °C – 240 °C). The relationship between the structural changes that occur upon the exchange of glass-formers along with certain physico-chemical properties of obtained glass(-ceramics) is discussed in detail.

Keywords: glass, glass-ceramic, structural properties, electrical properties

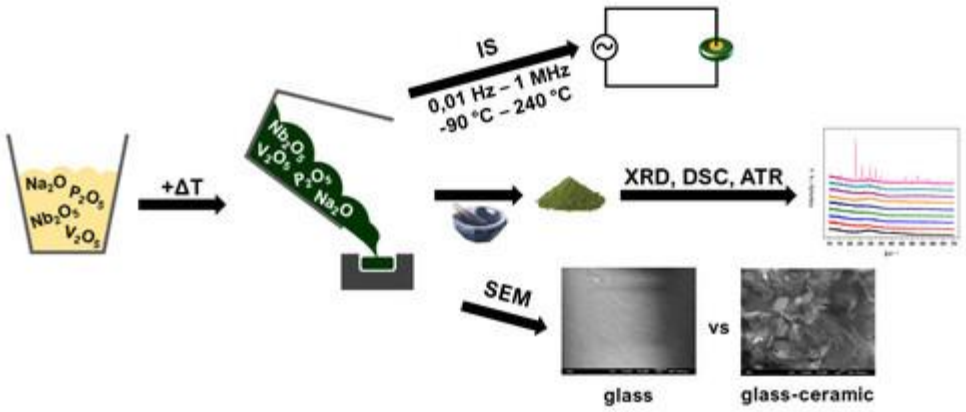

Figure 1. A schematic representation of the study of the quaternary system Na_2O–V_2O_5–P_2O_5–Nb_2O_5.

References:
1. M. Storek et al., J. Phys. Chem. B 120 (2016) 4482–4495.
2. T.K. Pietrzak et al., Nanomaterials 11 (2021) 1321–1345.

This work is supported by the Croatian Science Foundation, POLAR-ION-GLASS project IP-2018-01-5425.

Chemical synthesis of manganite catalysts for simultaneous oxidation of aromatic compounds

Jelena Macan (1), Andreja Žužić (1), Filip Car (1), Vesna Tomašić (1), Andreja Gajović (2)

1) University of Zagreb, Faculty of Chemical Engineering and Technology, Zagreb, Croatia

2) Ruđer Bošković Institute, Zagreb, Croatia

The development of efficient and affordable catalysts for the removal of volatile organic compounds is a pressing issue in environmental protection. Strontium-doped lanthanum manganites, $La_{1-x}Sr_xMnO_3$ (LSMO) have potential as catalysts, since the level of doping influences both the Mn oxidation state and oxygen non-stoichiometry and thus redox properties and possible catalytic activity of LSMO [1]. LSMO catalysts (x = 0, 0.1, 0.2 and 0.3) were prepared by the citrate-nitrate autocombustion (CNA) and coprecipitation synthesis. Pure manganite phases of desired composition were obtained in all cases, as confirmed by energy dispersive spectroscopy, X-ray diffraction and Rietveld refinement analysis. Oxygen content as calculated from occupancy factors matched the one determined by Mohr's salt permanganate titration. Morphology and porosity of prepared catalysts were investigated by scanning electron microscopy and N_2 adsorption/desorption analysis. It was observed that both synthesis methods yield catalysts of similar average pore size diameter and specific surface area, but the pore size distribution differed: CNA-prepared catalysts had a multimodal pore size distribution, while the coprecipitated ones had a single maximum at 4 nm. Furthermore, the LSMO catalysts prepared by the CNA synthesis were voluminous with a porous 'sponge-like' morphology, which is expected to allow a better exchange of reactants and products. Catalytic activity was tested on oxidation of BTEX (benzene, toluene, ethylbenzene and *o*-xylene) gas mixture in the temperature range 373 – 723 K. Catalysts prepared by the CNA method have shown a higher catalytic activity, reaching 100 % conversion in catalytic oxidation of all components except benzene. Temperatures required to reach 50 % conversion were 10 – 50 K higher for catalysts prepared by the coprecipitation method. Catalytic activity was further increased by Sr-doping, as the presence of Mn^{3+}/Mn^{4+} mixed valences increased their reducibility [2]. Samples prepared by coprecipitation had higher oxygen deficiency, which would decrease their reducibility and thus their activity as oxidative catalysts. The catalytic activity of these samples could be improved by controlling their morphology and crystallite size.

Keywords: autocombustion synthesis, coprecipitation, catalytic oxidation, doped lanthanum manganites, volatile organic compounds

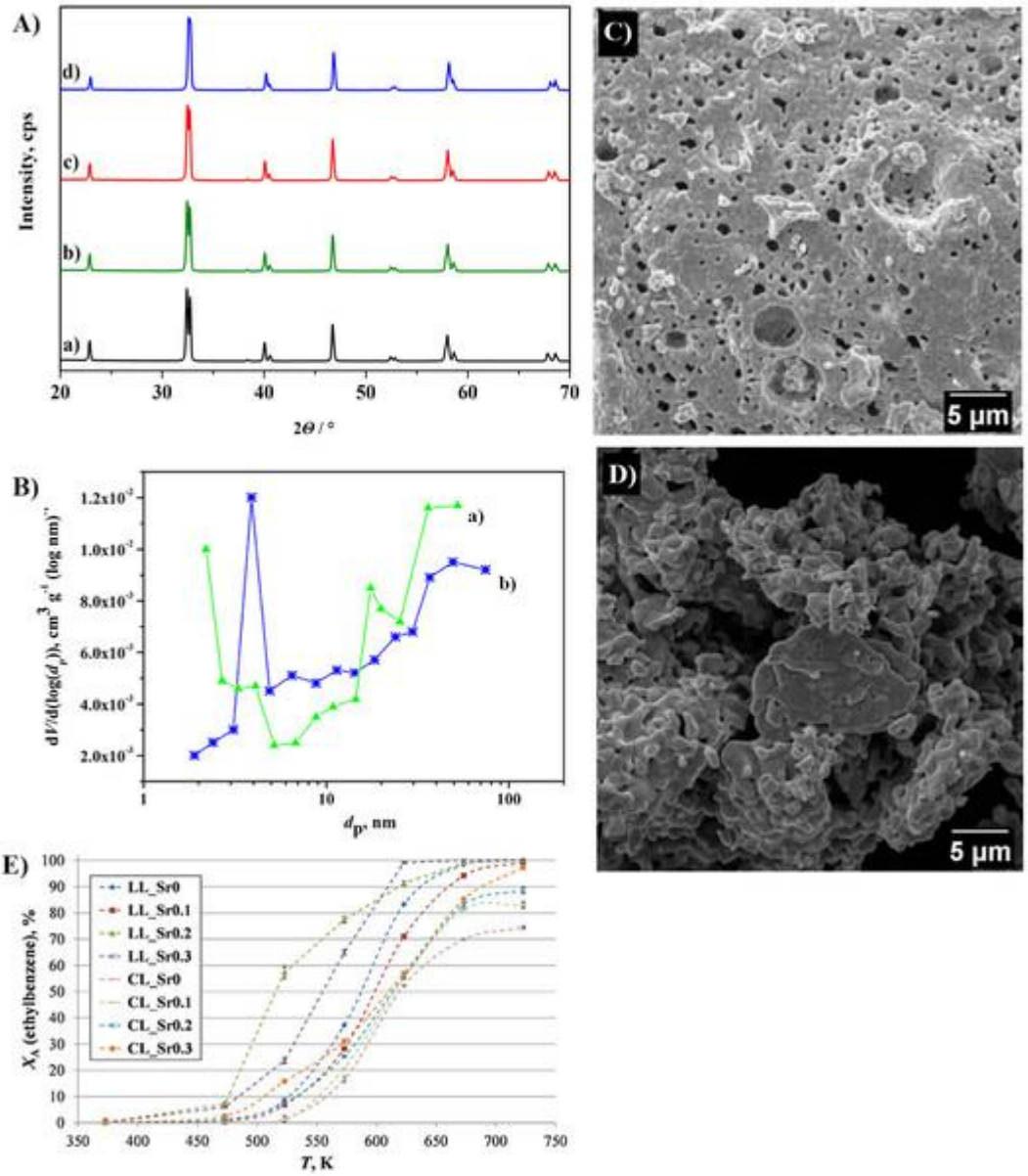

Figure 1. A) XRD of LSMO prepared by CNA. B) Pore size distribution for a) CNA and b) coprecipitation. SEM of LSMO prepared by C) CNA and D) coprecipitation. E) Conversion of ethylbenzene for all samples.

References:
1. A. Žužić et al., Open Ceram. 5 (2021) 100063.
2. E.G. Vrieland, J. Catal. 32 (1974) 415-428.

This work has been supported by Croatian Science Foundation under the projects IP-2018-01-5246 and IP-2018-01-8669, and by the Virtulab project (KK.01.1.1.02.0022) co-funded by the European Regional Development Fund.

Tungsten doped titania porous thin films for photocatalytic purification of water

Tayebeh Sharifi (1), Mario Bohač (1), Vedran Kojić (1), Krešimir Salamon (1), Krunoslav Juraić (1), Andreja Gajović (1)

1) Ruđer Bošković Institute, Zagreb, Croatia

Nanostructured TiO_2 has taken the scientific focus because of the large specific surface area compared to bulk, increased photo-induced reactions, light absorption, photo-generated charge carrier densities, photo-reduction and contact with pollutants in photo-catalysis. TiO_2 nanostructures, in general, have drawbacks in photo-catalysis, since their wide band gaps (anatase E_g = 3.2 eV, rutile E_g = 3.0 eV) limit absorbance of the whole solar spectrum and lead to fast recombination of photo-generated electron–hole pairs. Properties of nanostructured TiO_2 materials can be improved by doping or decorating with other materials. In this work, TiO_2 nanostructures were doped by tungsten with the aim to narrow the band gap of TiO_2. A series of transparent thin films ($W_xTi_{1-x}O_2$) are obtained by co-sputtering tungsten-titanium in different atomic ratios on FTO glass substrates and then anodizing them in ethylene glycol solution containing 0.6 % NH_4F. The morphology and structure of thin films were characterized by SEM, XRD and Raman spectroscopy. Different techniques were used for photo-electrochemical characterization, while photocatalytic activity under solar irradiation was studied using methylene blue as the target pollutant. SEM images (Fig. 1(A)) showed that the $W_xTi_{1-x}O_2$ thin films have a nanoporous structure resembling an open honey-comb construction, while EDS results indicated incorporation of tungsten in the crystal lattice of TiO_2. XRD results showed that anatase is the dominant crystalline phase (Fig. 1(B)); exhibiting major peaks at 25.3° and 38.0° (2θ) which were indexed to the lattice planes of (101) and (004), respectively (ICDD-JCPDS 01-086-1156) [1]. The characteristic Raman bands of anatase were also observed at 146, 397, 513 and 634 cm^{-1} (Fig. 1(C)) which can be assigned to E_g, B_{1g}, doublet of A_{1g}+B_{1g} and E_g modes of the anatase phase, respectively [2]. The incorporation of W slightly decreased the band gap of $W_xTi_{1-x}O_2$. The thin film with 1 % W showed the maximum photocurrent. Photoelectrochemical results also revealed that the charge recombination decreased with increasing the amount of W. Photocatalytic activity was evaluated by degradation of methylene blue solution at different pH, in which higher pH showed enhanced removal rate. The obtained functional properties will be discussed in the view of structural study.

Keywords: $W_xTi_{1-x}O_2$, magnetron co-sputtering, photoelectrochemical, photocatalyst, water treatment

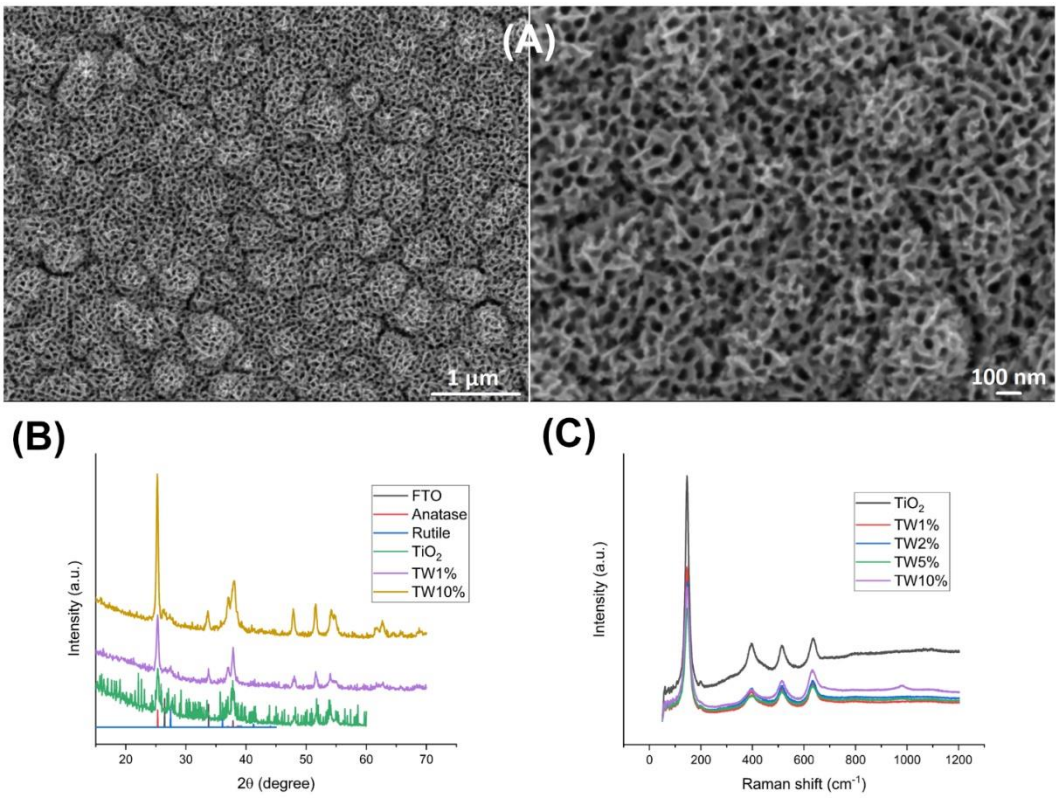

Figure 1. SEM images of thin films after anodization (A), XRD (B), and Raman spectra of $W_xTi_{1-x}O_2$ thin films (C).

References:
1. T. Sharifi et al., Dalton. Trans. 47 (2017) 11593.
2. T. Čižmar et al., Appl. Surf. Sci. 569 (2021) 15102.

Supported by the HrZZ-IP-2018-01-5246, and ERDF project „OS-Mi“, KK.01.1.1.04.0006.

Nanostructured CuO@TiO_2: an efficient photocatalyst for degradation of diclofenac from the aqueous solution

Tihana Čižmar (1), Ivana Panžić (2), Lidija Brkljačić (1), Zaoli Zhang (3), Andreja Gajović (1)

1) Ruđer Bošković Institute, Zagreb, Croatia

2) University of Zagreb, Faculty of Chemical Engineering and Technology, Zagreb, Croatia

3) Erich Schmid Institute of Materials Science, Austrian Academy of Sciences, Leoben, Austria

Environmental pollution and the absence of cost-effective renewable energy resources are acknowledged problems nowadays. Consequently, the development of low-cost, sustainable, clean and energy-efficient technologies is required. Various studies proved that titanium dioxide is environmentally friendly, chemically stable, commercially available, non-toxic and efficient photocatalyst, widely used for water and air purification. Despite these benefits, the energy efficiency of photo-activated processes is limited since the photocatalytic activity only appears under the UV light irradiation. To overcome the limits of TiO_2 and to enhance overall photoactivity, a more efficient photocatalyst, active also under visible light irradiation, has to be synthesized. Various approaches have been proposed to improve TiO_2 photocatalytic activity and reduce the high rate of recombination between photogenerated electrons and holes, including metal/ non-metal doping, surface modifications, semiconductor heterostructures, etc. [1]. Copper is a non-expensive alternative, it can be used for the surface modification of TiO_2 and induce visible-light photocatalytic activity of the photocatalyst in a simple process that does not introduce impurities or vacancy levels into the crystal [2]. Using titanium tetraisopropoxide and copper nitrate as titania and copper sources, a sol-gel method was used to synthesize Cu-modified TiO_2 with different Cu concentrations. The objective of this research was to investigate how CuO modifications can improve the photocatalytic activity of CuO@TiO_2 under the UV-Vis light irradiation. In our work, we showed full degradation of diclofenac [3], a non-steroidal anti-inflammatory drug used to treat pain and inflammatory diseases, and explained the correlations between the photocatalytic activity and the chemical structure of the CuO@TiO_2 photocatalysts.

Keywords: CuO modification, TiO_2, photocatalysis, diclofenac

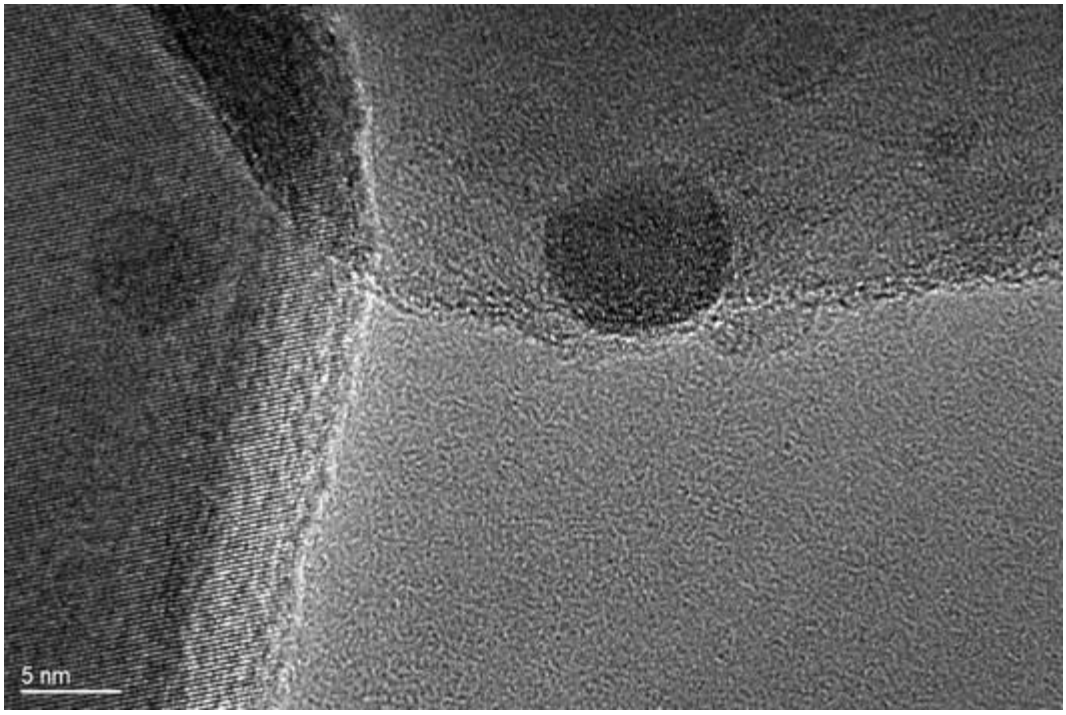

Figure 1. HR-TEM micrographs of $CuO@TiO_2$ sample confirming that CuO nanoparticles are highly dispersed on TiO_2.

References:
1. H. Park et al., J. Photochem. Photobiol. C 15 (2013) 1–20.
2. M.B. Gawande et al., Chem. Rev. 116 (2016) 3722–3811.
3. N. Vieno et al., Env. Intern. 69 (2014) 28–39.

This work was supported by the Croatian Science Foundation under the project HrZZ-IP-2018-01-5246. We thank Dr. Giuliana Aquilanti and Luca Olivi from XAFS beamline at synchrotron radiation facility Elettra, Trieste, Italy.

Surface morphology of textured transparent conductive oxide thin film seen by various probes: visible light, X-rays, electron scattering and contact probe

Krunoslav Juraić (1), Pavo Dubček (1), Mario Bohač (1), Andreja Gajović (1), Sigrid Bernstorff (2), Miran Čeh (3), Davor Gracin (1)

1) Ruđer Bošković Institute, Zagreb, Croatia

2) Elettra-Sincrotrone Trieste, Basovizza (TS), Italy

3) Jožef Stefan Institute, Ljubljana, Slovenia

Fluorine doped tin oxide thin films (SnO_2:F) are widely used as transparent conductive oxide electrodes in thin-film solar cells because of their good electrical and optical properties. Thus, the surface morphology has an important influence on the optical properties of SnO_2 thin films. On a rough surface light is diffusely scattered, which extends the optical path of light inside the active layer of the solar cell and in that way improves light absorption and solar cell conversion efficiency. In this work, we investigated the surface morphology of undoped and doped SnO_2 thin films and its influence on the optical properties of the films. We have compared and analysed the results obtained by several complementary methods for thin film surface morphology investigation: atomic force microscopy (AFM), scanning electron microscopy (SEM), transmission electron microscopy (TEM) and grazing-incidence small-angle X-ray scattering (GISAXS). Based on the AFM, SEM and TEM results, we propose a theoretical model that reproduces well the GISAXS scattering patterns.

Keywords: surface morphology, surface roughness, thin films, tin oxide, light scattering, grazing-incidence small angle X-ray scattering

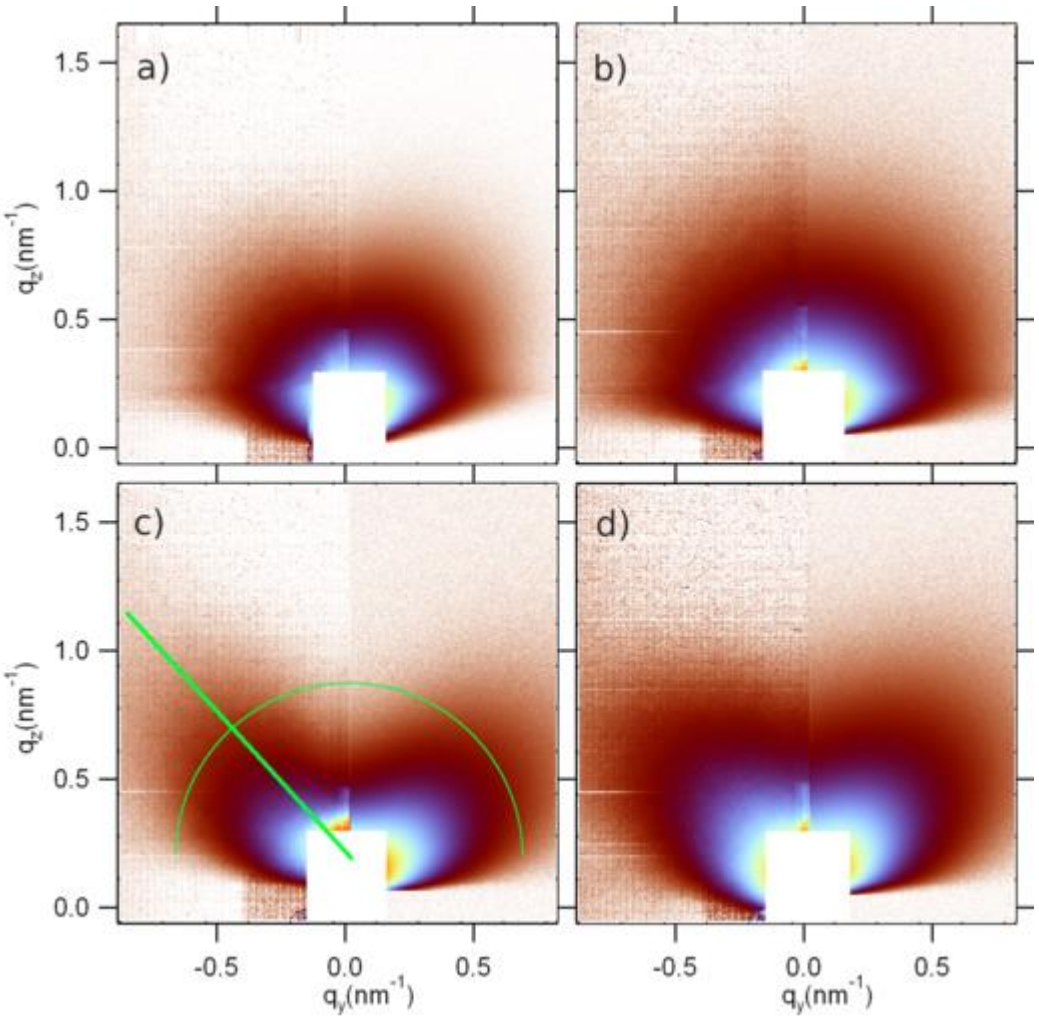

Figure 1. GISAXS pattern for SnO_2 single- and double-layer films on glass substrate for a grazing angle of incidence equal to α_c+0.1°. The left side of each subfigure represents experimentally obtained data, and the right side represents the result of the theoretical model application.

Specific and abstract feature analysis of wide area CVD grown 2D islands using deep learning

Antonio Supina (1), Ana Senkić (1), Antun Lovro Brkić (1), Marko Jaklin (2), Marko Kralj (1)

1) Institute of Physics, Zagreb, Croatia

2) Universidade de Santiago de Compostela, Santiago de Compostela, Spain

Atmospheric pressure chemical vapour deposition (APCVD) is considered to have the most potential for large-scale synthesis of 2D materials such as graphene and transition metal dichalcogenides (TMDs). These atomically thin materials have vast potential for novel applications. Although the synthesis produces samples with sufficient crystallinity and size, shapes and shape-related properties of the crystal islands are non-uniform with respect to lateral position on the growth substrate. Owing to this problem, experienced researchers usually assess the usable areas of the substrate and disregard the remaining crystals. To tackle this problem, we propose a quantifiable method to characterise the sample non-uniformity to reduce its effect or at least to have a more efficient way of property mapping. We utilise a motorized optical microscope to map the complete substrate surface which was used for sample synthesis. The individual images are processed through a series of neural networks which extract desired features, as well as abstract shape and morphological information which are most prominent in the latent space of image data. The extracted information is arranged in a map of features which give us a deeper understanding of different processes occurring on micro scale during APCVD synthesis, thus allowing us to optimise the synthesis to be more homogeneous. We anticipate the proposed method will be extended to other mapping techniques such as AFM, SEM and Raman microscopy.

Keywords: 2D materials, chemical vapour deposition (CVD), neural networks

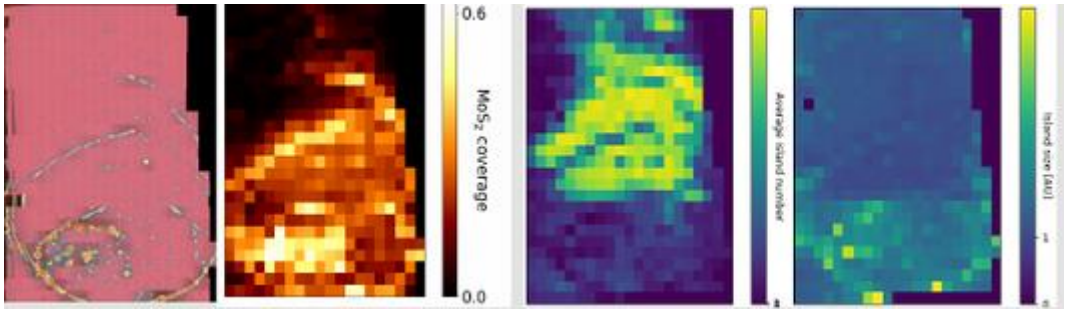

Figure 1. Left-most image shows a stitched map of optical microscopy images of solution-based CVD MoS_2. Following maps show the lateral distribution of coverage, island number and average island size extracted by different neural networks.

References:
1. D. Dumcenco et al., ACS Nano 9 (2015) 4611–4620.
2. B. Han et al., Adv. Mater. 32 (2020) 2000953.
3. J. Redmon et al., arXiv:1506.02640 [cs.CV] (2016).

Large-scale synthesis and electrochemical transfer of borophene

B. Radatović (1), V. Jadriško (1), S. Kamal (1), M. Kralj (1), D. Novko (1), N. Vujičić (1), M. Petrović (1,2)

1) Institute of Physics, Zagreb, Croatia

2) University of Duisburg-Essen, Faculty of Physics, Duisburg, Germany

Large-scale fabrication procedures and mechanical manipulation techniques are crucial for the investigation and technological utilization of 2D materials (2DMs). While for some 2DMs (such as graphene) these challenges have already been addressed in detail, many other 2DMs still require a lot of optimization from the aspect of synthesis and deterministic transfer. Among those materials is borophene, a 2D form of boron, which has a metallic character [1] and holds the potential to serve as a conductive layer in future flexible electronics. Here we perform (i) scalable synthesis of borophene by executing segregation-enhanced epitaxy on Ir(111) substrate, followed by (ii) electrochemical transfer of borophene to an oxide-covered Si wafer. Borazine is used as a source of B atoms, which are dissolved in subsurface layers of Ir at high synthesis temperatures. During sample cooling, B atoms segregate back to the surface and self-assemble into a borophene mesh [2]. The process of B atom dissolution and segregation is tracked in real time by low-energy electron microscope (LEEM) [Fig. 1(a)], and borophene crystallography and morphology are characterized by low-energy electron diffraction (LEED) and *ex situ* atomic force microscopy (AFM). In the transfer process, which includes temporary mechanical support by a PMMA layer, borophene monolayer is electrochemically delaminated from the Ir substrate [3] and placed on a Si wafer. Scanning electron microscopy (SEM) and AFM confirm a successful transfer of millimeter-sized borophene flakes and also reveal nanoscopic modifications and imperfections in the material [Fig. 1(b)]. Preservation of an intrinsic structure of borophene after the transfer is confirmed by means of Raman spectroscopy and density functional theory (DFT) calculations. Our results demonstrate a new route for the fabrication of extended 2D boron layers and their transfer to arbitrary substrates, thus bringing borophene closer to integration into novel devices.

Keywords: 2D materials, borophene, electrochemical transfer

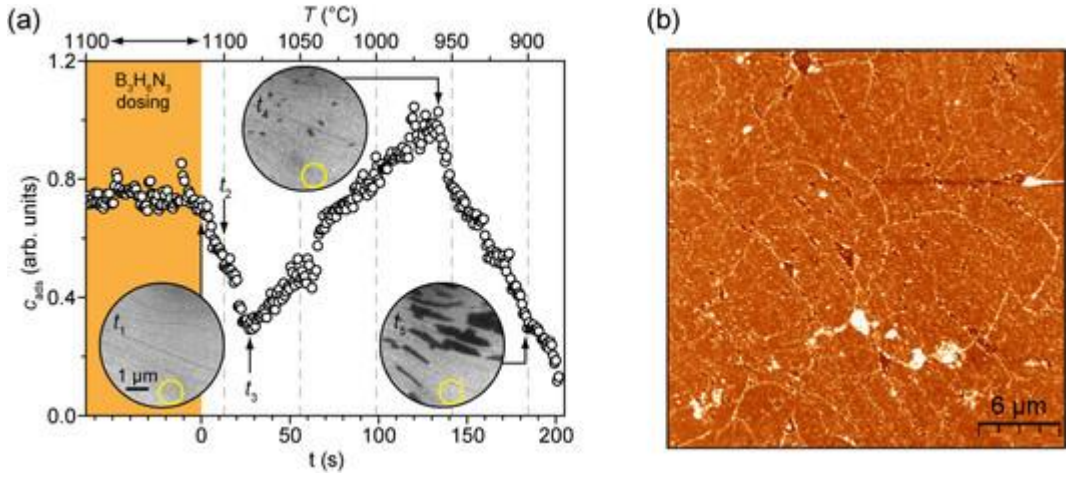

Figure 1. (a) Concentration of adsorbates on the Ir(111) surface as a function of temperature and time. Emerging borophene islands are visible as black patches in the insets. (b) AFM topography of borophene transferred to a Si wafer by using the electrochemical transfer method.

References:
1. B. Feng et al., Phys. Rev. B 94 (2016) 041408.
2. K.M. Omambac et al., ACS Nano 14 (2021) 7421.
3. L. Koefoed et al., J. Phys. D: Appl. Phys. 48 (2015) 115306.

Simultaneous influence of titanate nanomaterials and chitosan on precipitation of calcium phosphate

Ina Erceg (1), Ana–Marija Milisav (1), Vida Strasser (1), Maja Dutour Sikirić (1)

1) Ruđer Bošković Institute, Division of Physical Chemistry, Laboratory for Biocolloids and Surface Chemistry, Zagreb, Croatia

The increased frequency of hard tissue diseases, which commonly can be treated only by implantation, is motivating research of materials' new innovative designs as well as green and low-cost routes of fabrication. In this sense, composites of calcium phosphates (CaPs) with inorganic nanomaterials or organic macromolecules attract special attention. In addition to replacing missing tissue or enabling its regeneration, they can have improved mechanical properties and/or act as a local drug delivery system [1]. In order for these materials to be functional and to rationalize their design, the interactions between CaPs and additives should be understood. This is very often not the case, and success stories are often a result of a more empirical rather than a systematic approach. To fill this void, in this study the simultaneous influence of titanate nanomaterials and chitosan on the precipitation of CaPs was investigated. Titanate nanomaterials are proposed as additives which can improve CaP mechanical properties, while chitosan is biocompatible [2]. To the best of our knowledge, the studies on the precipitation of CaP in the simultaneous presence of two additives are rare. Four different classes of TiNMs, namely nanoparticles (TiNP), nanowires (TiNW), nanotubes (TiNT), and nanoplates (TiNPl), were synthesized by hydrothermal methods, and their composites with CaPs were synthesized by precipitation from solutions. In order to obtain multifunctional composites, chitosan was added simultaneously with TiNM in the precipitation systems. The progress of precipitation was followed by potentiometric measurements. The precipitated composites were characterized by Fourier transform infrared spectroscopy (FTIR), powder X-ray diffraction (PXRD) and scanning electron microscopy (SEM). The obtained results show that precipitation of CaP in the presence of TiNMs and chitosan can be used as a fast and versatile method for the preparation of CaP/TiNM composites. Neither class of additives had an effect on the structure or composition of the formed composites, either added alone or simultaneously. However, an effect on the morphology of the CaPs was observed. The obtained results will provide a deeper insight into the precipitation processes on nanosurfaces, which will enable a rational approach in synthesis of novel composites for hard tissue regeneration and various other applications.

Keywords: calcium phosphates, chitosan, titanate nanomaterials

References:
1. S. Bose et. al., Acta Biomater. 8 (2012) 1401–1421.
2. E.J. Tobin, Adv. Drug Deliv. Rev. 112 (2017) 88–100.

This work has been fully supported by Croatian Science Foundation under the project HrZZ-IP-2013-11-5055 and HRZZ-IP-2018-01-1493.

SEM and EDS analyses of zeolite clinoptilolite water supernatants upon centrifugation

Rumenka Markoska (1), Vedrana Spada (2), Dean Marković (1), Krešimir Pavelić (3), Sandra Kraljević Pavelić (4)

1) University of Rijeka, Department of Biotechnology, Rijeka, Croatia

2) Research Center for Materials of Region of Istria METRIS, Pula, Croatia

3) University "Juraj Dobrila" Pula, Pula, Croatia

4) University of Rijeka, Faculty of Health Studies, Rijeka, Croatia

Zeolite clinoptilolite is a natural mineral of volcanic origin, non-toxic to mammals. Due to its crystalline structure with pores and cavities, it is an ion-exchanger that may be useful for certain detoxification purposes *in vivo*. The physical-chemical structure of clinoptilolite materials is due to a large surface and cavities containing the exchangeable cations, features relevant for observed biological effects. We present, accordingly, the surface study of the different clinoptilolite materials, namely TMAZ-zeolite clinoptilolite (Tribomechanically Activated Zeolite), PMA-zeolite clinoptilolite (Panaceo Micro Activation) and PMAO2-zeolite clinoptilolite (Panaceo Micro Activation by Oxygenation). The surface study was done by use of an electronic microscope (SEM analysis) and element analysis by EDS. Obtained results show different surface appearance and Si/Al ratio in zeolite clinoptilolite water supernatants upon centrifugation at 4000 rpm, 14 000 rpm and 140 000 rpm. Interestingly, the largest percentage of crystals formed from zeolite clinoptilolite water supernatants upon centrifugation were silicon and oxygen-containing crystals. Si mass percentage in clinoptilolite water supernatants after centrifugation was on average 34.4 %. Al was present in 0.75 % average value mass percentage. This gives a Si/Al ratio of 46, which does not correspond to the zeolite clinoptilolite surface Si/Al ratio of 5.6. We hypothesize that the clinoptilolite water supernatants after centrifugation contain polymerized forms of Si. Such structure can bind positively charged cations, for example the trivalent cation aluminum, which may be relevant for its elimination *in vivo*.

Keywords: zeolites, clinoptilolite surface, silicon, detoxification, Si/Al ratio

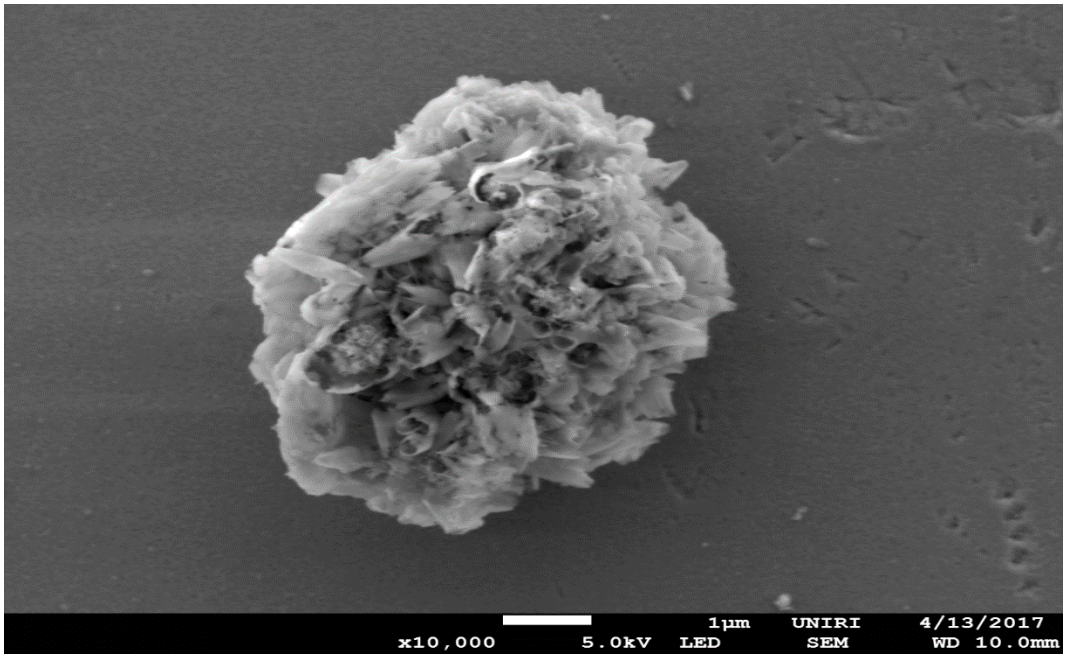

Figure 1. Supernatant of zeolite TMAZ in water upon centrifugation at 140 000 rpm.

References:
1. F.A. Mumpton, Proc. Nat. Acad. Sci. USA. 96 (1999) 3463–3470.
2. K. Pavelić and M. Hadžija, In: Handbook of Zeolite Science and Technology, Eds. S.M. Auerbach, K.A. Carrado., P.K. Dutta, Marcel Dekker, New York, 2003, pp. 1141-1172.
3. K. Pavelić and S. Kraljević Pavelić, Zeolites in Medicine: Current Achievements and Research of Zeolites in Medicine, Nova Science Publishers, New York, 2019.

POSTER PRESENTATIONS

(Life Sciences)

Pancreatic islet surface and share of insulin granules after streptozotocin treatment in wild-type and Tff3 knock-out mice

Nikola Bijelić (1), Edi Rođak (2), Kate Šešelja (3), Iva Bazina (3), Tatjana Belovari (2), Mirela Baus Lončar (3)

1) Department of Histology and Embryology, Faculty of Medicine Osijek, Josip Juraj Strossmayer University of Osijek, Osijek, Croatia

2) Department of Histology and Embryology, Faculty of Medicine Osijek, Josip Juraj Strossmayer University of Osijek, Osijek, Croatia

3) Ruđer Bošković Institute, Department of Molecular Medicine, Zagreb, Croatia

Trefoil Factor 3 (Tff3) is a small peptide mainly expressed in gastrointestinal epithelial cells with a known role in the protection and repair of the mucosal barrier. It promotes cellular migration and angiogenesis. Tff3 is also found expressed in pancreas islet cells, where it co-localizes with insulin and some glucagon-expressing cells [1]. Some studies indicate that Tff3 could be involved in islet-cell proliferation [2]. To investigate the effect of Tff3 deficiency on the integrity of the pancreas, we have performed a study on a novel congenic *Tff3-/-* C57Bl6NCrl mouse strain using a multiple low-dose streptozotocin (STZ) protocol [3]. STZ is selectively toxic to insulin-producing pancreatic β cells and is commonly used to induce Type 1 diabetes (T1D) in animal models. Seven week-old *Tff3-/-* male and female mice and wild type controls were administered low 50 mg/kg, multiple intraperitoneal STZ injections (for 5 consecutive days). We have monitored weight and blood glucose levels during the experiment, and after 6 weeks of STZ induced hyperglycemia, mice were sacrificed. Pancreases were collected and tissue was fixed in 4 % paraformaldehyde and embedded into paraffin. The organs were cut into 6 μm sections. Three different sections through the whole pancreas, up to 1 mm apart, were taken for each animal, and two largest pancreatic islets found on the section were used for measurements. Sections were deparaffinized and stained using Gomori's aldehyde fuchsin for pancreatic beta-granules. Six digital photographs were taken per animal, islets were separated from the rest of the tissue in GIMP software, and islet surface and beta granule surface were measured using FIJI software. Brightfield microscopy showed only a small number of detectable islets in pancreatic tissue. There was no significant difference in average pancreatic islet surface in a share of beta granules in the islets among the examined groups. Although, there were no differences in pancreas tissue between groups, during the experiment *Tff3-/-* male and female mice had statistically reduced body weight and higher mortality rate compared to WT animals. These results indicate an important role of Tff3 in response to STZ treatment but its exact role remains yet to be determined.

Keywords: Tff3, pancreas, pancreatic islets, streptozotocin

References:
1. M. Jackerott et al., Endocrinology 147 (2006) 5752–5759.
2. P.T. Fueger et al., Mol. Endocrinol. 22 (2008) 1251–1259.
3. A.A. Like and A.A. Rossini, Science 193 (1976) 415–417.

This work was supported by Croatian Science Foundation grant IP-06-2016-2717 and "Young researchers career development project – training of doctoral students" of the Croatian Science Foundation funded by the European Union from the European Social Fund (I. Bazina).

Lipid profile of epicardial adipose tissue in obese individuals – preliminary data

Nikola Bijelić (1), Milorad Zjalić (2), Edi Rođak (1), Domagoj Vučić (3), Željko Debeljak (4), Boris Dumenčić (5), Jasmina Rajc (5), Tatjana Belovari (1), Kristina Selthofer Relatić (6)

1) Department of Histology and Embryology, Faculty of Medicine Osijek, Josip Juraj Strossmayer University of Osijek, Osijek, Croatia

2) Laboratory of Neurobiology, Department of Medical Biology and Genetics, Faculty of Medicine Osijek, Josip Juraj Strossmayer University of Osijek, Osijek, Croatia

3) Department for Internal Medicine, Division of Cardiology, General Hospital Doctor Josip Benčević, Slavonski Brod, Croatia

4) Clinical Institute of Laboratory Diagnostics, University Hospital Osijek, Osijek, Croatia and Department of Pharmacology, Faculty of Medicine Osijek, Josip Juraj Strossmayer University of Osijek, Osijek, Croatia

5) Department of Pathology and Forensic Medicine, University Hospital Center Osijek, Osijek, Croatia

6) Department of Internal Medicine, Faculty of Medicine, Josip Juraj Strossmayer University of Osijek, Osijek, Croatia and Department of Heart and Vascular Diseases, University Center Hospital Osijek, Osijek, Croatia

With its endocrine and metabolic activity, visceral adipose tissue (VAT) is more than a storage organ. Research shows that VAT has a role in the development of cardiovascular disorders. The influence of epicardial adipose tissue (EAT, a subset of VAT) morphology on cardiovascular function and health is still limited [1]. Furthermore, the data on the content of lipids and their metabolites in the EAT depending on the amount of VAT are scarce or non-existent. The aim of this pilot study was to characterize lipids and their metabolites in EAT in relation to visceral obesity. EAT from 6 obese and 6 non-obese subjects (based on waist circumference) was collected post-mortem and homogenized in 20 mM ammonium acetate buffer using Dounce homogenizer. Lipid extraction from the homogenate was performed with Blight and Dyer's two-phase method [2]. Both polar and nonpolar phases were imaged in positive and negative imaging mode on Bruker UltrafleXtreme MALDI-TOF device in the 200-1500 m/z range. The matrices used were dihydrobenzoic acid and 9-aminoacridine, respectively. Collected data were analyzed using R statistical software with FELLA and KEGGREST packages. Out of 106 determined putative metabolites, C08320 – Lignoceric acid was 2.37 times more abundant in the obese group ($p = 0.0396$). Out of the 106 molecules, 13.5 % were upregulated, 11.9 % were downregulated in the obese group, and the rest were unchanged compared to the non-obese group. FELLA enrichment revealed alteration in fatty acid biosynthesis and degradation accompanied with upregulation in glycosphingolipid biosynthesis. Preliminary data indicate a metabolic difference in EAT of obese patients. None of the subjects suffered from Gaucher's disease, so it may be assumed that lignoceric acid is exogenous in nature (from food). This also explains upregulation in glycosphingolipid biosynthesis, lignoceric acid being one of its

precursors. The preliminary data showed some changes in EAT of obese patients, which are potentially food-related. Larger groups are necessary to draw more definite conclusions.

Keywords: heart, adipose tissue, MALDI-TOF, lipids

References:
1. D. Vučić et al., Clin. Med. Insights Cardiol. 15 (2021) 1-9 .
2. E.G. Bligh and W.J. Dyer, Can. J. Biochem. Physiol. 37 (1959) 911-917.

The golden days are back: modern application of gold impregnation technique on rat brain cryosections

Milorad Zjalić (1), Sara Cibok (2), Edi Rođak (3), Marija Heffer (1), Tatjana Belovari (3), Nikola Bijelić (3)

1) Laboratory of Neurobiology, Department of Medical Biology and Genetics, Faculty of Medicine Osijek, Josip Juraj Strossmayer University of Osijek, Osijek, Croatia

2) Faculty of Medicine Osijek, Josip Juraj Strossmayer University of Osijek, Osijek, Croatia

3) Department of Histology and Embryology, Faculty of Medicine Osijek, Josip Juraj Strossmayer University of Osijek, Osijek, Croatia

Around 150 years ago, the silver impregnation method for histological sections of nervous tissue was published by Camillo Golgi [1]. Different impregnation methods were used extensively for some time, and they contributed significantly to the development of neuroscience. With the development of new methods, such as electron and confocal microscopy, silver and gold impregnation methods were used less. However, they can still produce useful data, especially when used in combination with modern image analysis software. In this research, the impregnation technique was used to visualize nerve fibers in the areas of interest in the rat brain. The animals were divided into 5 groups (sham-operated control group, ovariectomized untreated group, ovariectomized and treated with alendronate, hop extract and a combination of the two). Rat brains were fixed in 4 % paraformaldehyde, cryoprotected and frozen in pre-chilled isopentane. Coronal 35 μm-thick sections were prepared on a cryostat. 0.2 % gold chloride solution in 0.02 M neutral phosphate buffer and 0.9 % sodium chloride was used for impregnation. After the impregnation, the slides were dehydrated and coverslipped. Samples were photographed and analyzed in a free and open-source program ImageJ [2]. For staining intensity quantification, images were separated into 8-bit channels, and the blue channel was used for analysis. Parameters chosen for measurement in ImageJ were area, standard deviation, min and max grey value, integrated density and mean grey value. Brightfield microscope examination showed the excellent quality of the nerve fiber impregnation. Significant changes in the staining intensity were found in several brain regions of interest between examined groups (primary motor cortex, dentate gyrus and *cornu ammonis* 3). The impregnation technique was very useful for the quantification of nerve fibers when combined with ImageJ image analysis software. Although impregnation methods in neuroscience are 150 years old, gold impregnation can be effectively used in modern research for the quantification of nerve fibers on brain cryosections using freely available image analysis software.

Keywords: hop extract, image processing, impregnation, neuroscience

References:

1. C. Golgi, Gazzetta Medica Italiana, Lombardia 33 (1873) 244–246.
2. J. Schindelin et al., Mol. Reprod. Dev. 82 (2015) 518–529.

Particle surface functionalization affects mechanism of endocytosis of silver nanoparticles in mammalian kidney cells

Maja Beus (1), Marija Ćurlin (2), Igor M. Pongrac (3), Ivona Capjak (4), Krunoslav Ilić (1), Ena Vrček (5), Mirta Milić (1), Ana Marija Marjanović Čermak (1), Ivan Pavičić (1)

1) Institute for Medical Research and Occupational Health, Zagreb, Croatia

2) Catholic University of Croatia, School of Medicine, Zagreb, Croatia

3) University of Zagreb, School of Medicine, Zagreb, Croatia

4) Croatian Institute of Transfusion Medicine, Zagreb, Croatia

5) University of Zagreb, Faculty of Pharmacy and Biochemistry, Zagreb, Croatia

Silver nanoparticles (AgNPs) are widely used due to their antimicrobial properties. The present study indicates the effect of AgNPs' surface coating on their *in vitro* toxicity and internalization in kidney cells. AgNPs were toxic at a concentration of 10 ppm and higher. Positively charged AgNPs were internalized to a greater extent than negative. All types of AgNPs were internalized by the PK15 cells in a dose-dependent manner with greater internalization of AgNPs bearing positive surface charge. Transmission electron microscopy (TEM) experiments showed that AgNPs were located in the lysosomal compartments, while the co-treatment with known inhibitors of endocytosis pathways suggested macropinocytosis as the preferred internalization pathway. All AgNPs induced oxidative stress while comet assay revealed possible genotoxicity.

Keywords: electron microscopy, PK15 cells, cellular uptake, cytotoxicity, genotoxicity

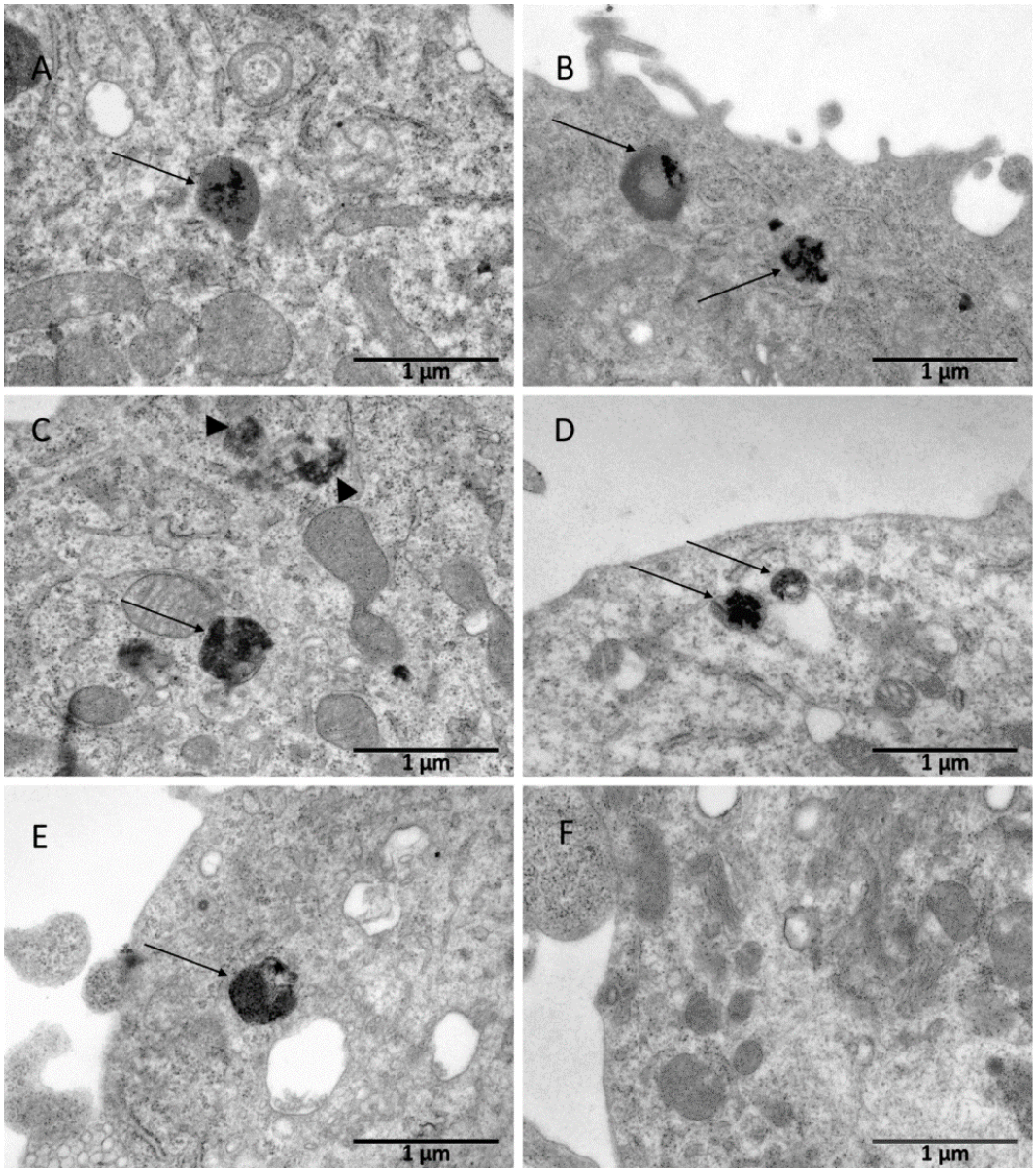

Figure 1. Intracellular localization of different silver nanoparticles (AgNPs) in PK15 cells: (a) AOT-AgNPs, (b) PVP-AgNPs, (c) BSA-AgNP, (d) PLL-AgNP, (e) CTAB-AgNP, and (f) untreated cells. All AgNPs were found in lysosomes (black arrows), while BSA-AgNPs were also present in the cell cytoplasm (arrowheads).

References:
1. M. Milić et al., J. Inorg. Biochem. 224 (2021) 111565.
2. R. Barbir et al., Part. Part. Syst. Charact. 36 (2019) 1900174.
3. L. Brkić Ahmed et al., Food Chem. Toxicol. 107 (2017) 349–361.

Dependence of cell shape on spatial confinement

Blaž Ivšić (1), Tomislav Vuletić (1), Marko Šoštar (2), Igor Weber (2)

1) Institute of Physics, Zagreb, Croatia

2) Ruđer Bošković Institute, Division of Molecular Biology, Zagreb, Croatia

Cell migration is one of the basic properties of almost all eukaryotic cells and is crucial in a large number of biological processes. The shape of migrating cells is primarily determined by the spatial and temporal dynamics of the intracellular actin cytoskeleton and associated proteins. However, the shape and migratory properties of cells in two-dimensional culture depend also on the specific interactions of cells with the underlying surface. It is known that amoebae *Dictyostelium discoideum* dynamically change their shape when migrating. In order to quantitatively classify cell shapes, one possible approach is to use descriptors based on invariant moments of mass distribution. For example, elongation (E) is equal to the ratio of the long and short radii of an ellipse that best fits the contour of a cell, and dispersion (D) describes how much mass is dispersed away from the centroid of the cell shape [1]. In order to quantify the dependence of the shape of *D. discoideum* cells on spatial confinement, we engineered patterned surfaces coated with anti-adhesive co-polymer PLL-*g*-PEG (polylysine grafted to polyethylene glycol), except for small patches of uncoated glass several square micrometers in size [2]. Contours of fluorescently labelled cells, which were deposited either onto the confined adhesive patches or onto the plain glass coverslips, were obtained by analysing the images obtained by confocal fluorescence microscopy. Comparison of the shape descriptors of confined vs. nonconfined cells showed that ranges of, and ratios between, cell elongation and dispersion values depended on the state of confinement. The methodology developed here will be useful in characterizing the role of proteins involved in the regulation of the cell-substratum adhesion and the cell shape dynamics by analysing the phenotypes of mutant cells devoid of these proteins.

Keywords: cell shape, cell confinement, anti-adhesive substrates, shape descriptors

References:

1. G.A. Dunn and A.F. Brown, In: Biological motion, Eds. W. Alt and G. Hoffmann, Springer, Berlin – Heidelberg, 1990, pp. 10-34.
2. A. Azioune et al., Lab Chip. 9 (2009) 1640-1642.

Effect of silver nanoparticles and ions on oxidative stress formation and antioxidative machinery of *Chlorella vulgaris*

Bruno Komazec (1), Daniel Mark Lyons (2), Petra Peharec Štefanić (1)

1) Department of Biology, Faculty of Science, University of Zagreb, Zagreb, Croatia

2) Center for Marine Research, Ruđer Bošković Institute, Rovinj, Croatia

Silver nanoparticles (AgNPs) are used in a variety of industries and, due to their tendency to agglomerate in various media, they are commonly stabilised with various surface coatings such as carboxylic acids (citrate) or surfactant cetyltrimethylammonium bromide (CTAB), among others [1]. As the use of AgNPs increases, so does the potential for their release into the aquatic environment. Since *Chlorella vulgaris* is one of the most ubiquitous algae inhabiting aquatic ecosystems, it is widely used as a model organism for assessing the impact of materials of anthropogenic origin, e.g. AgNPs, on aquatic habitats [2]. To evaluate the impact of AgNP on *C. vulgaris*, algal cultures were grown in a liquid BBM nutrient medium for four days, after which they were exposed to AgNPs coated with citrate or CTAB and to $AgNO_3$, which was used as ionic Ag control. Concentration endpoints were obtained by growth inhibition test (72 h) and the estimated 25 % inhibition of growth rate (EC25) values for the AgNP-citrate, AgNP-CTAB and $AgNO_3$ were 0.188 mg L^{-1}, 0.895 mg L^{-1} and 0.130 mg L^{-1}, respectively. After 72 h treatment, the quantity of newly synthesised oxygen, damage to membrane lipids as measured through malondialdehyde (MDA) content, levels of reactive oxygen species (ROS) and activity of antioxidant enzymes (superoxide dismutase-SOD, catalase-CAT, ascorbate and pyrogallol peroxidase-APX and PPX) were analysed. To understand the ROS formation, algal suspensions were incubated with fluorogenic dyes through which hydroxyl and peroxyl activity within the cells (H_2DCFDA) or superoxide ($O_2^{\cdot-}$) generation (DHE) were determined, with both dyes providing a measure of other ROS activity through non-specific oxidation. Moreover, to further examine the interaction between AgNPs and algal cells, the treated organisms were observed directly by transmission electron microscopy (TEM). Obtained results showed a detrimental effect of all treatments on the photosystem of *C. vulgaris* since a significant decrease in oxygen synthesis was reported. Similarly, all treatments have increased ROS formation and MDA content, which is indicative of membrane lipids damage. Interestingly, only increases in PPX and CAT activity were observed after treatment with AgNP-citrate, while for APX and for other treatments a trend of decreasing activity of antioxidant enzymes was observed. TEM analysis of algae cells showed multiple NPs in extracellular polymeric substances (EPS) of algae cells which could aid in decreasing toxic effect of AgNPs on algal cells (Fig. 1). In conclusion, all silver nanoparticles (AgNP-citrate and AgNP-CTAB) and ionic silver showed damaging effects on the photosynthetic apparatus of *C. vulgaris* algae. The parallel increase in ROS formation and decrease in the activity of the antioxidant machinery after 72 h treatment can be explained by an overproduction of ROS (Fig. 1), which consequently results in a change of enzyme structure and activity [3].

Keywords: *Chlorella vulgaris*, oxidative stress, silver nanoparticles

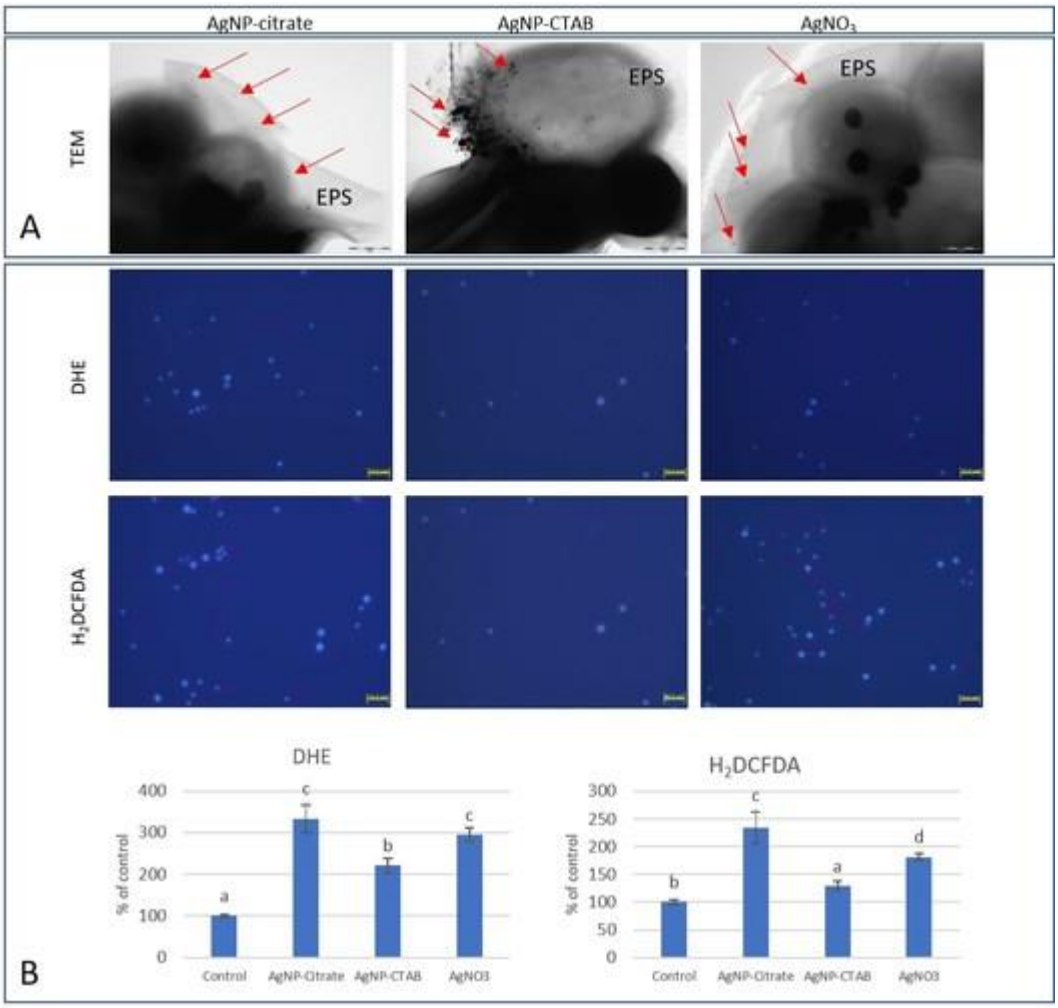

Figure 1. *C. vulgaris* cells after AgNP-citrate, AgNP-CTAB or $AgNO_3$ treatment obtained by (A) TEM, showing NPs (arrows) in the EPS (scale = 1 μm); (B) fluorescence microscopy showing ROS increase via fluorescent probes DHE or H_2DCFDA (scale = 10.8 μm).

References:
1. R. Biba et al., Nanomaterials 12 (2022) 24.
2. S. Wu et al., Environ. Eng. Sci. 31 (2014) 9–17.
3. R. Van der Oost et al., Environ. Toxicol. Pharmacol. 13 (2003) 57–149.

In situ fluorescence-based confocal imaging for detecting early stress responses of tobacco plants after exposure to silver nanoparticles or silver nitrate

Karla Košpić (1), Renata Biba (1), Petra Peharec Štefanić (1), David Vondrášek (2), Ilse Letofsky Papst (3), Biljana Balen (1)

1) Department of Biology, Faculty of Science, University of Zagreb, Zagreb, Croatia

2) Department of Biomathematics, The Czech Academy of Sciences, Prague, Czech Republic

3) Institute of Electron Microscopy and Nanoanalysis (FELMI), Graz University of Technology, Graz, Austria

Antimicrobial properties of silver and enhanced reactivity when applied in the nanoparticle form (AgNPs) led to their growing utilization in consumer products. Consequently, their increasing release into water or soil represents a potential environmental hazard and poses an indirect threat to human health. AgNP phytotoxic effects have been mainly attributed to the excess generation of reactive oxygen species (ROS), leading to the induction of oxidative stress [1]. However, most studies so far have been performed *in vitro* and at the whole plant or whole organ level, where oxidative stress symptoms were observed after plant exposure to stress conditions was long enough to produce extensive cell damage. In this work, detached roots of *in vitro* grown tobacco (*Nicotiana tabacum)* plants were exposed for 24 h to either AgNPs stabilized with polyvinylpyrrolidone (PVP) coating or ionic silver ($AgNO_3$), applied in the 100 μM concentration with the aim to investigate *in situ* early physiological responses as first signs of stressful conditions. Generation of ROS in root cells was monitored by confocal laser scanning microscope (Leica TCS SP8) using highly sensitive and specific fluorescent probes: dihydroethidium (DHE), to detect superoxide radical (O_2^-), and 2',7'-dichlorofluorescein-diacetate (H_2DCF-DA), to detect hydrogen peroxide (H_2O_2) [2]. Moreover, monochlorobimane (MCB) was applied for the detection of glutathione (GSH), an important constituent of the cell antioxidant defence [3]. Additionally, propidium iodide (PI) was used as a counterstain to verify cell viability. The results showed an increased amount of H_2O_2 and O_2^- and a decreased amount of GSH in roots exposed to both types of treatments in comparison to control, which was accompanied with an increased number of dead cells detected with PI. All observed changes were more prominent upon $AgNO_3$-exposure compared to AgNPs. AgNPs were visualized within root cells upon both types of treatments by observing reflection and transmission with the excitation light source of 476 nm, and by employing a longer excitation wavelength (760 nm) of a multiphoton pulsed laser at which AgNP exhibit fluorescence properties. This suggests that not only AgNPs can enter roots cells, but also new AgNPs are being synthesized upon exposure to $AgNO_3$. Fluorescence lifetime imaging microscopy (FLIM) revealed that the observed reflective and luminescent particles have a relatively short fluorescence lifetime, which could distinguish them from the natural compounds of plant cells. AgNPs were mostly found attached to the root surface and inside root hairs. Employment of transmission electron microscope (TF20, FEI Tecnai G2) coupled with energy-dispersive X-ray (EDX) detector confirmed AgNP localization in root cells. In conclusion, AgNPs and $AgNO_3$ not only compromised cellular redox-homeostasis, but possibly caused cell necrosis, while different level of impact was observed depending on the form of the applied silver.

Keywords: confocal microscopy, fluorescent probes, phytotoxicity, reactive oxygen species, silver nanoparticles

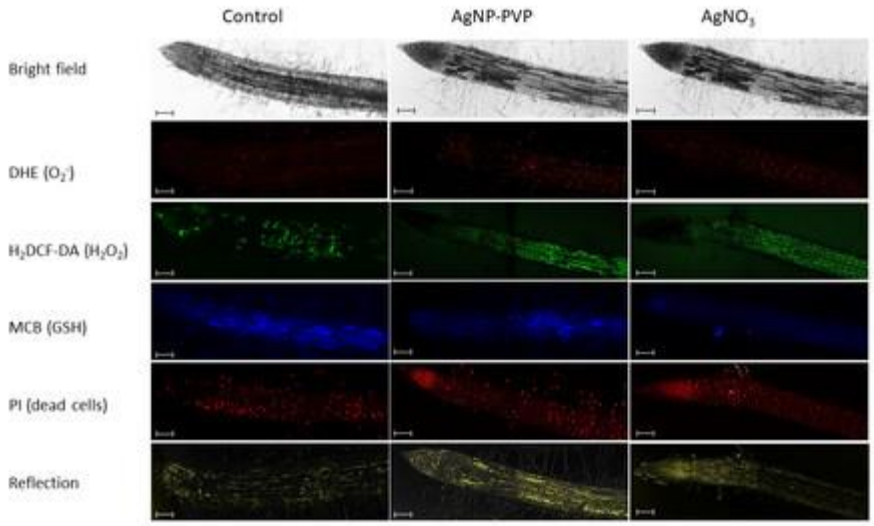

Figure 1. Confocal imaging of tobacco roots stained with fluorescent probes specific for ROS or glutathione upon AgNP or $AgNO_3$ treatment. Images represent maximum intensity projection of Z-stack (30 images, Z-step: 0.03 μm, magnification: 20 x, bar: 100 μm).

References:

1. R. Biba et al., Nanomaterials 12 (2022) 24-54.
2. V.C. Mai et al., Phytochemistry 93 (2013) 49–62.
3. C. Ortega-Villasante et al., J. Exp. Bot. 56 (2005) 2239-2251.

Morphometric characteristics of *Dreissena polymorpha* oocytes in the Drava River and in the Dubrava Reservoir

Jasna Lajtner (1)

1) Department of Biology, Faculty of Science, University of Zagreb, Zagreb, Croatia

Freshwater mussel *Dreissena polymorpha* (Pallas, 1771) is one of the most dominant invasive species in the European freshwaters, which began to spread in Croatia during the 1980s. Their rapid invasion is enabled by the ability of adult mussels to adapt to a wide range of habitats and by their reproductive cycle flexibility. The aim of this study was to investigate the annual development of gonads in two populations living in the Drava River (site 1) and in the accumulation lake of Dubrava Hydroelectric Power Plant (site 2), differing in environmental parameters. The analyses included measuring the size and diameter of oocytes and their nuclei in the period from March to August. The histological sections were made by the classical histological technique. Measurements were done with the image analysis system (Lucia G 4.8), and the digital video camera Nikon DXM 1200, linked to a Nikon's Eclipse E600 light microscope, was used for taking images. A total of 13 731 oocytes were analysed, of which 6 680 from site 1 and 7 051 from site 2. Based on this analysis, but also the known gonadal volume, the following values were calculated: number of oocytes per mm^2, percentage of oocytes in total ovarian volume, oocyte volume in ovary, and finally the total number of oocytes per female. The difference between the mean values of oocyte and nucleus diameters between sites, by months, was statistically significant ($p < 0.0001$; Wilcoxon rank sum test). In addition, differences in diameters between months at the same site were also statistically significant ($p < 0.0001$; ANOVA). All other calculated variables were higher at site 1, but only the percentage of oocytes in the total ovarian volume differed significantly ($p = 0.0063$; Wilcoxon sum test). The differences in all calculated variables at the same station, by months, were statistically significant (Kruskal-Wallis test). The highest number of oocytes, 801 977, was recorded in a female sampled in April at site 1. In general, the values of all measured parameters were highest in spring, before spawning, and then decreased. The observed differences between sites are possibly a consequence of the fact that mussels at site 2 have faster development of gonads, due to more uniform living conditions, and have a smaller shell width (body volume), due to high population density. Finally, it is important to emphasize that it has been proven that the oocytes became mature in successive cohorts within one gonad, which means that a female may spawn several times during the reproductive season.

Keywords: reproductive cycle, gonads, invasive species, image analysis

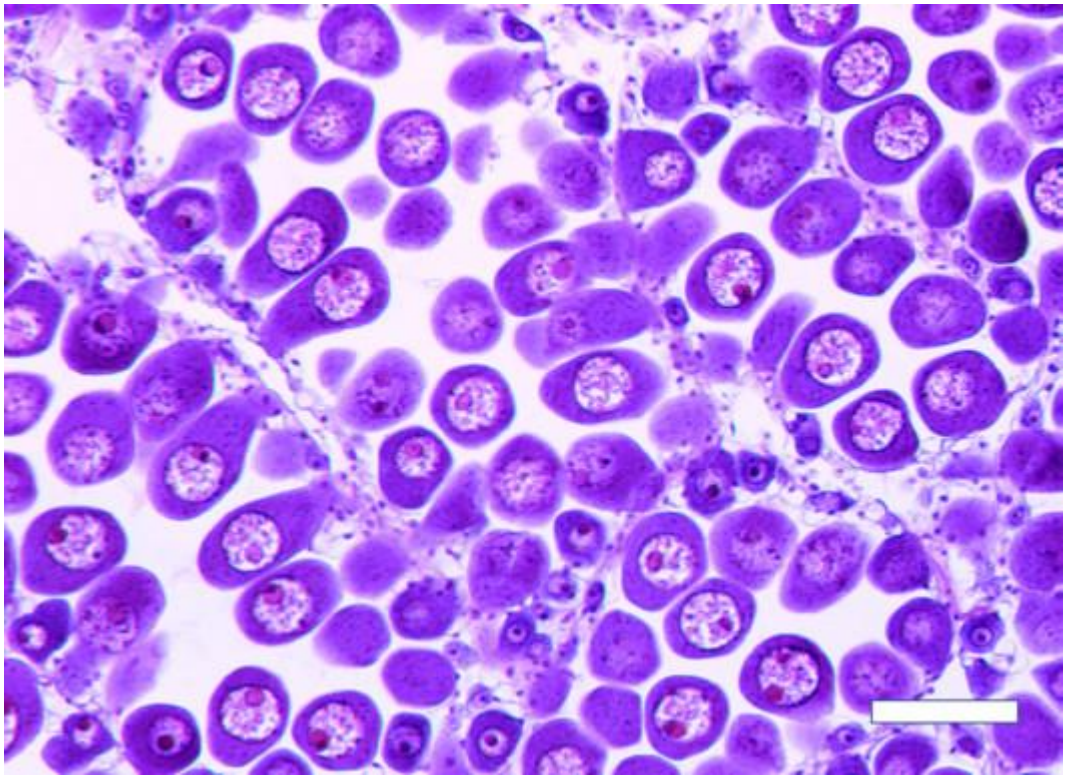

Figure 1. Mature oocytes in the female gonad of *Dreissena polymorpha*, site 1, April. Scale bar 100 μm.

References:
1. J. Borcherding, Oecologia 87 (1991) 208-218.
2. J. Lajtner et al., Acta Parasitol. 53 (2008) 85-92.

Histomorphometric evaluation of toxic effects of Na-PCP on the gill of the freshwater snail *Holandriana holandrii*

Romana Gračan (1), Jasna Lajtner (1), Maria Špoljar (1), Ines Tkalčec (1), Goran Kovačević (1), Blaženka Banjad Ostojić (2), Martina Ivšić (1), Ana Miletić (3), Radovan Erben (1)

1) Department of Biology, Faculty of Science, University of Zagreb, Zagreb, Croatia

2) Institute IGH, Zagreb, Croatia

3) Association for Nature, Environment and Sustainable Development SUNCE, Split, Croatia

Compounds of pentachlorophenol and particularly the sodium salt (Na-PCP) have been widely used for a variety of agricultural and industrial purposes. The pollution of aquatic ecosystems by Na-PCP has assumed serious proportions due to its toxicity and accumulative effect in organisms and the environment. The objective of this laboratory study was to examine and quantify the histopathological effects of Na-PCP on the structure of the gill, as one of the most important organs targeted by phenol entries, in the freshwater snail, *Holandriana holandrii*. Based on the results of a preliminary mortality test, three experimental concentrations were chosen: 0.56, 1.00 and 5.6 mg L^{-1} Na-PCP for the semi-static test. Histological sections, stained with hematoxylin and eosin, were observed under a light microscope equipped with a digital camera and analysed with image analysis software to quantify histopathological lesions. Results indicated serious structural changes in epithelial cells and underlying connective tissue of gills, which were accelerated with an increase of Na-PCP concentrations and more pronounced in relation to the exposed period. Significant gill structural changes appeared as a progressive necrosis at epithelial cells, and the epithelial lining was interrupted, while connective tissue exhibited vacuolization, formation of large irregular spaces and damaged chitinous rods. Epithelial height measured showed significant difference among experimental groups exposed to different concentrations of Na-PCP and control. Further on, measured connective tissue width also showed a statistically significant difference. We can conclude that the histomorphometric approach in quantifying of toxicant effects on animal tissue could be applied in legislative prevention of adverse effects in freshwater ecosystems, and *H. holandrii* can serve as a good indicator of freshwater deterioration.

Keywords: gill, tissue and cell morphometry, vacuolisation, necrosis, image analysis

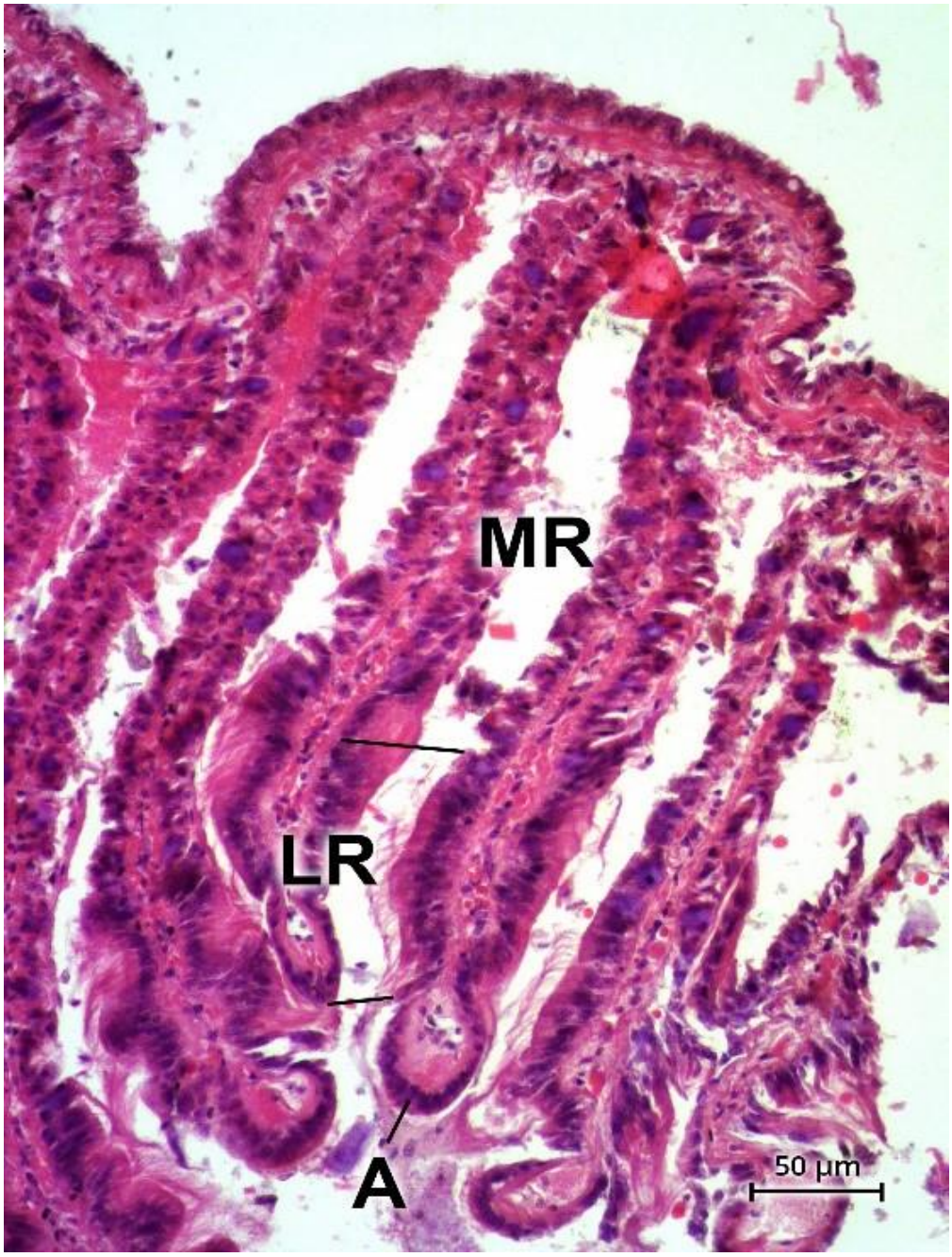

Figure 1. Representative gill tissue of *Holandriana holandrii* in control group with three selected regions of interest and marked features analysed after exposure to Na-PCP. Abbreviations: MR–middle region, LR–lateral region, A–apex region.

References:
1. J. Lajtner et al., Period. biol. 105 (2003) 157-162.
2. M. Špoljar et al., Biologia, Bratislava 60 (2005) 201-205.
3. J.M. Besser et al., Arch. Environ. Contam. Toxicol. 70 (2016) 321-331.

Tracking polystyrene nanoparticles and resolving their effect on the immune system in mussel *Mytilus galloprovincialis*

Matea Marelja (1), Petra Peharec Štefanić (2), Daniel Mark Lyons (1)

1) Center for Marine Research, Ruđer Bošković Institute, Rovinj, Croatia

2) Department of Biology, Faculty of Science, University of Zagreb, Zagreb, Croatia

Microplastics, deriving from the breakdown of macro-scale polymer-based products, have become the focus of much research over the past number of years due to their ubiquity in the environment and their potentially negative impact on biota. Moreover, the possibility of bioaccumulation and biomagnification in the food chain may ultimately impact upon human health. However, continued environmental weathering of microplastics likely gives rise to increasingly smaller particles, eventually reaching the nano-scale size range. Nanoplastics are particularly interesting as their small size (1 – 1000 nm) overlaps with the size of the particles ingested by filter feeders. However, determining the distribution and fate of such polymer nanoparticles in biota is particularly challenging using instrumental methods of analysis. The aim of the work reported herein was to synthesise labelled polystyrene nanoparticles of tailored diameter and to investigate their uptake, bio-distribution and impact on Mediterranean mussel *Mytilus galloprovincialis*. Non-surface-functionalised virgin polystyrene nanoparticles with encapsulated ethidium bromide were characterised by scanning electron microscopy and transmission electron microscopy. Subsequently, *M. galloprovincialis* was treated with the nanoparticles at concentrations in the range of 100 – 1000 mg L^{-1} with an exposure time of 24 h. The accumulation of nanoplastics on the gills was tracked by epi-fluorescence microscopy with significant quantities agglomerated among the gill filaments. As an indicator of toxicity, the impact of the nanoplastics on the immune system of the mussels was investigated by determining cell viability and changes to the number of circulating haemocytes. Even though the exposure time was short, higher concentrations of nanoplastics were found to reduce both the number and cell viability of mussel haemocytes. Furthermore, the stability of lysosomal membranes in haemocytes was also found to have significantly decreased at higher nanoparticle concentrations. Overall, this work has used a range of microscopy and spectroscopy techniques to demonstrate how *M. galloprovincialis* rapidly takes up nanoplastics from the water column where they accumulate on gills and pass into the digestive system. The presence of these nanoplastics were found to deleteriously impact on the mussel's immune system, even after a short experimental exposure. Ultimately, this work is a step in the direction of creating tailored polymer nanoparticles that will allow tracking of nanoplastics' pathways through tissues and cells.

Keywords: nanoplastic, polystyrene, mussel, immune system

References:
1. P.J. Thomas et al., Sci. Total Environ. 780 (2021) 146534.
2. J.M. Gonçalves et al., Environ. Pollut. 273 (2021) 116426.

This work has been fully supported by the Croatian Science Foundation under grant IP-2018-01-5351.

Glandular trichomes micromorphology of aerial parts of *Sideritis romana* L. and *Sideritis montana* L.

T. Marić (1), M. Friščić (1), Ž. Maleš (1)

1) Department of Pharmaceutical Botany, University of Zagreb, Faculty of Pharmacy and Biochemistry, Zagreb, Croatia

Sideritis romana L. and *Sideritis montana* L. (Lamiaceae) are annual herbs covered in hairs inhabiting arid meadows and grazings of Europe and the Mediterranean area. In this study, micromorphological observations were performed using light microscopy on the rehydrated dry aerial parts (stems, leaves, calyces and corollas) of three different individual plants from each species collected from wild populations in Croatia, in order to compare these two plant species based on the type and size of occurring glandular trichomes. The gland sizes were assessed based on the measurement of stalk length and/or head width of ten glands of each of the three established gland types, sessile glandular trichomes, unicellular-stalked glandular trichomes and multicellular-stalked glandular trichomes, in triplicate. All three types of glandular trichomes were found on stems, leaves and calyces of *S. romana* (Sr) and on calyces of *S. montana* (Sm), while stems and leaves of Sm had only sessile and unicellular-stalked glands (Fig. 1). On corollas of both species, only unicellular-stalked glands were found. Head diameter of sessile glandular trichomes ranged from 20.5 to 36.3 μm in Sr and from 19.5 to 38.8 in Sm. Stalk length of unicellular-stalked glandular trichomes ranged from 6.7 to 70.2 μm in Sr and from 6.4 to 159.4 μm in Sm, while their head diameter ranged from 13.9 to 52.6 μm in Sr and from 20.1 to 48.8 μm in Sm. Stalk of multicellular-stalked glandular trichomes ranged from 65.1 to 562.2 μm in Sr and from 95.3 to 190.6 μm in Sm, while the head diameter ranged from 24.6 to 38.0 μm in Sr and from 25.4 to 48.1 μm in Sm. Glandular classification reported previously for these two species [1,2] could not have been made here due to the lack of information on glandular structure obtained only by light microscopy. Scanning and transmission electron microscopy imaging would be needed for the more precise systematization of observed glands, which will be the focus of our future studies.

Keywords: *Sideritis*, light microscopy, morphology

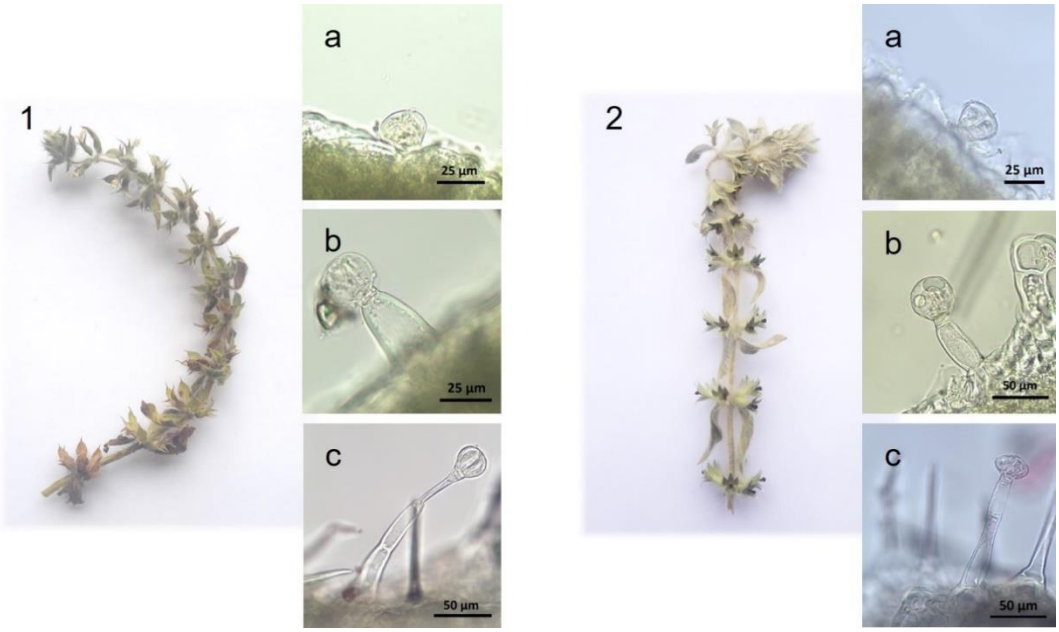

Figure 1. Dry sample of *Sideritis romana* L. (1) and *S. montana* L. (2) with corresponding light microscopy images of sessile glands (a), unicellular-stalked glands (b) and multicellular-stalked glands (c).

References:
1. C. Giuliani and L.M. Bini, Plant Syst. Evol. 276 (2008) 199-208.
2. A. Venditti et al., Chem. Biodiversity 13 (2016) 1380-1390.

IqgC at the crossroads of RasGAP and IQGAP protein families

Lucija Mijanović (1), Darija Putar (1), Vedrana Filić (1), Igor Weber (1)

1) Ruđer Bošković Institute, Division of Molecular Biology, Zagreb, Croatia

Ras-specific GTPase activating proteins (RasGAPs) constitute a diverse group of proteins characterized by their GAP domain. This domain binds and inactivates small GTPases from the Ras family by stimulating their GTP hydrolytic activity. Despite having a highly homologous GAP-related domain (GRD), members of the IQ-motif containing Ras GTPase-activating-like protein (IQGAP) family do not function as RasGAPs. They are multidomain proteins that serve as scaffolds for various pathways and modulate diverse cellular processes [1]. Amoeba *Dictyostelium discoideum* encodes four IQGAP-related proteins – DGAP1, GAPA, IqgC and IqgD. DGAP1 and GAPA are extensively studied and exhibit traditional IQGAP activity, i.e. they participate in the formation of large protein complexes involved in the regulation of actin cytoskeleton and are unable to inactivate Ras GTPases. We showed recently that IqgC, despite apparently belonging to the IQGAP family, is a genuine RasGAP [2]. It binds and inactivates small GTPase RasG, acting as a negative regulator of large-scale endocytosis. Based on the observation that *iqgC*-null cells detach easily from the cell culture dishes, we set out to characterize the role of IqgC in the cell-substratum adhesion. Shaking assays showed that *iqgC*-null cells adhere considerably more weakly to the glass surface than the wild-type cells, and expression of recombinant IqgC in mutant cells rescued this phenotype. IqgC localizes to the punctate adhesion structures together with the adhesion marker paxillin B, as shown by total internal reflection fluorescence (TIRF) microscopy. We expressed fluorescently labeled IqgC in *rasG*-null cells and examined them using confocal microscopy. Normal localization of IqgC to the adhesion foci was observed, indicating that RasG is not necessary for its role in adhesion. To further dissect the role of IqgC in the cell-substratum adhesion, we expressed its individual fluorescently labeled domains in wild-type cells and examined their localization: the GRD domain with GAP activity towards RasG, and the RGCt domain unique to IQGAPs. YFP-RGCt, but not YFP-GRD, localized to the adhesion foci. The same constructs were tested for their ability to rescue the adhesion phenotype of *iqgC*-null cells in shaking assays, but neither could completely rescue the defect. We conclude that the interaction of IqgC with RasG and its GAP activity is not essential for the role of IqgC in the cell-substratum adhesion. The RGCt domain of IqgC is necessary and sufficient for the proper localization of the protein to the adhesion foci, but the expression of the full-length protein is necessary to restore normal adhesion. Since the RGCt domain is a hallmark of IQGAPs, our results suggest that IqgC unifies the features and activities of both RasGAP and IQGAP protein families in the regulation of various cellular processes.

Keywords: IqgC, *Dictyostelium discoideum*, adhesion, GAP, IQGAP

References:
1. J.M. Smith et al., Trends. Cell. Biol. 25 (2015) 171-184.
2. M. Marinović et al., PNAS USA. 116 (2019) 1289-1298.

This work was supported by the Swiss Enlargement Contribution in the framework of the Croatian-Swiss Research Programme (project number IZHRZ0_180584) and by Croatian Science Foundation under the project IP-2020-02-1572. The work of doctoral student Lucija Mijanović has been supported by the "Young researchers' career development project – training of doctoral students" of the Croatian Science Foundation funded by the European Union from the European Social Fund.

In vivo imaging to tackle the challenge of visualisation of dynamic processes – example of brain damage evolution after ischemic stroke

Daniela Petrinec (1), Dominik Hamer (1), Sanja Sarkočić (1), Paula Josić (1), Rok Ister (1), Monika Berecki (1), Laura Skukan (1), Marina Dobrivojević Radmilović (1), Siniša Škokić (1), Anton Glasnović (1), Srećko Gajović (1)

1) Croatian Institute for Brain Research, University of Zagreb School of Medicine, Zagreb, Croatia

The challenge of visualisation of the dynamic processes which change through time remains an important challenge, in particular if combined with methods with different magnification range. Together with light, some other visualisation modalities can be applied, for example magnetic resonance or X-ray-based micro-CT. In animal experiments, the additional issue is the need to reduce the number of animals, refine the animal procedures and replace animals by other experimental approaches. Subsequently, we have organised a platform for *in vivo* imaging of the laboratory animals, which allowed multiple imaging sessions during a single experimental protocol. This was applied to study the animal model of human ischemic stroke, where brain lesion was caused by transient middle cerebral occlusion (tMCAO). Two imaging modalities were used, magnetic resonance imaging (MRI) and optical imaging of bioluminescence (BLI), and the obtained *in vivo* imaging results were combined by histological analysis and immunohistochemistry of the mouse brain and flow cytometry of isolated and separated brain cells. Moreover, the imaging results were related to the functional outcomes of the animals obtained by neurological deficit scoring. The described approach was used to compare the mice deficient for the specific receptor on the microglia, Tlr2, to which particles of necrotic cells bind and subsequently elicit neuroinflammation [1]. The experimental paradigm included the follow up of animals for 28 days after ischemic lesion. The imaging sessions allowed us to compare the brain consequences between Tlr2-deficient to control wild-type animals. Tlr2-deficient animals survived better after ischemic lesion, however, had bigger lesions and neurological scores. After 28 days, Tlr2-deficient animals were comparable to their controls. Bioluminescence imaging showed higher Gap43 expression in Tlr2-deficient animals related to the processes of brain repair. The same was shown by modelling the relation between the ischemic lesion and functional outcome indicating that Tlr2-deficient animals recovered better than the wild-type controls. In conclusion, the *in vivo* imaging modalities combined with other microscopy methods provided a multimodal approach, giving insight into the time-dependent changes of the mouse brain after ischemic lesion. The animals are followed analogously to the human patients which allows testing the preclinical interventions with the aim to design future human therapies of the stroke.

Keywords: magnetic resonance imaging, optical *in vivo* imaging, bioluminescence imaging, mouse brain, ischemic lesion

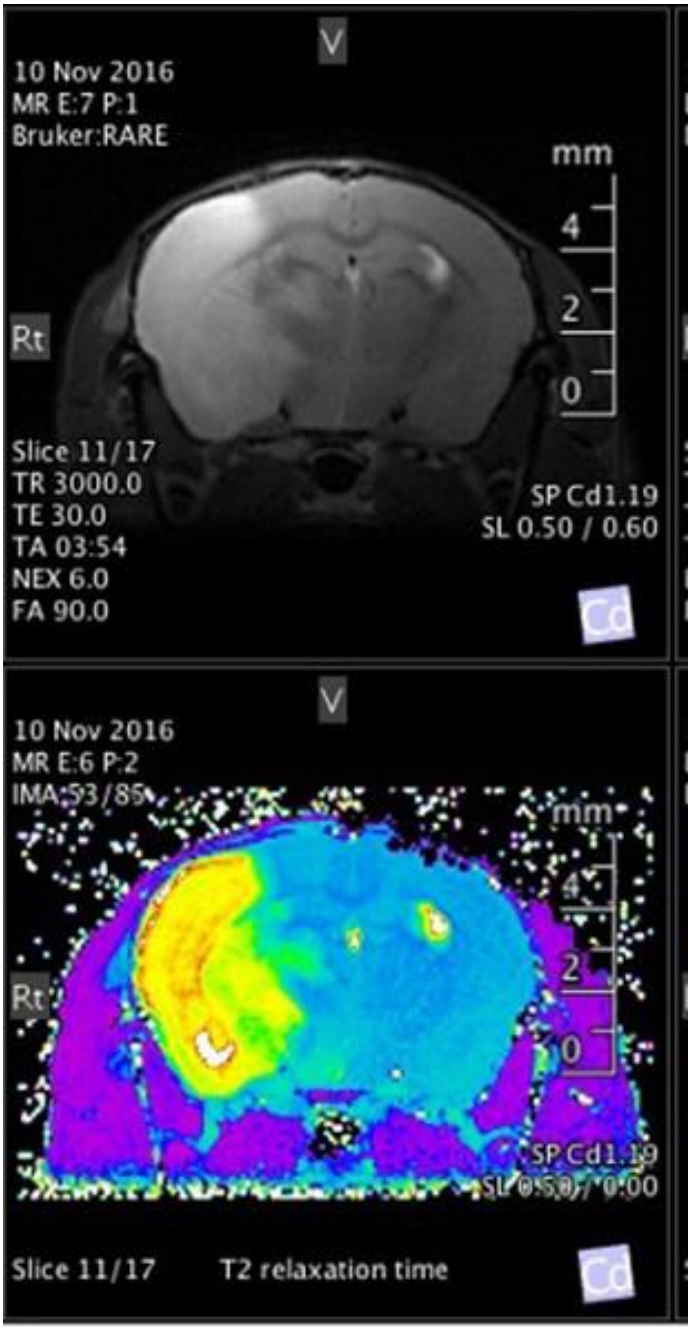

Figure 1. Magnetic resonance imaging of the mouse brain after ischemia shows the size of ischemic lesion by T2 (up) and T2map (down) modalities.

References:

1. I. Bohacek et al., J. Neuroinflammation 9 (2012) 191.

Dictyostelium IqgD is a Rho-regulated IQGAP involved in large-scale endocytosis

Anja Privara (1), Darija Putar (1), Igor Weber (1), Vedrana Filić (1)

1) Ruđer Bošković Institute, Division of Molecular Biology, Zagreb, Croatia

IqgD is an IQGAP-related protein from amoeba *Dictyostelium discoideum*. IQGAPs are evolutionarily conserved, multidomain proteins that serve as scaffolds to integrate diverse signaling pathways. Consequently, they regulate various cellular processes such as migration, adhesion, and vesicle trafficking [1]. IQGAP proteins directly bind actin filaments via their calponin homology domain (CHD). They can further cross-link them into bundles, and this F-actin-cross-linking activity is dependent on the dimerization and oligomerization of IQGAP molecules. Oligomerization is facilitated by binding of active Cdc42 and Rac1, members of the Rho family GTPases, to the GAP-related domain (GRD). IQGAPs also regulate actin dynamics via interaction with nucleation-promoting factor N-WASP and actin-assembly factors Arp2/3 complex and formin Dia1, thus promoting the generation of protrusive structures at the cell leading edge [2]. *Dictyostelium* IqgD is a fimbrin-related RasGAP that contains a CHD duplex, a coiled-coil region, a GRD/RasGAP domain, and a RasGAP_C-terminal (RGCt) extension [3]. It is the only *Dictyostelium* IQGAP that possesses an actin-binding domain and presumably binds actin filaments. We show by confocal microscopy that fluorescently labelled IqgD in live *Dictyostelium* cells localizes to the entire cell cortex. However, it is enriched at the membrane patches that are primed for macropinocytosis and subsequently enclose nascent macropinosomes. Similarly, IqgD is also strongly enriched at the base of the phagocytic cup during large particle engulfment. As the protrusion of the cup advances, IqgD translocates to the distal parts of the cup and reaches maximal intensity at the site of phagosome sealing. Soon after internalization is completed, the IqgD signal disperses. Next, we examined its presumed interactions with actin via CHD, and with Ras and Rho GTPases involved in large-scale endocytosis, via GRD. Using yeast two-hybrid assay, we demonstrated a direct interaction between IqgD and Rac1A and Rac1C GTPases. Interestingly, while IqgD showed a higher affinity for constitutively active Rac1A, it prefers binding to dominant-negative Rac1C. Interaction with endogenous actin was demonstrated using Co-IP. The presented data strongly suggest that *Dictyostelium* protein IqgD regulates actin cytoskeleton in large protrusions such as macropinocytic and phagocytic cups and that Rho GTPases Rac1A and Rac1C regulate its activity.

Keywords: IqgD, IQGAP, Rho, actin, *Dictyostelium*

References:
1. C.D. White et al., Cell. Signal. 24 (2012) 826–834.
2. T. Watanabe et al., Cell Struct. Funct. 40 (2015) 69–77.
3. F. Friedberg et al., Mol. Biol. Rep. 37 (2010) 2853–2862.

This work has been fully supported by Croatian Science Foundation under the project IP-2020-02-1572.

Small GTPases interacting with IqgC on *Dictyostelium* macropinosomes

Darija Putar (1), Tamara Ćutić (1), Igor Weber (1), Vedrana Filić (1)

1) Ruđer Bošković Institute, Division of Molecular Biology, Zagreb, Croatia

The *Dictyostelium* IQGAP-related protein IqgC is a GAP (GTPase-activating protein) specific for the small GTPase RasG [1]. It deactivates RasG and thus negatively regulates macropinocytosis in the amoeba *Dictyostelium discoideum*. Macropinocytosis is a Ras-regulated endocytic process for non-selective uptake of extracellular fluid [2]. Previous study has shown that IqgC strongly localizes to macropinosomes [1]. It colocalizes with active Ras during the formation of the macropinocytic cup and on the nascent macropinosome. However, IqgC remains on the internalized macropinosome even after Ras has dissociated from the vesicle. This dynamics suggests that IqgC has a role independent of RasG, probably in early macropinosome maturation. We aim to (I) clarify the role of RasG in the recruitment of IqgC to the forming macropinosomes, and (II) identify novel protein interactor(s) of IqgC that could retain it after RasG disappears. To examine the role of RasG in IqgC recruitment, we analyzed the localization of IqgC in *rasG*-null cells by confocal microscopy. We observed the loss of IqgC localization to macropinosomes in the absence of RasG. Next, we monitored the localization of a truncated version of IqgC, which lacked the RasG-binding RasGAP domain, in *iqgC*-null cells and again observed mislocalized IqgC. Finally, IqgC proteins mutated in amino acids important for its GAP activity and/or interaction with RasG again did not localize properly. Altogether, these data demonstrate that interaction with RasG is indispensable for the recruitment of IqgC to the macropinosome during its formation. To identify novel protein interactor(s) that could explain IqgC functions during early macropinosome maturation, we selected several protein candidates from the previously published IqgC interactome [1], based on their known involvement in early endocytic pathways. Using this approach, we found another small GTPase from the Ras superfamily, Rab5A, to co-immunoprecipitate with endogenous IqgC. By performing GST-Rab5A pull-down assay with purified IqgC, we have demonstrated a direct interaction between Rab5A and IqgC. Confocal microscopy of wild-type cells co-expressing fluorescently labelled IqgC and Rab5A showed their colocalization on internalised macropinosomes. More specifically, Rab5A associates with the macropinocytic vesicle when IqgC signal starts to diminish. By the time Rab5A, whose presence increases gradually, reaches maximal intensity, IqgC has dissociated from the vesicle. In summary, interaction with RasG is necessary for the correct localization of IqgC to forming macropinosomes. After macropinosome closure, RasG dissociates from the macropinocytic vesicle. However, IqgC remains on the vesicle where it interacts with the early endosome marker Rab5A [3]. Deciphering the physiological significance of this interaction requires further investigation.

Keywords: IqgC, RasGAP, RasG, Rab5A, macropinocytosis

References:
1. M. Marinović et al., Proc. Natl. Acad. Sci. 116 (2019) 1289-1298.
2. J.S. King and R.R. Kay, Philos. Trans. R. Soc. B Biol. Sci. 374 (2019) 20180158.
3. M.E. Maxson et al., J. Cell Sci. 134 (2021) 252411.

This work was supported by the Swiss Enlargement Contribution in the framework of the Croatian-Swiss Research Programme (project number IZHRZ0_180584) and by Croatian Science Foundation under the project IP-2020-02-1572. The work of doctoral student Lucija Mijanović has been supported by the "Young researchers' career development project – training of doctoral students" of the Croatian Science Foundation funded by the European Union from the European Social Fund.

Microscopic insight into the intriguing world of broccoli

Ivana Šola (1), Danijela Poljuha (2)

1) Department of Biology, Faculty of Science, University of Zagreb, Zagreb, Croatia

2) Department of Agriculture and Nutrition, Institute of Agriculture and Tourism, Poreč, Croatia

Brassicaceae family counts around 350 genera and 3500 species [1], including crops of great economic importance, such as *Brassica oleracea* and *B. rapa,* which represent a significant part of human and animal diet [2]. The vegetables from this family have diverse morphological forms, such as leaves that form a head of cabbage, non-heading kale, collard greens and Chinese kale, an enlarged stem of kohlrabi, axillary buds of brussels sprouts, immature inflorescences of cauliflower and broccoli. Broccoli (*Brassica oleracea botrytis* var. *cymosa*) has a characteristic miniature tree-like appearance with a lot of elongated lateral shoots starting at the maturation of the terminal inflorescence [3]. What about the broccoli organism from the inside? Using a light microscope, we captured the structure of its tissues, cells, cell walls, tubes, vessels and pits. It is just as attractive and picturesque on the inside as it is on the outside.

Keywords: broccoli, morphology, light microscopy

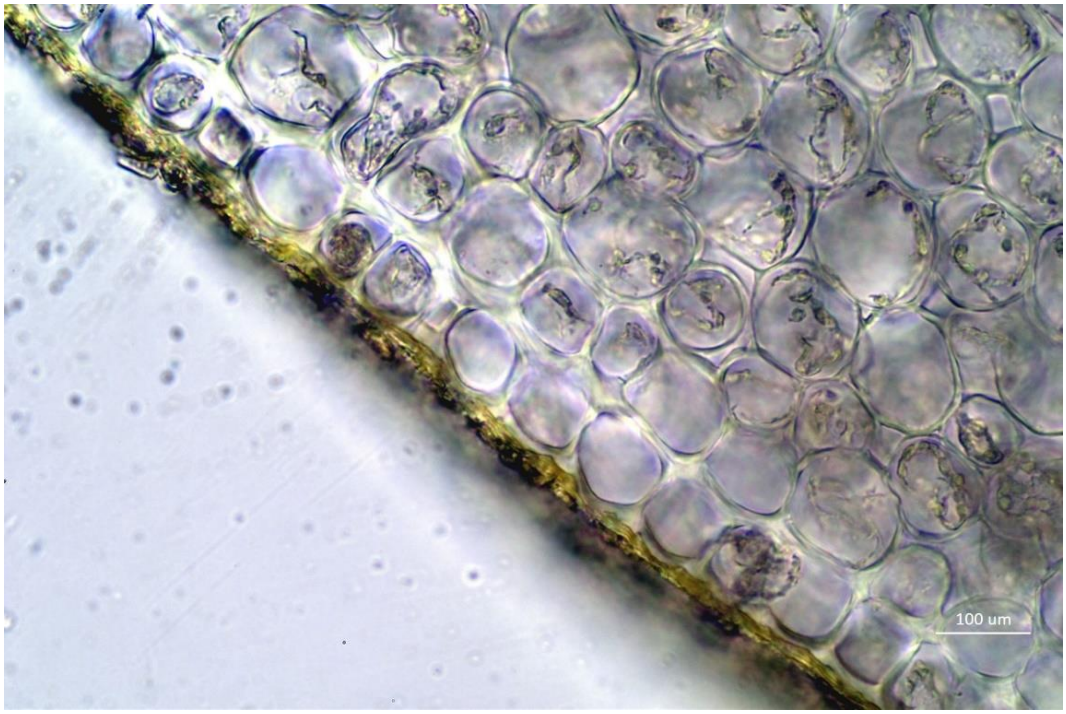

Figure 1. Epidermal cells and cuticle of the broccoli stem tissue.

References:
1. K. Sasaki and T. Takahashi, Phytochemistry 61 (2002) 339–343.
2. M. Jahangir et al., Compr. Rev. Food Sci. Food Saf. 8 (2009) 31-43.
3. E. Pressman et al., Sci. Hort. 26 (1985) 1-7.

This work was supported by the Croatian Science Foundation research project IP-2020-02-7585 „Indirect Effect of Global Warming on Mammals Physiological Parameters via High Temperature-Stressed Plant Diet (TEMPHYS)“.

A new approach to teaching about invasive species using a pocket paper Foldscope microscope

Mirela Uzelac (1), Ida Linić (1), Barbara Sladonja (1), Danijela Poljuha (1)

1) Institute of Agriculture and Tourism, Poreč, Croatia

The world of microscopy is constantly evolving, and in just a few decades, microscopes have become a window into almost everything we can imagine. Just like microscopy, invasive alien plant species (IAPS) have become our everyday topic to deal with. Education is one of the primary measures in response to the problem of the spread of invasive species. The invention of the Foldscope paper microscope in 2014 has made micro-world education more accessible. Foldscope combines low-cost materials with precision optics. With a magnification of 140 x, Foldscope can visualize microorganisms as well as larger samples such as tissues, organs, insects or plants. It is portable, waterproof and can be attached to mobile phones and is, therefore, an excellent educational tool. Here we will present a new approach to the education on IAPS through microscopy, developed in the framework of the Croatian Science Foundation project NATURALLY (IP-2020-02-6899) and intended for the young student population (10-14 years old). The targeted microscopy workshops were held in the outdoor classroom at the Institute of Agriculture and Tourism in Poreč (Croatia). The workshops were designed for upper-grade elementary school students. The first step of the workshop was an introduction to microscopy and invasive species, followed by assembling the paper microscope and preparation of microscopy sections. Leaf and flower tissue preparations of four invasive alien plants (*Ailanthus altissima* (Mill.) Swingle, *Solidago canadensis* L., *Helianthus tuberosus* L. and *Robinia pseudoacacia* L.) were made. Every sample was examined under different magnifications and photographed. The obtained images were sent to Foldscope Microcosmos – an online community platform. In general, this approach has proven successful in raising student motivation to learn and apply microscopic methods in exploring the environment and encouraging discussion on ecological topics.

Keywords: education, microscopy, invasive alien plants, science popularization

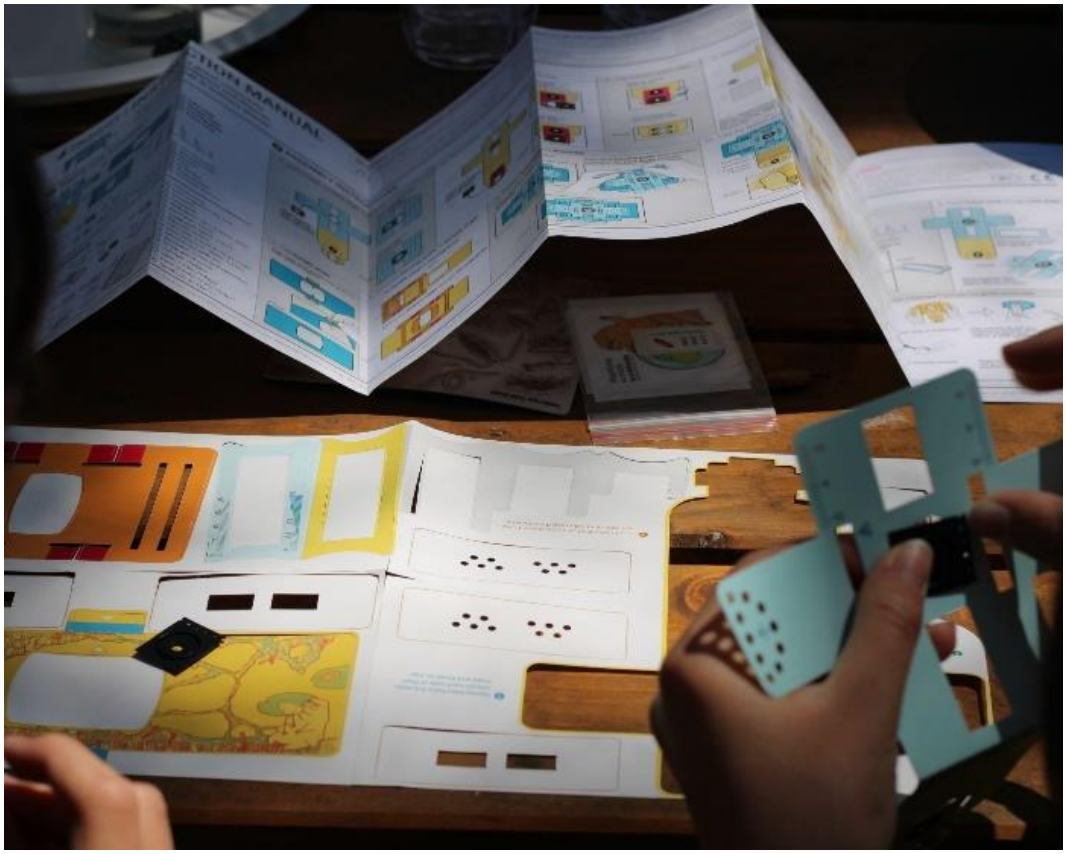

Figure 1. The process of assembling the Foldscope paper microscope.

This work has been supported by the Croatian Science Foundation under the projects IP-2020-02-6899 and DOK-2021-02-6899.

DNA damage and morphological changes to symbiotic and free-living hydra caused by norflurazon and UVB radiation

Goran Kovačević (1), Davor Želježić (2), Ana Matijević (3), Petra Korać (1), Katarina Caput Mihalić (1), Martina Ivšić (1)

1) Department of Biology, Faculty of Science, University of Zagreb, Zagreb, Croatia

2) Institute for Medical Research and Occupational Health, Unit for Mutagenesis, Zagreb, Croatia

3) Department of Laboratory Diagnostics, University Hospital Zagreb, Zagreb, Croatia

Individuals of symbiotic green hydra (*Hydra viridissima* Pallas, 1766) and free-living brown hydra (*Hydra oligactis* Pallas, 1766) were treated with aqueous solutions of herbicide norflurazon ($2x10^{-7}$, $2x10^{-6}$ mol/L) for 72 h and hydras were also exposed to simultaneous treatment to norflurazon and UVB radiation (λ = 254 nm, 2 min), along with control groups. The experiment was performed in triplicate. Migration and change of body shape (relaxed, contracted), as the evasion signs of deleterious effects, were observed by stereo microscope, and responses to mechanical stimuli were also noted. Comet assay was applied to measure the level of primary DNA damage of exposed green and brown hydras. Beside single and double strand breaks, it detects DNA base alkylation, oxidatively changed bases, DNA-adducts, covalently bound proteins to DNA, cross-linking and base dimers. Each hydra was put into a conical tube containing chilled homogenization buffer (75 mM NaCl, 24 mM Na_2EDTA, pH 7.5, +4 °C) and its cells were separated mechanically. The obtained homogenate was mixed with the low melting point agarose, spread across the microscopic slide and left for the gel to polymerize. Preparations were treated with a series of buffers to remove the cell structures and isolate nucleoids. By immersing the slides into alkaline buffer, pH 13.0, DNA denatures rapidly. At the spots of primary damage, DNA strands broke, which led to the formation of relaxed loops and free DNA fragments. In electrophoresis, these loops and fragments are pulled from the nucleoid core toward the anode, and following fluorescent staining, under the microscope, they appear as comets. Comet preparations were analysed under an epifluorescent microscope equipped with CCD camera, and the level of damage was measured by image analysis software for the comet assay. Based on the intensity of fluorescence of the tail compared to the nucleoid, the percentage of DNA affected by primary damage was calculated. The treatment did induce a concentration related increase in primary DNA damage, but no significant difference between green and brown hydra was observed (4.40 % vs. 5.23 %, respectively; negative controls 1.13 % and 1.17 %, respectively). On the other hand, in the presence of radiation, brown hydras showed significantly higher level of primary DNA damage already when exposed to the lowest concentration compared to the green ones (15.10 % and 3.77 %, respectively), proving the advantage of the symbiotic organism. The increase in damage was concentration dependent in either case.

Keywords: hydra, comet assay, morphology, norflurazon, UVB radiation

Deleterious effect of quercetin on green hydra and its endosymbiotic alga

Goran Kovačević (1), Ana Matulić (2)

1) Department of Biology, Faculty of Science, University of Zagreb, Zagreb, Croatia

2) Elementary school Dubrava, Dubrava, Croatia

Quercetin is a flavonoid that acts as an antioxidant, and it can also show a prooxidative effect. the effect of quercetin on freshwater invertebrate green hydra (*Hydra viridissima* Pallas, 1766) was studied under laboratory conditions. Green hydra forms an endosymbiotic relationship with unicellular photoautotrophic algae. Endosymbiosis requires at least two genomes of different evolutionary origin within the same cytoplasm. Here algae are placed in gastrodermal myoepithelial cells of hydra. Hydras were treated with aqueous solutions of quercetin (0.12, 0.2, 0.25, 0.3 g/L) for 72 h and compared to the controls. Static toxicity test was used and the experiment was performed in triplicate. For histological analysis standard preparation methods were used. The morphometrical analysis included thickness of mesoglea, area and diameter of algae and area of chloroplasts. By using stereo microscope and light microscopy we detected the following effects: concentration of 0.25 g/L was the threshold concentration at which intensive sublethal changes and changes of the histological structure appeared; concentration of 0.3 g/L led to irreversible changes and presented ca. LC_{50}; cytological changes of algae included shape and size of algae and chloroplasts. Altogether, quercetin exerted dose-dependent deleterious effects on green hydra and endosymbiotic alga. At lower concentrations (0.05, 0.07 and 0.1 g/L), no remarkable sublethal effects such as morphological and locomotory changes were noticed, whereas higher concentrations (0.4 and 0.5 g/L) induced increased mortality.

Keywords: toxicity, histological and cytological changes, morphometry

Microalgae as „triggers“ to dynamics in freshwater microcosm

Goran Kovačević (1), Daniela Petrinec (2), Petra Tramontana (3), Damir Sirovina (1), Siegfried Reipert (4), Davor Želježić (5), Petra Peharec Štefanić (1)

1) Department of Biology, Faculty of Science, University of Zagreb, Zagreb, Croatia

2) Croatian Institute for Brain Research, University of Zagreb School of Medicine, Zagreb, Croatia

3) Zagreb, Croatia

4) Cell Imaging and Ultrastructure Research (CIUS), University of Vienna, Vienna, Austria

5) Institute for Medical Research and Occupational Health, Unit for Mutagenesis, Zagreb, Croatia

The microcosm is a laboratory method used in the study of population dynamics, in the research of food chains etc. It simultaneously brings into interaction different species in the same controlled laboratory experimental area, which provides an opportunity for modelling and reconstruction of relationships in populations and biocenoses in nature. *Desmodesmus subspicatus* is an endosymbiotic alga isolated from green hydra and belongs to the *Chlorella zagrebiensis* group. Algae were cultured on a sterile deep stock agar in test tubes in an air chamber under sterile conditions at 24 °C. Besides *D. subspicatus*, the constituents of microcosms were also green hydras, freshwater turbellarians and large water fleas. Microalgae take an important place as the primary producers and food resources in aquatic ecosystems, but previously we have already noted the ability of isolated *D. subspicatus* to form algal nets and contribute to predation upon large water flea in freshwater microcosm. Herewith we proposed a possible mechanism of microalgal net formation in the freshwater microcosm. We studied the ultrastructure of cryopreserved microalgae by transmission electron microscopy (TEM) to get an explanation for formation of net-like structures and observation of abdominal microalgal filaments attached to water fleas that managed to escape from the nets. For this, we processed algae by high-pressure freezing (HPF) within milliseconds, followed by accelerated freeze substitution (FS) and embedding in epoxy resin. We also processed algae by chemical fixation, post-fixation, dehydration and embedding in epoxy resin. Ultrathin TEM sections revealed rod-like entities at the cell wall surface of isolated endosymbiotic algae, structures that could possibly fit and bond together, pointing to the possibility of microalgal net formations. These rod-like profiles could not only explain the formation of microalgal nets themselves, but also the basics of isolated algal species *D. subspicatus* itself: morphology and colour of the culture, formation of coenobia, and transitional forms and tetrads.

Keywords: *Chlorella zagrebiensis*, high-pressure freezing, freeze substitution, TEM, algal nets

POSTER PRESENTATIONS

(Materials Science)

Photocatalytic properties of thin PE-ALD ZnO films: the role of crystal structure

D. Jardas (1), R. Peter (1), M. Podlogar (2), D. Vengust (2), K. Salamon (3), M. Petravić (1), A. Omerzu (1)

1) University of Rijeka, Department of Physics & Centre for Micro- and Nanosciences and Technologies, Rijeka, Croatia

2) Jožef Stefan Institute, Ljubljana, Slovenia

3) Ruđer Bošković Institute, Zagreb, Croatia

Atomic layer deposition (ALD) is a sophisticated deposition technique that can be used to synthesize high-quality thin ZnO films. Moreover, films with different structural and physical properties can be obtained by varying the synthesis parameters [1-3]. The most important parameter is the deposition temperature – it determines the structure and material properties of the deposited films [2,3]. For conventional (i.e. thermal) ALD, the temperature range for the deposition of high-quality films is between 120 °C and 180 °C, and the best photocatalytic activity has been observed for films deposited above 150 °C [2,3]. An upgrade of thermal ALD is plasma-enhanced atomic layer deposition (PE-ALD), which allows deposition at lower temperatures without compromising the film's quality and growth rate. The photocatalytic activity of the films deposited by the PE-ALD method shows a maximum value for films deposited at temperatures lower than 100 °C and their efficiency is higher than that of the best thermal ALD films. In the present study, we compare the crystal structure of thin films deposited by the PE-ALD method at 60 °C, 80 °C, 100 °C, and 200 °C. For that purpose, we have analysed our samples with transmission electron microscopy (TEM) and X-ray diffraction (XRD). From the TEM images (Fig. 1), it can be seen that the films synthesized at lower temperatures are composed of smaller, round-shaped grains and the films synthesized at higher temperatures consist of larger, elongated crystals that are perpendicular to the substrate. Smaller grains mean more grain boundaries and thus lower carrier mobility. This leads to a longer charge carrier separation time and thus, a lower electron-hole recombination rate. Since the photocatalytic activity depends mainly on the concentration of photoinduced charges on the surface of the catalyst, the material with longer charge lifetimes (in our case, the films with smaller grains) is expected to exhibit higher photocatalytic activity, which was indeed observed in our measurements.

Keywords: zinc oxide, thin film, atomic layer deposition, plasma, photocatalysis

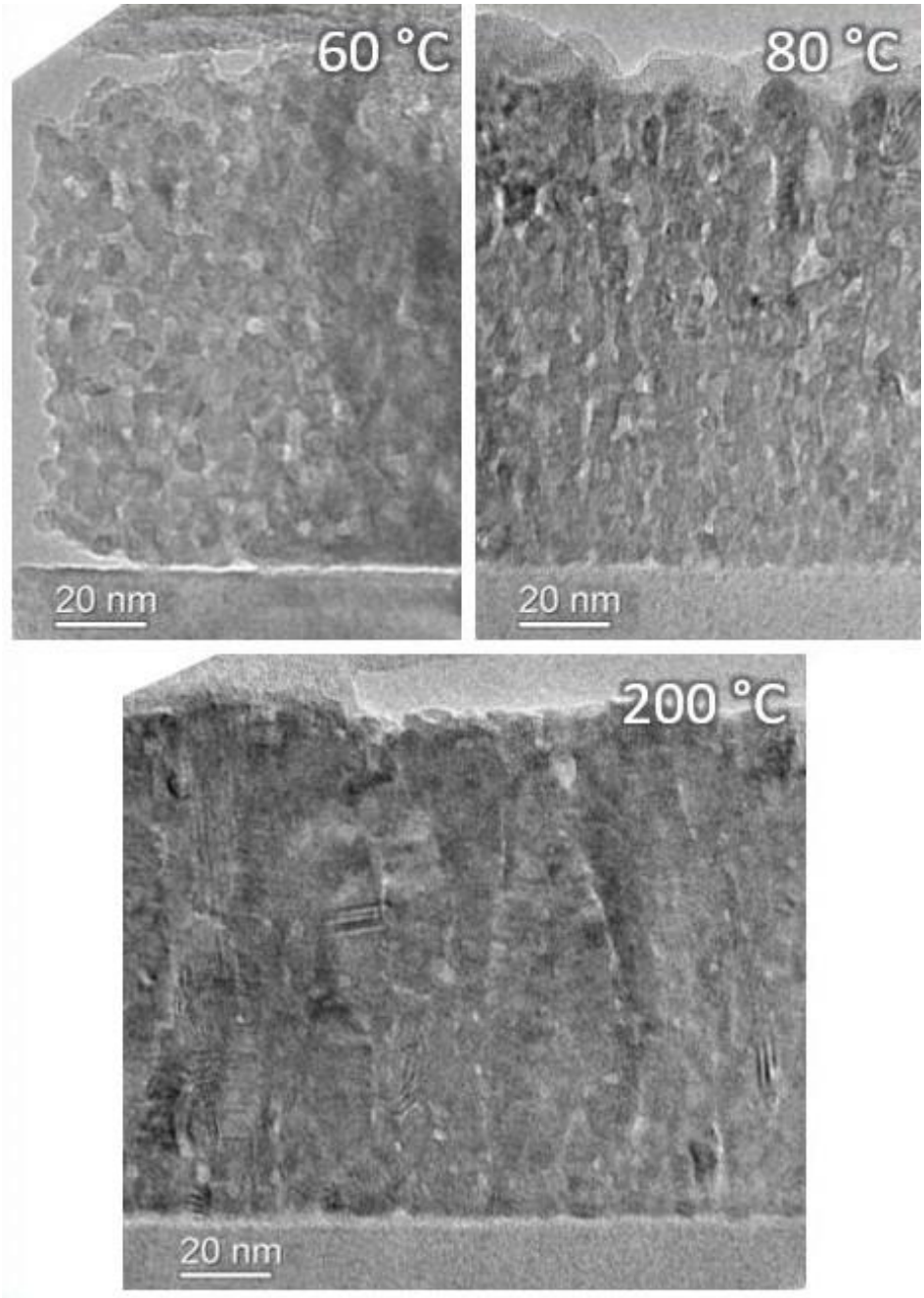

Figure 1. HRTEM images of the thin film cross sections for PE-ALD thin ZnO deposited at 60 °C, 80 °C and 200 °C.

References:
1. A. Omerzu et al., Surface. Interfac. 23 (2021) 100984.
2. R. Peter et al., J. Phys. Chem. C 124 (2020) 8861-8868.
3. V. Roge et al., J. Mater. Chem. A 3 (2015) 11453–11461.

Atomic layer deposition of ZnO and Al_2O_3 on cellulose for photocatalytic antibacterial performance

Ivana Jelovica Badovinac (1), Silvestar Mežnarić (2), Dalibor Broznić (3), Iva Šarić (1), Robert Peter (1), Maria Kolympadi Marković (1), Gabriela Ambrožić (1), Ivana Gobin (2)

1) University of Rijeka, Department of Physics and Centre for Micro- and Nanosciences and Technologies, Rijeka, Croatia

2) University of Rijeka, Faculty of Medicine, Department of Microbiology and Parasitology, Rijeka, Croatia

3) University of Rijeka, Faculty of Medicine, Department of Medical Chemistry, Biochemistry and Clinical Chemistry, Rijeka, Croatia

In the last 20 years, photocatalysis has become an important strategy for wastewater treatment. Various types of semiconductor-based photocatalysts, such as nano-sized metal oxides (TiO_2, Fe_2O_3, ZnO, etc.), are used in water purification [1]. Among them, zinc oxide (ZnO) has attracted much attention as a promising candidate for environmental applications due to its important properties, such as the ability to generate strong oxidants like hydroxyl and superoxide radicals, low toxicity and high chemical and thermal stability, wide band gap (E = 3.37 eV) and low cost. Many studies have shown that ZnO efficiently degrades organic and biological pollutants in addition to its antibacterial property [2]. Recently, atomic layer deposition (ALD) proved to be a suitable technique for the preparation of highly uniform and conformal inorganic layers with defined composition and structure on thermally sensitive polymer substrates. In this work, conformal coatings of ZnO and Al_2O_3 on cellulose fibers were prepared by atomic layer deposition (ALD) at low temperature. The antibacterial activity of cellulose, cellulose coated with a monolayer of Al_2O_3, and cellulose coated with Al_2O_3 and ZnO was tested against two bacterial species: gram-positive *Staphyloccocus aureus* and gram-negative *Escherichia coli* at UV-A and in the dark. Surface morphology, conformity, composition and film thickness were studied using a field emission scanning electron microscope (FE-SEM) and SEM in transmission mode (TSEM). We also used X-ray photoelectron spectroscopy (XPS) to study composition and chemical bonding, and secondary ion mass spectrometry (SIMS) to study film uniformity and approximate thickness in detail. Cellulose samples coated with both Al_2O_3 and ZnO achieved higher photoinhibition for *Escherichia coli* and *Staphyloccocus aureus* within only 15 and 60 min after UV irradiation, respectively, compared with cellulose coated with a monolayer of Al_2O_3. Cell damage was assessed by analysis of FE-SEM and TSEM images. Our results show that cellulose fibers coated with Al_2O_3 and ZnO are a suitable material for efficient photocatalytic disinfection of water.

Keywords: photocatalytic antibacterial activity, atomic layer deposition, zinc oxide, thin films, cellulose

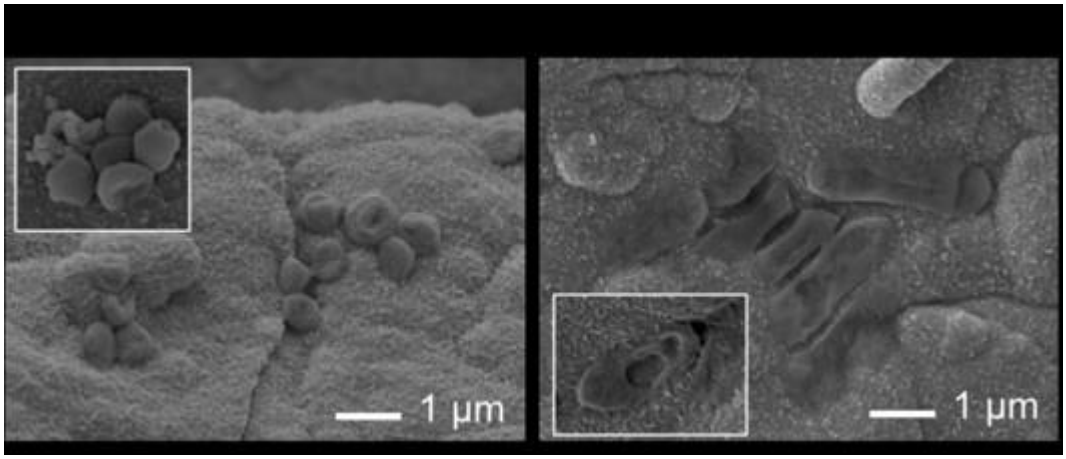

Figure 1. SEM images of *S. aureus* and *E. coli* on cellulose samples coated with Al_2O_3 and ZnO thin films after treatment with UVA light. The insets show images taken at higher magnification.

References:
1. A.M. Elgarahy et al., Nanotechnol. Environ. Eng. 6 (2021) 9.
2. K.-H. Park et al., Chem. Eng. J. 328 (2017) 988–996.
3. E. Kontturi and S. Spirk, Front. Chem. 7 (2019) 448.

This work has been mainly supported by Croatian Science Foundation under the project IP-2016-06-3568, and in part by the University of Rijeka under the project number uniri. biomed. 18-171. The characterization instruments applied in this work were acquired under the project Research Infrastructure for Campus based Laboratories at the University of Rijeka (RC.2.2.06-0001).

Photocatalytic activity of thin ZnO ALD films deposited on porous substrates

Ivna Kavre Piltaver (1), Ivana Jelovica Badovinac (1), Karlo Veličan (1), Aleš Omerzu (1)

1) University of Rijeka, Department of Physics and Center for Micro- and Nanosciences and Technologies, Rijeka, Croatia

Zinc oxide (ZnO) is a wide bandgap semiconducting material with a wide range of applications, including UV light emitters, solar cells, gas sensors, piezoelectricity, environmental engineering and photocatalysis. Recently, ZnO thin films have attracted much attention due to their unique advantages such as high photocatalytic ability, transparency and reusability. Atomic layer deposition (ALD) represents an excellent technique for the synthesis of ZnO thin films because it allows precise control of the film thickness, is easy to handle, exhibits high conformality of the obtained films and enables reproducible growth of defect-free films. In recent years, it has been shown that photocatalytic ZnO films grown on flat solid substrates or nanoparticles can be used in water purification systems [1-3]. On the one hand, powders or colloidal suspensions of nanoparticles are particularly efficient systems because they have a high surface-to-volume ratio, which increases the number of available surface states serving as reaction sites. Moreover, the nanoparticles are easily mixed with the contaminated solution. However, their subsequent separation from the solution is a challenging and expensive process. Therefore, the design of highly-efficient photocatalytic materials for water purification should be optimised to have a practical benefit. Both large surface area and high optical efficiency are required for the high photocatalytic activity of metal oxide films. In this study, the growth of thin ZnO ALD films on self-assembled nanoporous anodic aluminium oxide (AAO) surfaces and porous silicon wafers (MacroPor Template, SmartMembranes) was investigated. AAO samples were obtained by anodizing finely polished aluminium plates in phosphoric acid electrolytes under appropriate electrochemical conditions. The pore size was tuned and tailored by varying the acid molarity to produce a multifunctional nanoporous material with a high surface area. The morphology and the pore size of the samples were characterized by scanning electron microscopy (SEM). The photocatalytic activity of samples coated with ZnO films was evaluated by monitoring the degradation of methylene blue dye in an aqueous solution under UV light irradiation. We have demonstrated that the photocatalytic activity can be greatly increased by changing the porosity of underlying substrates.

Keywords: zinc oxide, thin films, photocatalytic activity, porosity, scanning electron microscopy

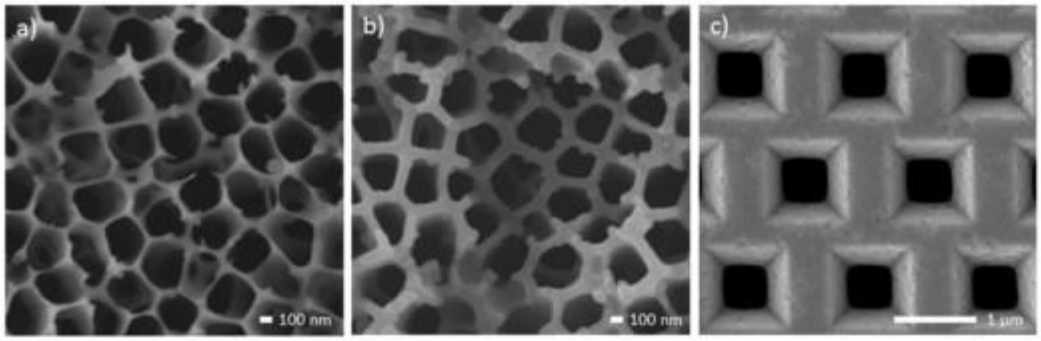

Figure 1. SEM images of porous structures: (a) AAO obtained by anodization, (b) same as (a) but coated with 20 nm ZnO ALD film and (c) porous silicon wafer.

References:

1. K.H. Park et al., Ceram. Int. 45 (2019) 18823-18830.
2. B. Jeong et al., Appl. Surf. Sci. 307 (2014) 468-474.
3. A. Di Mauro et al., Appl. Catal. B 196 (2016) 68-76.

Ceria-zirconia-based high entropy oxides as catalysts for pinacol-type reactions

J. Kojčinović (1), D. Tatar (1), I. Szenti (2), S. Balász Nagy (3), S. Ziegenheim (3), Y. Tang (4), D. Stenzel (4), G. Varga (5), I. Djerdj (1)

1) Josip Juraj Strossmayer University of Osijek, Department of Chemistry, Osijek, Croatia

2) University of Szeged, Department of Applied and Environmental Chemistry, Szeged, Hungary

3) University of Szeged, Department of Organic Chemistry, Szeged, Hungary

4) Karlsruhe Institute of Technology (KIT), Institute of Nanotechnology, Eggenstein-Leopoldshafen, Germany

5) University of Szeged, Department of Physical Chemistry and Materials Science, Szeged, Hungary

Novel high entropy oxides (HEOs) were synthesized in nanocrystalline powder form using a modified citrate sol-gel route. These compounds were further structurally characterized using powder X-ray diffraction (PXRD), Raman spectroscopy, scanning electron microscopy coupled with energy-dispersive X-ray spectroscopy (SEM-EDS), high resolution transmission electron microscopy (HRTEM), BET physisorption measurements and thermogravimetric analysis. HEOs were further used as catalysts for efficient Lewis acid-catalyzed direct conversion of aldehydes to 1,2-diketones in liquid phase. The synergistic effect of various cations incorporated in the same oxide structure (framework) is partially responsible for the efficiency of multi-cationic materials compared to corresponding single-cation oxide forms. Furthermore, a clear, linear relationship between the Lewis acidity and the catalytic activity of the HEOs is observed. Due to the developed strategy, exclusively diketone selective, recyclable, versatile heterogeneous catalytic transformation of aldehydes can be realized under mild reaction conditions.

Keywords: 1,2-diketone selective conversion of aldehydes, ceria, ceria-zirconia-based multimetallic oxides, high entropy oxides

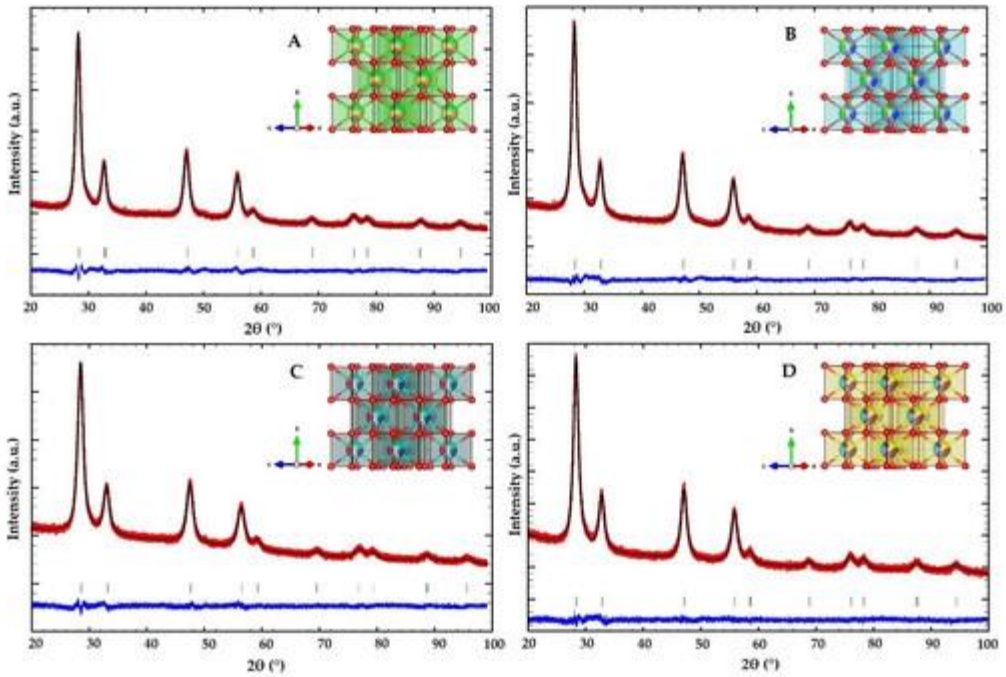

Figure 1. PXRD patterns and structures of synthesized HEO catalysts.

This research has been fully funded by the Croatian Science Foundation under the project number PZS-2019-02-2467, entitled “The study of the role of rare earth metal promoters and ordering on the redox properties of CeO_2 - ZrO_2 system”.

Experimental validation of novel fluorite-type rare earth high-entropy oxides for photocatalytic water splitting applications

D. Tatar (1), J. Kojčinović (1), S. Nundy (2), H. Ullah (2), A. Ghosh (2), A. A. Tahir (2), R. Meinusch (3), B. M. Smarsly (3), I. Djerdj (1)

1) Josip Juraj Strossmayer University of Osijek, Department of Chemistry, Osijek, Croatia

2) University of Exeter, Environment and Sustainability Institute, Penryn, United Kingdom

3) Physikalisch-Chemisches Institut and Center of Materials Research, Justus Liebig University, Giessen, Germany

Five different rare-earth-based nanocrystalline high-entropy oxides (HEOs) with fluorite type of structure and average crystallite sizes between 6 and 8 nm were prepared and their photocatalytic behaviour towards AZO dye degradation and photoelectrochemical water splitting for hydrogen generation was examined. The cationic site in the fluorite lattice consists of five equimolar elements selected from the group of rare-earth elements, including La, Ce, Pr, Eu, and Gd and second-row transition metals, Y and Zr. They reveal high photocatalytic activity which is mostly attributed to the accessibility of more photocatalytically active sites [1] which provided radicals responsible for the AZO dye degradation [1-3]. The materials successfully produce hydrogen by photocatalytic water splitting, suggesting the potential of HEOs as new photocatalysts. The photocatalytic performances of all studied HEOs outperform the single fluorite oxides or equivalent mixed oxides. The $Ce_{0.2}Zr_{0.2}La_{0.2}Pr_{0.2}Y_{0.2}O_2$ (CZLPY) engender hydrogen in the quantity of 9.2 μmol mg^{-1} per hour, which is much higher content than for pristine CeO_2 material which amounts to 0.8 μmol mg^{-1} per hour.

Keywords: high-entropy oxides, photocatalyst, photoelectrochemical water-splitting, hydrogen evolution

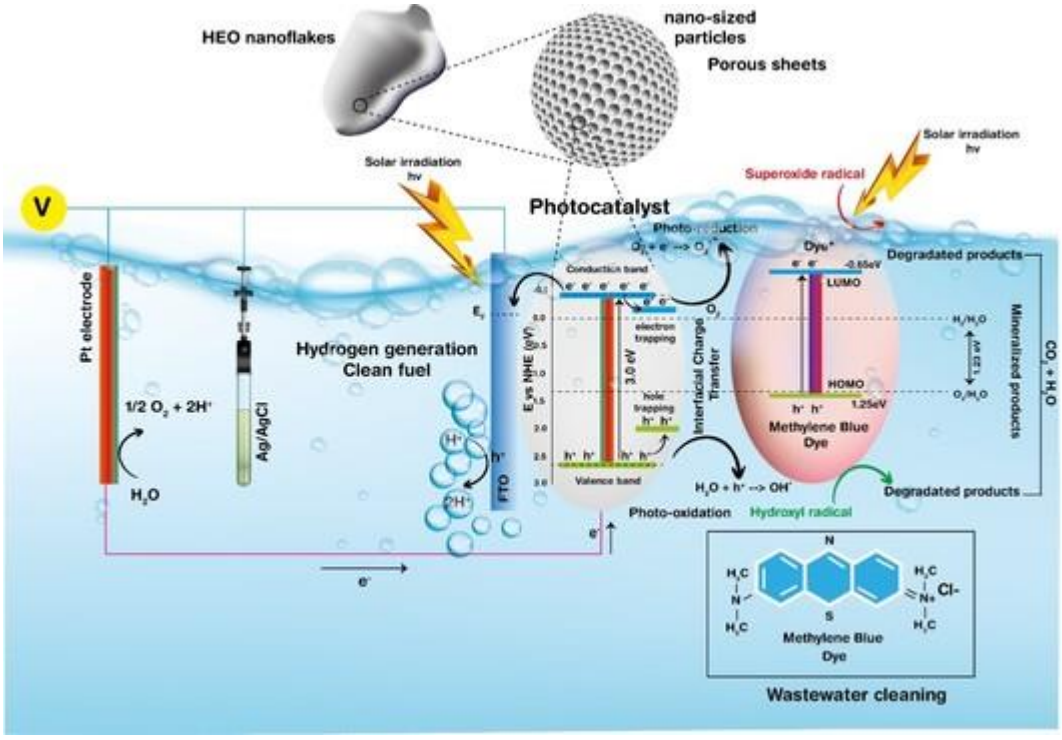

Figure 1. Schematic representation of the energy levels in high-entropy oxides (HEOs) with possible photocatalytic mechanism of AZO dye degradation.

References:

1. S. Chu and A. Majumdar, Nature 488 (2012) 294.
2. X. Zheng et al., Nat. Chem. 10 (2018) 149.
3. B. You and Y. Sun, Acc. Chem. Res. 51 (2018) 1571.

Split-second photothermal processing of thin film titania nanotubes using intense pulsed (white) light

M. Bohač (1), M. Zubak (2), V. Kojić (1), P. Kassal (2), K. Juraić (1)

1) Ruđer Bošković Institute, Zagreb, Croatia

2) University of Zagreb, Faculty of Chemical Engineering and Technology, Zagreb, Croatia

Semiconducting metal oxides (tin oxide, zinc oxide, titanium oxide, indium tin oxide, etc.) have been a hot topic in materials science since the mid-20th century due to their advantageous structural and optoelectrical properties. TiO_2, one of the most researched materials in this group, stands out because of its low cost, non-toxicity and excellent chemical and mechanical stability. Also, the plethora of possible TiO_2 nanostructures that can be prepared show immense application potential, since nanostructuring of TiO_2 leads to an increase in the specific surface area of the material, which in turn increases the efficiency in applications where TiO_2 interacts with its environment, e.g. catalysis, sensors, third-generation photovoltaics. In addition to the large increase in specific surface area, 1D nanostructures such as nanotubes provide superior charge separation and transport due to their ordered structure, elongated shape and thin walls. In most cases, the synthesis routes of ordered TiO_2 nanotubes (TNTs) result in amorphous products that require some sort of thermal processing to induce crystallinity. This in term is costly, time-consuming, energy inefficient and limits the final use of the product as all of the components must be thermally stable at the relatively high temperatures of annealing (> 450 °C). As an alternative approach to the annealing method, we used Intense Pulsed Light (IPL) irradiation to induce crystallinity. The IPL technique induces crystallization by the use of short pulses (μs) of white light without over-heating the substrate. The findings presented in this poster presentation indicate high potential for the development of thin-film TNTs on flexible plastic substrates that could potentially open up new implementation possibilities for thin-film TNTs like flexible solar cells, sensors or photocatalysts, something we will cover in future papers. We have prepared TNTs by anodizing Ti thin films that were deposited using radio frequency magnetron sputtering on FTO (fluorine-doped tin oxide) coated glass substrates and flexible polymer substrates. The as-prepared TNTs were amorphous and with IPL treatment we successfully induced crystalline changes (the formation of anatase with a small amount of rutile). We have tested the parameters of IPL treatment (number of pulses, pulse intensity) in a wide range and optimized them to obtain fully crystalline and transparent TNT layers. Using SEM, XRD, and UV-Vis spectroscopy, we tracked the changes in surface morphology, crystallinity, opto-electric properties and compared them with the results obtained for the samples annealed in a conventional way in a tube furnace at high temperature.

Keywords: intense pulsed light, titania nanotubes, crystallization, thin films

We acknowledge the Croatian Science Foundation (projects: IP-2018-01-5246, DOK-2018-09-7558 and UIP-2020-02-9139)

Correlation between synthesis parameters and optical/morphological properties of PbI_2 nanocrystals

Tomislav Damjanović (1), Livio Žužić (1), Antonio Supina (2), Ana Senkić (2), Iva Šrut Rakić (2), Nataša Vujičić (2)

1) University of Zagreb, Faculty of Science, Physics Department, Zagreb, Croatia

2) Institute of Physics, Zagreb, Croatia

In recent years two-dimensional (2D) semiconductors have seen extensive research for their promising properties for use in various electronic and optoelectronic devices. Most known examples of 2D semiconductors are transitional metal dichalcogenids (TMDs) [1] such as MoS_2. Another example of 2D semiconductors are transitional metal halides such as PbI_2, which have a large bandgap suitable for optoelectronic use [2,3] and are the focus of this work. In this work, we have synthesized 2D PbI_2 using precipitation of PbI_2 from its solution in ultrapure water onto a flat substrate. We used a Si substrate with a 300 nm layer of SiO_2 on top. The goal was to maximize the lateral size of PbI_2 crystals which would still retain a regular (triangular or hexagonal) shape while keeping thickness at the minimum. This was achieved by systematically varying synthesis parameters such as concentration and drying temperature of the solvent. Different methods of substrate preparation were also analyzed. After we systematically varied these parameters, obtained nanocrystals were investigated using optical microscope, atomic force microscope (AFM), Kelvin probe force microscopy (KPFM) and scanning electron microscopy (SEM) in order to establish a correlation between samples' morphology and synthesis parameters. Here we implemented machine learning (ML) techniques to map the sizes of crystals on a given wafer in order to determine the average size of a crystal. It was observed that precipitation at lower temperatures yields thinner crystals, while the temperature increase leads to laterally smaller and bulkier PbI_2 islands. These findings could provide a route for single- and few-layer PbI_2 growth.

Keywords: 2D semiconductors, PbI_2, atomic force microscope (AFM), Kelvin probe force microscopy (KPFM)

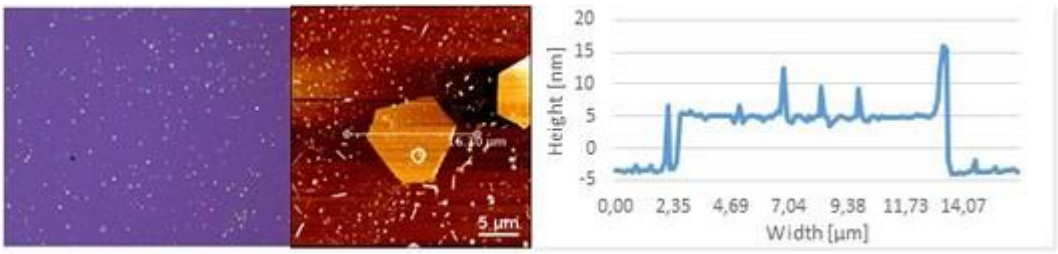

Figure 1. A typical wafer surface with multiple PbI_2 islands after synthesis (left), AFM topography map of a few layer island (middle) and the corresponding cross section (right).

References:
1. G.R. Bhimanapati et al., ACS Nano 9 (2015) 11509–11539.
2. Mohd. Shkir et al., Sci. Rep. 8 (2018) 13806.
3. T. Zhao et al., Nanoscale 8 (2016) 233–242.

Role of polyvinylpyrrolidone glass transition temperature in the performance of formamidinium perovskite solar cells

Vedran Kojić (1), Mario Bohač (1), Tihana Čižmar (1), Krešimir Salamon (1), Pavo Dubček (1), Andreja Gajović (1)

1) Ruđer Bošković Institute, Zagreb, Croatia

Since their discovery in 2009, organometal halide perovskites (OHP) have garnered attention from the scientific community as a cheap active layer for the production of photovoltaic diodes and devices. In a record-breaking time, OHP materials have surpassed silicon semiconductors in their energy conversion efficiencies, owing to their ability to form simple tandem solar cell configurations. However, one of the biggest problems of OHP materials is their instability in the ambient environment in the form of phase and structural degradation. Only the cubic unit cell perovskite phase exhibits efficient photovoltaic properties. Water, derived from air moisture, catalyses the phase conversion of the perovskite into a hexagonal unit cell which is well known for the absence of the strong photovoltaic effect. Alongside the phase conversion, adsorption of water leads to irreversible material degradation via organic cation sublimation and the formation of lead halide products. Several authors [1-3] have reported the use polyvinylpyrrolidone (PVP) as a stabilising agent for OHP materials. The role of PVP in perovskite thin films is the passivation of the crystallite grain boundaries from water adsorption. In this work, we have used PVP as an additive for formamidinium based perovskites and report its impact on the performance of formamidinium based photovoltaic device. The impact of the PVP addition inside the formamidinium lead iodide perovskite thin films was analysed from the viewpoint of structure, morphology, and its optical as well as electrical properties. We have found that the annealing temperature of the perovskite and the glass transition temperature of the additive have to be taken into account in the choice of an adequate stabilizing agent.

Keywords: formamidinium, perovskite, thin films, solar cells, stabilization

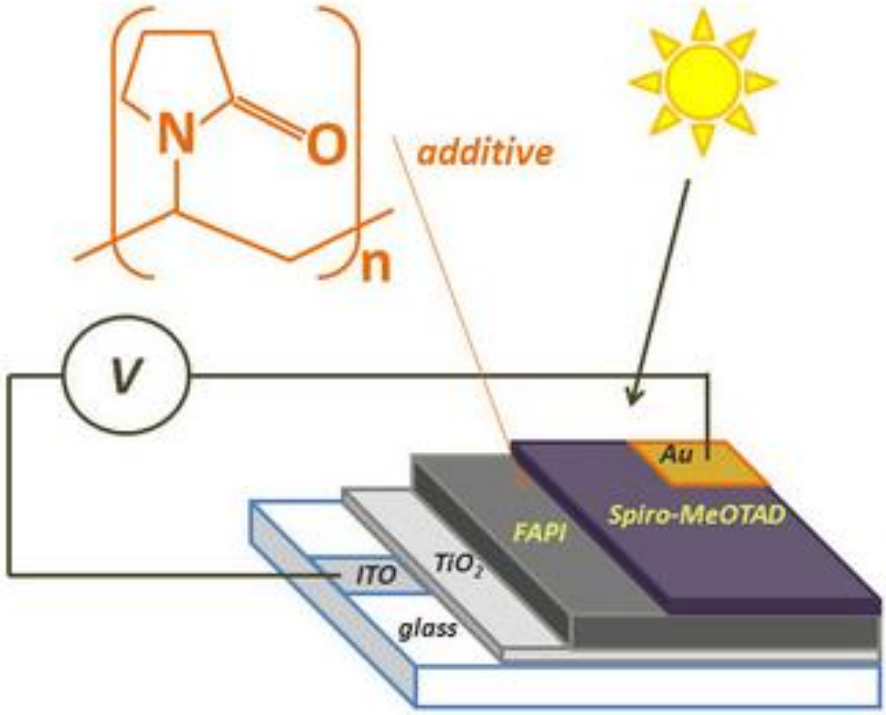

Figure 1. Graphical representation of formamidinium (FAPI) based perovskite solar cell.

References:
1. J. Yan et al., Sustain. Energy Fuels 3 (2019) 3448–3454.
2. H. Xiong et al., ACS Appl. Mater. Interfaces 10 (2018) 35385–35394.
3. B. Li et al., Nat. Commun. 9 (2018) 1076.

Morphological analysis of fibres extracted from lignocellulosic biomass – resources of renewable bioenergy

Zorana Kovačević (1), Sofia Šoufek (1), Ksenija Višić (1), Sandra Bischof (1)

1) University of Zagreb, Faculty of Textile Technology, Zagreb, Croatia

Lignocellulosic biomass is one of the best known raw materials for obtaining sustainable and environmentally friendly energy. The morphological characteristics of the cross section of two energy crops: miscanthus (*Miscanthus giganteus*) and Virginia marshmallow (*Sida hermaphrodita*), as well as two self-seeding crops: giant reed (*Arundo donax*) and Spanish broom (*Spartium junceum*) were examined in this paper. Fibres or sclerenchyma are present in plants as supporting tissue whose irregularly shaped cells are "framed" by a lignified cell wall to allow the plant to withstand weight, stretch, strain and bend. In addition to the production of renewable energy, these crops can also be used as raw materials for the production of fibres that can be used as reinforcements in the production of biocomposite materials. The establishment of such a production process where the waste of one industry becomes the input raw material of another industry respects the main task of the circular economy with the aim of reducing waste. Scanning electron microscopy was employed to analyse morphological characteristics of cross sections of plant stems and their inner fibres in order to determine the quality of fibrous reinforcement, which will be used in biocomposite production. SEM proved to be an efficient tool for the determination of structural features of lignocellulosic biomass and its degradation after performed pretreatments.

Keywords: scanning electron microscopy, circular economy, lignocellulosic biomass, natural fibre reinforcement, biocomposites

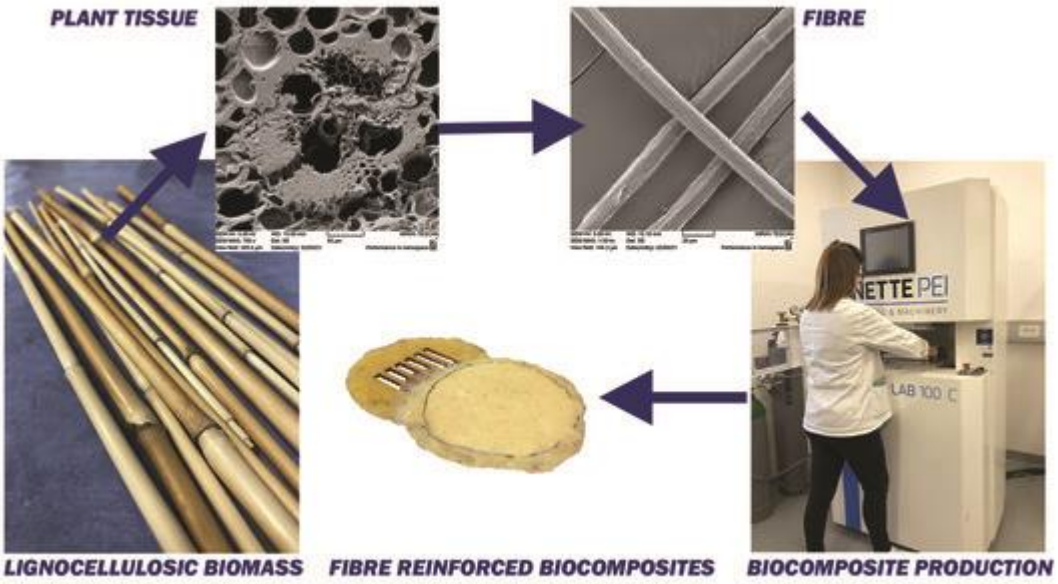

Figure 1. From biomass to biocomposites.

References:
1. Z. Kovačević et al., Holistic Approach Environ. 9 (2019) 44-52.
2. A. Balzano et al., Forests. 13 (2022) 161.

This research was supported by the European Regional Development Fund via K.K.01.1.1.04.0091 project ''Design of Advanced Biocomposites from Renewable Energy Sources – BIOCOMPOSITES''

Voltage cycling induced surface changes for enhancing sensing characteristics of graphene paste modified screen-printed electrodes

P. Živković (1), M. Medvidović Kosanović (1), A. Sečenji (1)

1) J.J. Strossmayer University of Osijek, Department of Chemistry, Osijek, Croatia

Graphene is a material with extraordinary chemical and physical properties and due to them is emerging as a promising material for a wide range of applications. Among them is the application for electrode material or surface modification of electrochemical sensors [1]. Using voltage cycling in electrolyte solution, it is possible to induce surface changes in electrodes modified with graphene paste. Induced surface changes cause enhancement of electrochemical sensing characteristics. In this study, screen-printed electrode with a graphene paste modified surface is prepared and electrochemical sensing characteristics are investigated. The electrode surface is investigated by Raman spectroscopy, energy-dispersive X-ray spectroscopy, and scanning electron microscopy before and after voltage cycling treatment. After voltage cycling electrode shows enhanced sensing characteristics, higher heterogeneous electron transfer rate, lower electron transfer resistance, lower capacitance, and higher sensitivity. Raman spectroscopy indicates a higher amount of available basal and edge plane graphene, while energy dispersive X-ray spectroscopy indicates the presence of intercalated oxygen species.

Keywords: screen-printed electrodes, graphene paste, surface modification, sensing characteristics enhancement

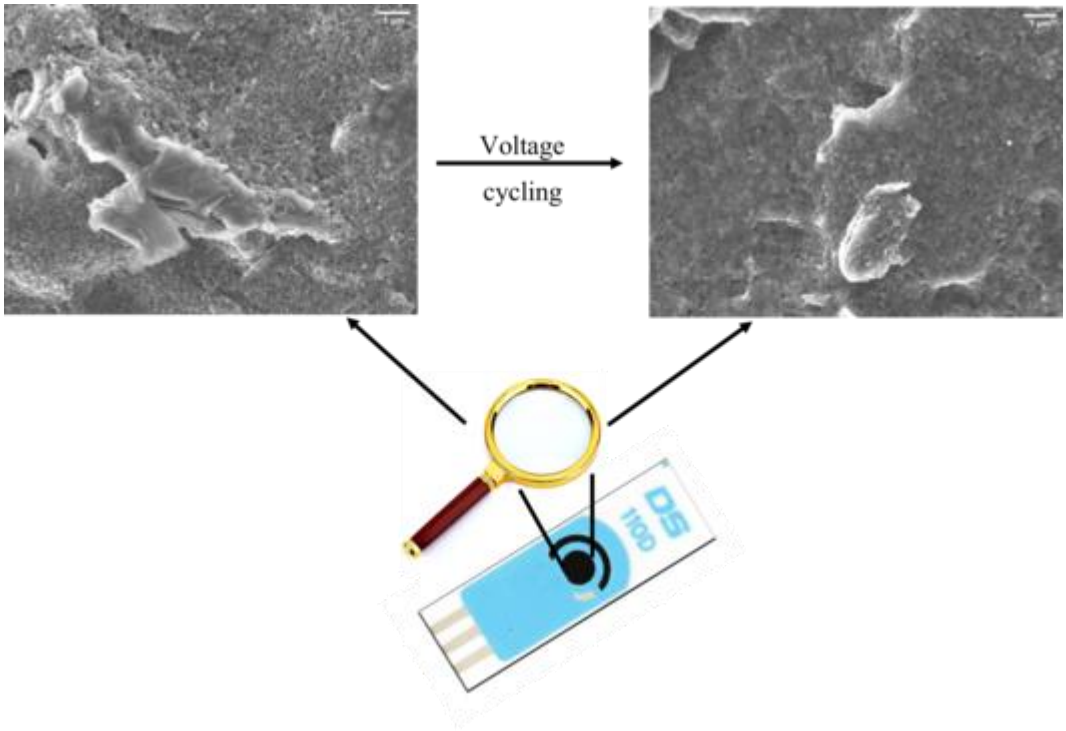

Figure 1. SEM image of electrode surface before (left) and after (right) anodic pretreatment.

References:
1. D.A.C. Brownson et al., Analyst 137 (2012) 1815-1823.

Determination of morphology, dopant amount and oxygen nonstoichiometry in lanthanum manganites by SEM-EDXS technique

Andreja Žužić (1), Jelena Macan (1)

1) University of Zagreb, Faculty of Chemical Engineering and Technology, Zagreb, Croatia

Sr-doped lanthanum manganites (LSMO, $La_{1-x}Sr_xMnO_3$) belong to a wide group of perovskite ceramics with promising electrical and magnetic properties and potential application in solid oxide fuel cells (SOFCs) and data storage devices. These properties can be enhanced via partial substitution of La^{3+} with an alkaline-earth divalent metal cation (most often Sr^{2+}) in order to promote the formation of mixed Mn^{3+}/Mn^{4+} valences and oxygen or cation vacancies [1]. Furthermore, properties depend on the synthesis method. In our study, LSMO (x = 0, 0.1, 0.2 and 0.3) were prepared by two different methods: citrate-nitrate autocombustion (CNA) and coprecipitation, and then calcined at 1200 °C/2 h. The structural analysis was conducted by the Rietveld refinement analysis of X-ray diffractograms. However, since the Rietveld profiles are mathematical models, the obtained results were checked by scanning electron microscopy (SEM) and energy-dispersive X-ray spectroscopy (EDXS). Furthermore, oxygen nonstoichiometry was determined by a direct analytical method – permanganate titration with Mohr's salt. All obtained results were in agreement showing that pure LSMO phases with targeted Sr-dopant amount were prepared. It was observed that coprecipitation has yielded samples with higher oxygen nonstoichiometry. Additionally, morphological differences were observed. CNA synthesis has yielded powders with a 'sponge-like' morphology, while powders prepared by coprecipitation were composed of large and porous spherical aggregates [2,3]. The morphology was also examined on the fracture of pellets prepared by raw powder pressing and sintered at 1200 °C/ 2 h. The densification of the sintered pellets was confirmed with the presence of sub-micrometer pores. Therefore, the sintering process has resulted in good particle-to-particle contact, as well as in porosity which makes LSMO a promising SOFC material due to electronic conductivity ensured by densification and gas permeability due to the porosity [1].

Keywords: lanthanum manganites, morphology, oxygen nonstoichiometry, synthesis

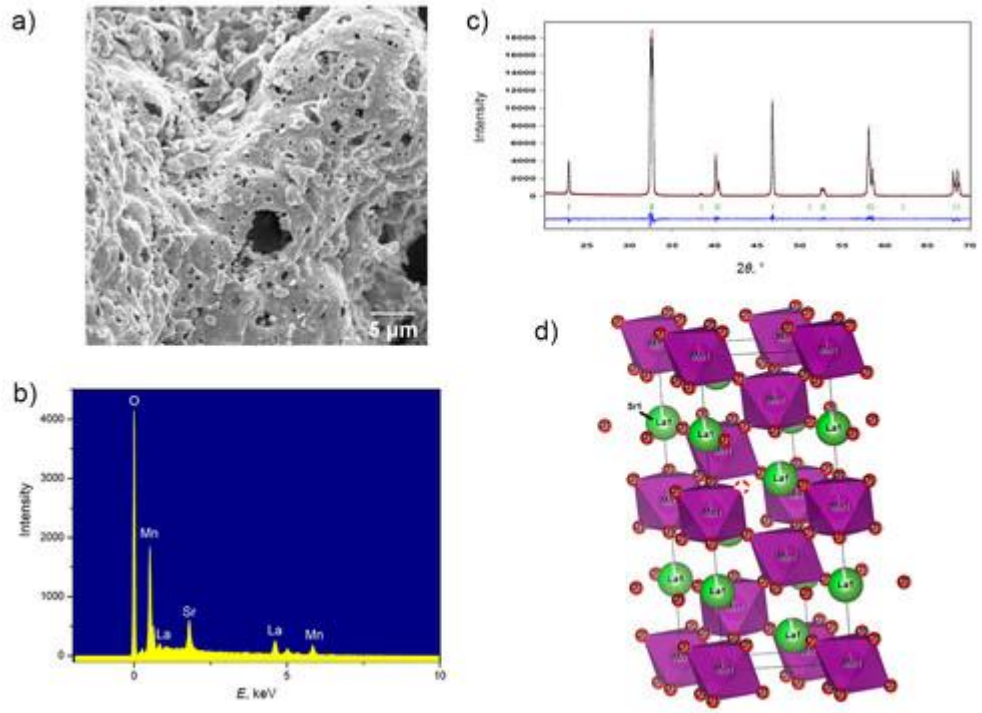

Figure 1. Importance of scanning electron microscopy (a) and energy-dispersive X-ray spectroscopy (b) technique along with X-ray diffraction analysis (c) for $La_{1-x}Sr_xMnO_3$ structure determination (d).

References:
1. P. Recio et al., Materials 14 (2021) 7831.
2. A.E. Danks et al., Mater. Horiz. 3 (2006) 91-112.
3. J. Macan et al., Ceram. Int. 46 (2020) 18200-18207.

This work has been supported in part by Croatian Science Foundation under the project IP-2018-01-5246.

Optical characterization of PbI_2 nanosheets prepared by a simple precipitation process

Livio Žužić (1), Tomislav Damjanović (1), Ana Senkić (2), Antonio Supina (2), Iva Šrut Rakić (2), Nataša Vujičić (2)

1) University of Zagreb, Faculty of Science, Physics Department, Zagreb, Croatia

2) Institute of Physics, Zagreb, Croatia

Two dimensional (2D) PbI_2 is a direct bandgap semiconductor material which shows promise as a base for electronic and optical devices [1,2] due to the direct bandgap in the visible spectrum [3]. PbI_2 belongs to the transition metal halides (TMH) family and its bulk form has been well characterized, but its 2D counterpart has only recently become the focus of interest. The synthesis process was done on a home-built setup under atmospheric conditions with slightly elevated temperature. Due to low solubility in cold water, the water solution of PbI_2 was kept at a high temperature of 90 °C with continuous stirring. We drop-cast 5 μL of the PbI_2 water solution of 400 mg/L concentration on a pre-treated Si/SiO_2 wafer surface and let it dry on a hot plate at temperatures in the range of 35 – 55 °C. Optical micrographs (Fig. 1) of prepared samples show how the crystallization process depends on solution concentration and drying temperature. The quality of obtained samples was assessed by atomic force microscopy (AFM) in order to correlate the thickness of the PbI_2 crystals with the optical properties of the material and its crystalline phase obtained by photoluminescence and Raman spectra measurements, respectively.

Keywords: 2D semiconductors, PbI_2, optical properties, Raman, photoluminescence

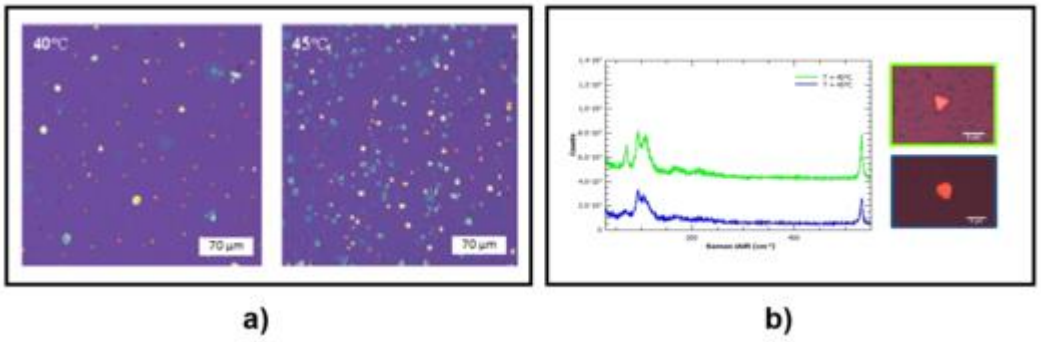

Figure 1. a) Optical micrograph at 10 x magnification of PbI_2 crystals on Si/SiO_2 wafer from an optical microscope for the concentration of 400 mg/L at different drying temperatures. b) Optical micrographs of two PbI_2 crystals synthesized at the two different drying temperatures and their Raman spectra.

References:
1. J.S. Manser et al., Chem. Rev. 116 (2016) 12956–3008.
2. M. Zhong et al., J. Mater. Chem. C 4 (2016) 6492–6499.
3. R. Frisenda et al., Nanotechnology 28 (2017) 455703.

Microscopy study of calcium phosphates and calcium carbonates precipitation in the presence of differently charged liposomes

Ina Erceg (1), Jasminka Kontrec (1), Vida Strasser (1), Atiđa Selmani (1), Darija Domazet Jurašin (1), Marija Ćurlin (2), Branka Njegić Džakula (1), Nives Matijaković Mlinarić (1), Suzana Šegota (1), Daniel M. Lyons (1), Damir Kralj (1), Maja Dutour Sikirić (1)

1) Ruđer Bošković Institute, Zagreb, Croatia

2) Catholic University of Croatia, School of Medicine, Zagreb, Croatia

Liposomes, bilayered vesicles made of phospholipids, are often considered to be a versatile tool for the synthesis of advanced materials, as they allow various control mechanisms to tune the materials' properties. The synthesis of two classes of biominerals, calcium phosphates (CaPs) and calcium carbonates ($CaCO_3$), using liposomes has attracted particular attention in the development of novel (bio)materials. However, the preparation of materials using liposomes has not yet been fully exploited. Therefore, the aim of this study was to investigate and compare the influence of differently charged liposomes (zwitterionic DMPC, negatively charged DMPS and positively charged EPC) on CaPs and $CaCO_3$ formation. The presence of liposomes during the spontaneous precipitation of CaPs and $CaCO_3$ affected the morphology of formed precipitates as well as the precipitation and transformation kinetics. The morphology of the obtained precipitates was analysed by scanning and transmission electron microscopy. The most prominent effect for both materials was found in the presence of negatively charged liposomes as (nano)shell structures were formed in both cases (Fig. 1). The obtained results indicate possible strategies to fine-tune the precipitation process of CaPs and $CaCO_3$, which could be of interest for the preparation of novel materials.

Keywords: calcium phosphates, calcium carbonates, liposomes, amorphous phases, nanoshells

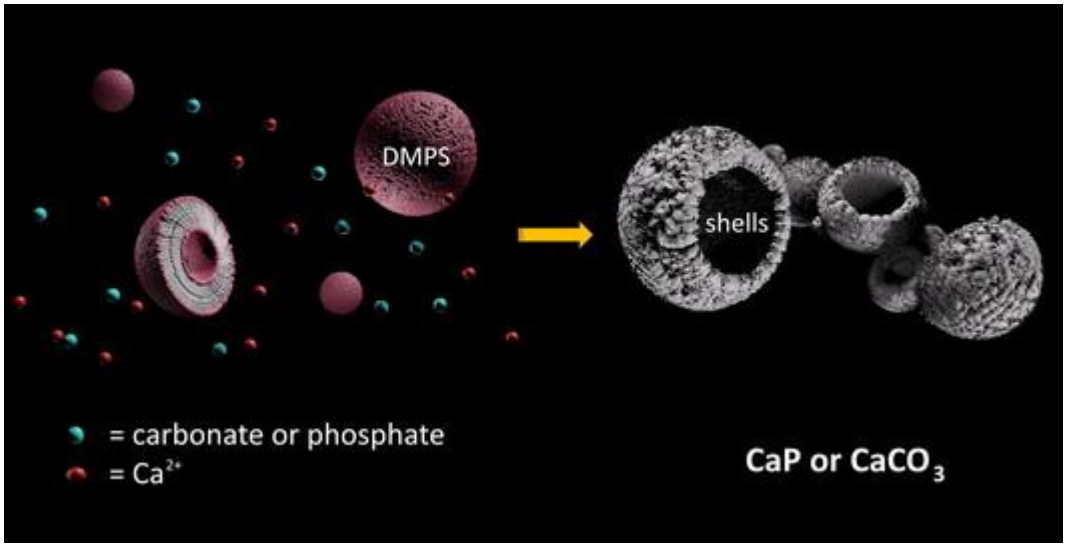

Figure 1. Schematic representation of the formation of calcium carbonate and calcium phosphate shell structures in the presence of DMPC liposomes.

Light microscopy application in determination of visible particles in injections

A. Giacobi Martinelli (1), N. Košutić Hulita (1), B. Martinić (1), B. Gudeljević (1)

1) Pliva Hrvatska d.o.o., Zagreb, Croatia

The use of light microscopy in pharmacy is almost necessary when determining foreign particles in parenteral dosage forms. Regulatory requirements listed in the USP Pharmacopoeia [1] and the European Pharmacopoeia [2] propose the method of determining foreign subvisible particles by light microscopy as one of two basic methods for determining the particulate matter in injections. In recent times there is a growing need for new approaches to methods for determining visible particles in injections. Looking with the human eye brings great subjectivity to the analysis itself, which pharmacy must avoid as much as possible. Also, basic methods for determining visible foreign particles are not suitable for special studies, such as simulation of the use of injections, in which the dosage of the drug is simulated as will be specified in the manufacturer's instructions. It is a great challenge, in addition to developing new methods for determining visible particles by a microscope, setting the criteria that a specific finished drug product must meet. Determination of foreign particles is the first point in the analysis, the next step would be possible identification of foreign particles using Raman microscope or SEM (morphology) and EDS (elementary) analysis. As part of this development, the materials used in the packaging of the finished drug product, such as the combi seal cap, are also evaluated. The research is aimed at finding a suitable material for closing the cartridges, which, after use and a certain number of needle punctures, will not impair the quality of the product, respectively have visible foreign particles under control and within the requirements specified during the method development.

Keywords: visible particles, combi seal cap, light microscopy, injections

References:
1. ⟨788⟩ particulate matter in injections, USP43-NF38 – 7017.
2. 2.9.19. Particulate contamination: sub-visible particles, EP 10.3., 01/2021:20919.

Effect of silver nanoparticles on the precipitation of calcium phosphates

Ana-Marija Milisav (1), Ina Erceg (1), Vida Strasser (1), Maja Dutour Sikirić (1)

1) Ruđer Bošković Institute, Division of Physical Chemistry, Laboratory for Biocolloids and Surface Chemistry, Zagreb, Croatia

Considering the increasing number of post-operative infections caused by antibiotic-resistant bacteria, research of therapeutic alternatives attracts special attention. The development of bioactive antimicrobial coatings for orthopaedic implants is of particular interest, as they can act locally and could reduce the use of oral antibiotics. In this sense, composite coatings based on calcium phosphates (CaPs) and metal or metal oxide nanomaterials have great potential, since CaPs occur naturally in the human body and inorganic nanoparticles do not in principle promote bacterial resistance [1]. Among different nanomaterials, silver nanoparticles (AgNPs) have shown optimal antimicrobial properties and cytocompatibility. In addition, their incorporation into various composite coatings within the organic or inorganic matrix was found to be beneficial, particularly with respect to their potential for controlled release system formulation *in situ* [2]. This study aimed to develop a green synthesis route for the preparation of novel CaP composites with AgNPs based on the precipitation of CaPs in the presence of AgNPs with different capping agents at different concentrations. For this purpose, two types of AgNPs were synthesised: one stabilised with polyvinylpyrrolidone (PVPAgNP) and the other stabilised with sodium bis(2-ethylhexyl) sulfosuccinate (AOTAgNP) [3]. The progress of precipitation was followed by monitoring the pH changes in the precipitation systems over time. The precipitates obtained after one hour of reaction time were filtered and characterised by powder X-ray diffraction (PXRD), Fourier transform infrared spectroscopy (FTIR), and scanning electron microscopy (SEM). The results showed that calcium-deficient hydroxyapatite (CaDHA) was formed both in the absence and presence of AgNPs. SEM micrographs revealed a significant difference in the morphology of the precipitates formed in the different systems, indicating the important influence of the stabilising agent, i.e., the surface composition of the NPs. The results of this study indicate that the formation of CaP composites with metallic nanoparticles should be studied in depth as various parameters can differently affect the process and ultimately the properties of the formed materials. The elucidation of this process is of great importance for the development of improved orthopaedic implants.

Keywords: calcium phosphates, silver nanoparticles

References:
1. L. Wang et al., Int. J. Nanomedicine 12 (2017) 1227–1249.
2. V.A. Spirescu et al., Int. J. Mol. Sci. 22 (2021) 4595.
3. I. Vinković Vrček et al., RSC Adv. 5 (2015) 70787–70807.

This project, Antimicrobial Integrated Methodologies (AIMed ITN), was supported by the European Union under the Horizon 2020 Research and Innovation Programme under Marie Sklodowska-Curie Grant Agreement No. 861138.

The impact of a novel photo-activation protocol on dental composite's degree of conversion – a Raman study

E. Novta (1), T. Lainović (1), S. Savić-Šević (2), D. Pantelić (2), E. Toth (3), Ž. Cvejić (3), L. Blažić (1)

1) University of Novi Sad, Faculty of Medicine, School of Dental medicine, Novi Sad, Serbia

2) University of Belgrade, Institute of Physics, Belgrade, Serbia

3) University of Novi Sad, Faculty of Sciences, Department of Physics, Novi Sad, Serbia

Bulk-fill dental resin-based composites (RBC) have been introduced into the market for facilitating material application into deep cavities. In such bulk layers (4 – 5 mm), the light transmission may be compromised, leading to the reduced monomer to polymer conversion (degree of conversion – DC). This study aimed to investigate the influence of a novel two-step photo-activation protocol on DC of a contemporary bulk-fill RBC using Raman spectroscopy. Replicas of standardized tooth cavities were made of dental gypsum and filled with the bulk-fill RBC (Beautifil-Bulk Restorative®, Shofu). Two groups of five samples each were formed (n = 5). In the experimental group, the proposed two-step curing was designed as follows: in the first step, two optical fibers (ϕ 1.5 mm) connected to a commercial dental LED curing unit were inserted into the dental filling to cure the RBC from within; in the second step, fibers were extracted, remaining voids were filled with the RBC, and final conventional curing was performed. In the control group, conventional curing was used. Spectra were collected at the top, middle, and bottom surface of the sample, immediately after curing and after 24 h of dark storage. DC was calculated as the ratio of the stretching mode peaks at 1660 cm^{-1} and 1640 cm^{-1} in the cured and uncured material. All spectral acquisitions were conducted with a Raman microscope (Thermo Scientific™ DXR™ 3) coupled with a 10 x objective. The excitation was a DPSS laser at 780 nm wavelength and laser power of 24 mW. The exposed sample surface was 3.1 μm, while the acquisition time for each spectrum was 50 times 10 s. Mean immediate DC in the control group ranged from 26.3 % – 39.0 % (bottom to top) and 35.4 % – 40.9 % (bottom to top) in the experimental group. A significant increase regarding 24 h post-cure DC was detected in the control group (39.2 % – 46.0 %), in comparison with the experimental group, where only slight changes during the dark cure period were measured (40.1 % – 43.8 %). Based on the presented results, it was concluded that the proposed two-step photo-activation protocol exhibited an increased immediate bottom DC compared with the conventional curing, without significant difference after 24 h of dark storage. Further examination of the proposed protocol is necessary on various bulk-fill RBCs with different material chemistry, to precisely determine its benefits.

Keywords: dental composite, photo-activation, optical fibers, degree of conversion, Raman spectroscopy

References:
1. P. Yu et al., Oper. Dent. 42 (2017) 82-89.

This research was supported by the Ministry of Education, Science and Technological development of the Republic of Serbia (contract No. NIO200114). The authors would also like to thank Mikodental depo (Šabac, Serbia), for providing the dental composite.

The importance of SEM BSED in paintings and wooden polychrome cross-sections analysis

Tea Zubin Ferri (1)

1) ArcheoLab, Pula, Croatia

Microscopy analysis on painting or polychrome cross-sections represents the first and most important step in archaeometry research of an artwork. Today microscopy and micro-analysis techniques provide a wide range of investigation possibilities in terms of elemental and molecular spectroscopy analysis aimed to determine the painting materials (pigments, binders, and fillers). Usually, in order to observe all the layers (support, ground layer, underdrawings, paint layers, varnish) constituting a painted artwork, a tiny sample is embedded in transparent epoxy or polyester resin and polished, so the whole analysis can be performed directly on the cross-section. Optical microscopy observation is the very first step. With the provision of UV, IR, and polarized light, additional useful information about the composition of the layers could be immediately collected (like the presence of gilding, modern varnishes etc.), and the assessment for chemical composition analysis can be done. The most appropriate following step is the analysis of the layers by means of electron microscopy using the detector for back-scattered electrons which provides exceptional information about the composition of each layer and, often, reveals layers and details not observed by optical microscopy analysis (Fig.1). Such analysis instantly provides visual data about the different composition of the painting materials, especially those containing metal oxides (due to their higher atomic number), the shape of the filler particles or cracks and detachment between layers. In accordance with this, it can be stated that in order to perform a complete microscopy analysis of a painting or a polychrome sample, optical microscopy observations on the cross-sections should be followed by SEM BSED observations. If the SEM analysis is skipped, it is possible to overlook important characteristics of the painted layers that can lead to wrong or incomplete assumptions, especially when the analysis is accomplished as a part of research aimed to provide information about the technique and the author or to prove the authenticity of an artwork.

Keywords: wooden polychrome cross-sections, optical microscopy, SEM BSED

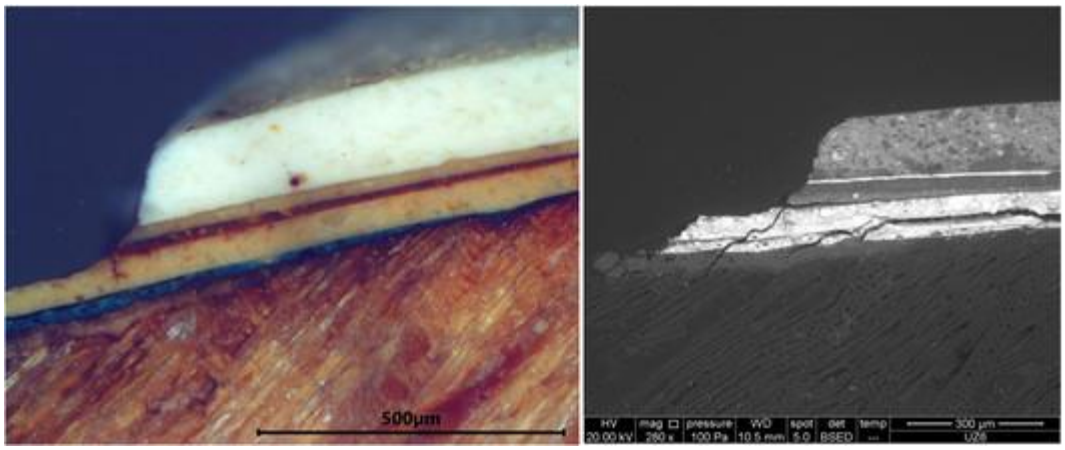

Figure 1. Cross-section of the wooden polychrome (The Mourning of Christ, Rovinj, Croatia) by optical and SEM BSED microscopy.

References:
1. M. Schreiner et al., Anal. Bional. Chem. 387 (2007) 737–747.
2. P. Lerotić et al., Portal 4 (2013) 153-167.

Author Index

Ambrožič, B. 14
Ambrožić, G. 93
Balász Nagy 97
Balen 67
Banjad Ostojić 71
Baus Lončar 34, 57
Bazina 34, 57
Belovari 34, 57, 59, 61
Berecki 32, 78
Bernstorff 47
Beus 62
Biba 67
Bijelić 34, 57, 59, 61
Bischof 106
Blažić 119
Bočina 30
Bohač 43, 47, 101, 104
Brkić 49
Brkljačić 45
Broznić 93
Capjak 62
Caput Mihalić 87
Car 17, 41
Chalet 28
Cibok 61
Cingesar 17
Cvejić 119
Čeh 1, 47
Čižmar 45, 104
Ćetković 8
Ćurlin 62, 114
Ćutić 81
Damjanović 102, 112
Debeljak 59
Djerdj 97, 99
Dobrivojević Radmilović 78
Dolinšek 37
Domazet Jurašin 114
Drenjančević 34
Drev 1
Dubček 47, 104
Dumančić 22
Dumenčić 59
Dutour Sikirić 53, 114, 117
Erben 71
Erceg 53, 114, 117
Erdani Kreft 5
Filić 7, 21, 76, 80, 81
Friščić 74
Fulgosi 22
Gajović, A. 41, 43, 45, 47, 104
Gajović, S. 32, 78
Ghosh 99
Giacobi Martinelli 116
Glasnović 78
Gobin 93
Gottschalk 28
Gracin 47
Gračan 71
Gudeljević 116
Guo 37
Hae Jin 37
Hamer 32, 78
Heffer 61
Herak Bosnar 8
Hreščak 1
Hwanuk 37
Ilić 62
Ister 78
Ivošević DeNardis 24
Ivšić, B. 64
Ivšić, M. 71, 87
Jadriško 51
Jaklin 49
Jardas 91
Jelen 37
Jelovica Badovinac 93, 95
Josić 78
Jukić 34
Juraić 43, 47, 101
Kamal 51
Kassal 101
Kavre Piltaver 95
Kelam 30
Kević 30
Klaser 39
Koblar 1
Kodba 20
Kojčinović 97, 99
Kojić 43, 101, 104
Kolympadi Marković 93
Komazec 65
Kontrec 114
Korać 87
Košpić 67
Košutić Hulita 116
Kovačević, G. 71, 87, 88, 89
Kovačević, Z. 106
Kozina 34
Koželj 37

Kralj, D. 114
Kralj, M. 49, 51
Kraljević Pavelić 54
Kreft, M. 9
Lainović 119
Lajtner 69, 71
Leitinger 28
Letofsky Papst 67
Levak Zorinc 24
Likozar 14
Linić 85
Lunkenbein 12
Lyons 65, 73, 114
Macan 41, 110
Machaček 25
Maleš 74
Marciuš 39
Marelja 73
Marić 74
Marijan 39
Marinović 21
Marjanović Čermak 62
Markoska 54
Marković, D. 54
Marković, M.P. 17
Martinić 116
Matijaković Mlinarić 114
Matijević 87
Matulić 88
Meden 37
Medvidović Kosanović 108
Meinusch 99
Mežnarić 93
Mijanović 76
Miletić 71
Milić 62
Milisav 53, 117
Mišić Radić 24
Nerl 12
Novko 51
Novosel 24
Novta 119
Nundy 99
Njegić Džakula 114
Obad 30
Omerzu 91, 95
Pantelić 119
Panžić 45
Pavelić 54
Pavičić 62
Pavić 39
Pavin 21
Peharec Štefanić 65, 67, 73, 89
Peter 91, 93
Petravić 91
Petrinec 32, 78, 89
Petrović 51
Pisk 39
Plodinec 12
Podlogar 91
Poljuha 83, 85
Pongrac 62
Prašnikar 14
Privara 80
Putar 76, 80, 81
Racetin 30
Radatović 51
Radić 8
Radulović 28
Rajc 59
Razum 39
Reipert 89
Restović 30
Risteski 20
Rođak 34, 57, 59, 61
Salamon 43, 91, 104
Sarkočić 78
Savić-Šević 119
Schlögl 12
Sečenji 108
Selmani 114
Selthofer Relatić 59
Senkić 49, 102, 112
Sharifi 43
Sirovina 89
Skoko 39
Skukan 32, 78
Slade 8
Sladonja 85
Smarsly 99
Spada 54
Stenzel 97
Strasser 53, 114, 117
Sunkara 27
Supina 49, 102, 112
Szenti 97
Šarić 93
Šegota 114
Šestan 1
Šešelja 34, 57
Škokić 78
Šola 83
Šoštar 8, 21, 64
Šoufek 106
Špoljar 71
Šrut Rakić 102, 112
Šturm 14
Tahir 99

Tang 97
Tatar 97, 99
Tkalčec 71
Tolić 20
Tomašić, N. 16
Tomašić, V. 41
Toth 119
Tramontana 89
Ullah 99
Uzelac 85
Varga 97
Veličan 95
Vengust 91
Vinicki 25
Višić 106
Vondrášek 67
Vrček 62
Vrsaljko 17
Vrtnik 37
Vučemilo 30
Vučić 59
Vujičić 51, 102, 112
Vukušić 20
Vuletić 64
Weber 8, 21, 64, 76, 80, 81
Wernitznig 28
Willinger 3
Zankel 28
Zhang 45
Ziegenheim 97
Zjalić 59, 61
Zubak 101
Zubin Ferri 121
Želježić 10, 87, 89
Živković 108
Žužek 14
Žužić, A. 41, 110
Žužić, L. 102, 112